Washington University in St. Louis
Washington University Open Scholarship

Arts & Sciences Electronic Theses and Dissertations

Arts & Sciences

Spring 5-15-2017

Mitochondrial damage accumulation in oocytes – a potential link between maternal obesity and increased cardiometabolic disease risk in offspring.

Anna Louise Boudoures
Washington University in St. Louis

Follow this and additional works at: https://openscholarship.wustl.edu/art_sci_etds

Part of the Cell Biology Commons, and the Developmental Biology Commons

WASHINGTON UNIVERSITY IN ST. LOUIS

Division of Biology and Biomedical Sciences
Program in Developmental, Regenerative, and Stem Cell Biology

Dissertation Examination Committee:
Kelle Moley, Chair
Jennifer Duncan
Joan Riley
Tim Schedl
James Skeath

Mitochondrial Damage Accumulation in Oocytes – A Potential Link Between Maternal Obesity
and Increased Cardiometabolic Disease Risk in Offspring.
by
Anna Boudoures

A dissertation presented to
The Graduate School
of Washington University in
partial fulfillment of the
requirements for the degree
of Doctor of Philosophy

May 2017
St. Louis, Missouri

Table of Contents

List of Figures

List of Tables

<u>Acknowledgments</u>

I must first and foremost thank Kelle Moley for her continued support, patience, generosity, and guidance for the duration of my time in her lab. None of this research would have been possible without her. I would like to thank the members of the Moley lab, especially thank Micheala Reid for keeping the lab running smoothly and keeping me clean and organized. Much of the work in this dissertation would not have been possible without the technical expertise of Andrea Drury and Suanne Scheaffer, who completed the *in vitro* fertilization and embryo transfers. Multiple lab members, past and present, contributed to this thesis through their scientific and technical advice. I am especially grateful for the support, advice and friendship of Emily Benesh, Jessica Saben, Zeenat Asghar, Claire Stephens, and Treeza Okeyo-Owour. I would also like to thank my thesis committee members who went above and beyond to give me scientific and personal advice throughout the years, especially Joan Riley.

I would not have made it to this point in my career without the undying support of my friends and family. Thank you to my parents, who would drop what they were doing to patiently listen and advise me despite knowing very little about biology. They encouraged me to keep going when I wanted to quit. Allyson Mayer was a crucial source of emotional and scientific support from the beginning; she showed me what dedication and hard work looks like and motivated me to always do my best. Thanks to Julia Fridrich, for having weekly coffee dates at Kaldi's to talk about our life goals. And to all of my friends who were there to give me a reprise from lab and make these past five years enjoyable, thank you.

Anna Boudoures

viii

Dedicated to Greg Sibbel.

Abstract of the Dissertation

Mitochondrial Damage Accumulation in Oocytes – A Potential Link Between Maternal Obesity

and Increased Cardiometabolic Disease Risk in Offspring.

by

Anna Boudoures

Doctor of Philosophy in Biology and Biomedical Sciences

Developmental, Regenerative, and Stem Cell Biology

Washington University in St. Louis, 2017

Professor Kelle H Moley, Chair

The developmental origins of health and disease (DoHAD) hypothesis suggests that negative

maternal lifestyle choices, such as obesity, affect the health of her offspring. Clinical and

laboratory studies support this hypothesis – offspring born to obese mothers are at increased risk

for health conditions including cardiometabolic syndrome and congenital abnormalities.

Maternal obesity damages the oocytes, contributing to the increased disease risk by transmitting

damaged organelles and epigenetic modifications to the offspring. Mitochondria, the most

abundant organelle in the oocyte, are damaged in oocytes from obese females. However, we do

not understand if mitochondrial damage in oocytes is reversible nor why offspring are at

increased risk for cardiometabolic syndrome like cardiomyopathy. Here we show that in mice

fed a high fat/high sugar (HF/HS diet), improving female health with moderate, voluntary

exercise does not reverse oocyte damage. We also tested if oocytes could activate mitophagy to repair obesity induced mitochondrial damage. Finally, we show that female offspring from obese mothers have mitochondrial damage in the heart that persists into adulthood. This damage causes dilated cardiomyopathy that worsens with age. These results provide an explanation for the persistence of damaged mitochondria in the oocytes of obese females. Additionally, they suggest that maternal obesity promotes the development of heart failure in offspring by inducing mitochondrial damage in the heart. Together, this data suggests mitochondrial damage caused by maternal obesity is non-reversible and contributes to cardiometabolic syndrome. The research provides potential mechanisms that support the DoHAD hypothesis and open new questions about how the changes to offspring health occur.

Chapter 1: Introduction to the Dissertation

1.1.   The Developmental Origins of Health and Disease

David Barker established the developmental origins of health and disease (DoHAD) hypothesis, which suggested that negative maternal lifestyle choices, such as obesity, affect the health of her offspring (Barker, 2004). Since then, numerous clinical and laboratory research studies have explored how maternal health affects future generations, including the effects of obesity, a growing risk factor for all individuals. In the most recent report of obesity trends in the United States, 37% of women who are of child bearing age are also obese (Flegal et al., 2016). Among lower income women, the maternal obesity rate climbs to 53% (Poston et al., 2016). Therefore, maternal obesity is a pressing health epidemic with long-term consequences that could span generations.

In line with the DoHAD hypothesis, maternal obesity can impact the long-term health of her offspring. For example, a mother who is obese prior to conception is 3.75 times more likely to give birth to an obese infant than a woman with a BMI in the normal range (Catalano et al., 2009a). In a follow-up study, the children were also more likely to have insulin resistance at birth (Catalano et al., 2009b). Both insulin resistance and obesity are risk factors for developing type 2 diabetes, a co-morbidity associated with obesity that is becoming increasingly prevalent in the adolescent population (Patterson et al., 2004; Pulgaron and Delamater, 2014). Obese mothers also have increased risk to give birth to children with more serious congenital abnormalities, including craniofacial defects, cardiovascular defects, and hydrocephalus (Stothard et al., 2009). These studies suggest that maternal obesity imparts negative effects during gestation and that obese women predispose their children to a variety of health conditions.

As children from obese mother age, additional health complications can arise or persist. Maternal BMI has also been associated with increased offspring systolic blood pressure and an increased likelihood for offspring to be hospitalized for a cardiac event in adulthood (Gaillard et al., 2014;

Godfrey et al., 2016). Obese mothers also have a higher risk of giving birth to a child with intellectual disabilities and this risk increased with increasing maternal BMI (Mann et al., 2013). Together, these results establish maternal obesity as a significant health risk to the next generation.

The effects of maternal obesity on offspring have been observed in mouse models. Pups born to mothers on a high fat/high sugar (HF/HS) diet were smaller than control pups at postnatal (PND) 18, likely due to intrauterine growth restriction (Jungheim et al., 2010). The disparity in weights between humans and mice is presumed to lie in the fact that mice are born prematurely (Clancy et al., 2001). HF/HS offspring growth caught up to control mice by PND 25. By the time the male offspring were 13 weeks old, they outweighed lean offspring, developed glucose intolerance, and had a higher body fat percentage (Jungheim et al., 2010). This phenotype is similar to that of humans and mirrors a pre-diabetic phenotype (American Diabetes Association, 2010). Additionally, mice born to obese mothers also develop heart failure later in life (Blackmore et al., 2014; Fernandez-Twinn et al., 2012). Taken together, these studies indicate that maternal obesity transmits multiple negative phenotypes to the offspring which can be recapitulated in animal models.

The negative effects of maternal obesity begin to manifest in utero. In mice, offspring from HF/HS dams have reduced crown-rump length and placenta diameter, two important parameters used to measure fetal growth. Organ systems are also affected by maternal obesity. Forty percent of the HF/HS embryos also had abnormal brain development in the HF/HS offspring in utero (Luzzo et al., 2012). Abnormal brain development in mice correlates with clinical data that indicated increased maternal BMI increased the likelihood for offspring to have intellectual disabilities (Mann et al., 2013). Even prior to implantation, embryo exposure to high

levels of fatty acids either *in vivo* or *in vitro* impairs growth and survival. Multiple groups reported obese mice and cattle have lower blastocyst formation rates (Desmet et al., 2016; Luzzo et al., 2012; Minge et al., 2008; Van Hoeck et al., 2011; Wu et al., 2010; Wu et al., 2012; Wu et al., 2015). The blastocysts from obese mothers also have significantly fewer cells in the inner cell mass, the portion of the blastocyst that will form the embryo after implantation.

Recently, two different groups designed embryo transfer experiments that the maternal diet effects the oocyte and these effects predispose embryos and offspring to growth restriction and poor health in adulthood. Oocytes from donor mice who were lean or obese were collected and fertilized *in vitro* with sperm from lean males. The two cell embryos were transferred to recipient mothers who were lean (Huypens et al., 2016; Sasson et al., 2015). In utero, embryos from obese donor mothers had reduced fetal/placental ratios, indicating fetal growth restriction. At birth, the pups from the obese donors were also smaller than pups from lean donors. The placentas from these embryos had significant changes in genes involved in lipid and steroid metabolism (Sasson et al., 2015), and changes to these pathways have been associated with placental insufficiency (Fowden et al., 2005). These data indicate pre-gestational exposure to obesity negatively impacts embryo development, potentially via changes to placental gene expression which cause placental insufficiency. A follow-up study observed that adult offspring from obese oocyte donors that developed in the lean uterine environment had decreased insulin sensitivity and increased body weight (Huypens et al., 2016). This research indicates a contribution by the oocyte to phenotypes observed throughout an offspring's life - from conception until adulthood. Oocyte exposure, prior to conception affects offspring health but the mechanism for how the oocyte specifically is contributing to the phenotype is not well understood.

1.2   Obesity and the Oocyte

Oocytes from HF/HS fed mice exhibit multiple signs of stress and have damaged organelles. These oocytes have a significant increase in lipid accumulation (Boudoures et al., 2016; Wu et al., 2010), abnormal meiotic spindles and inappropriate chromosome segregation (Luzzo et al., 2012, Boudoures et al., 2016, Boots et al., 2016) increased reactive oxygen species(Boots et al., 2016; Igosheva et al., 2010), and endoplasmic reticulum (ER) stress (Wu et al., 2012; Wu et al., 2015). Clinical studies of obese patients undergoing IVF also support a preconception contribution of oocyte damage to offspring health. Oocytes from obese women undergoing IVF are significantly smaller, have higher rates of anuploid, produce lower grade embryos, and significantly reduce blastocyst development rate (Luke et al., 2011; Marquard et al., 2011; Metwally et al., 2007; Wittemer et al., 2000). Finally, obese women undergoing IVF were more likely to achieve a successful pregnancy if they used an embryo fertilized from a lean donor women then if she used her own oocytes (Jungheim et al., 2013). These studies suggest multiple mechanisms for how the oocyte can transmit the negative health outcomes to offspring and support animal studies that show preconception exposure to obesity affects offspring health.

Multiple studies have shown that oocyte mitochondria from obese, HF/HS fed mice are damaged with significant decreases in mitochondrial membrane potential, changes in distribution within the oocyte, and structural abnormalities (Boots et al., 2016; Boudoures et al., 2016; Hou et al., 2016; Igosheva et al., 2010; Luzzo et al., 2012; Wu et al., 2010; Wu et al., 2015). It has been proposed that the mechanism of this damage is due to lipotoxicity, but no studies have definitively shown this effect to date. However, oocytes from obese animals have increased levels of reactive oxygen species, which can both cause and be produced by lipotoxicity (Boots et al., 2016; Hauck and Bernlohr, 2016; Igosheva et al., 2010). Chemically inducing oxidative damage to oocyte mitochondria prior to fertilization causes decreased blastocyst formation

(Thouas et al., 2004). Additionally, impairing the mitochondrial metabolism delays preimplantation embryonic cleavages, decreases the total cell numbers in blastocyst, and results in smaller fetuses and placentas at embryonic day 18 (Wakefield et al., 2011). This evidence suggests that oxidative damage to mitochondria, such as that caused by lipotoxicity, has similar effects to obesity on the embryo.

The most significant and heritable phenotype present in oocytes from obese females is damage to mitochondria. Oocytes have more mitochondria than any other cell (Piko and Taylor, 1987; Reynier et al., 2001). Additionally, all mitochondria are maternally inherited (sperm mitochondria are degraded rapidly upon fertilization (Al Rawi et al., 2011; Song et al., 2016; Sutovsky et al., 1999). Finally, embryos do not reactivate mitochondrial biogenesis until implantation(Piko and Taylor, 1987). Therefore, all of the mitochondria embryos rely upon to produce ATP, metabolic intermediates, and regulate signaling processes during cleavage stage divisions are inherited from the oocyte only. The damaged mitochondria may cause changes to embryo metabolism. Embryos have a unique metabolism prior to implantation. It is fine tuned to support the maternal to zygotic transition, rapid cell division, and an anoxic environment (Biggers JD, 1967; Dumollard et al., 2009; Ramalho-Santos et al., 2009). Research indicates embryos require approximately 150,000 oocyte mitochondria to complete these functions, and falling below this threshold results in embryo death (Cummins, 2004; Ge et al., 2012; Jacobs et al., 2006; Santos et al., 2006). Maternal obesity reduces mitochondrial DNA (mtDNA) copies in the embryo, which is used as a proxy for total number of mitochondria. Additionally, these embryos have changes in metabolic substrate preference (Binder et al., 2012; Minge et al., 2008; Wu et al., 2015). Finally, maternal obesity causes a significant reduction in blastocyst development rates (Dunning et al., 2011; Igosheva et al., 2010; Jungheim et al., 2010; Wu et al.,

6

2010; Wu et al., 2015). This research suggests that pre-conception and preimplantation exposure to obesity damages mitochondria and results in the observed developmental differences.

Multiple approaches have been taken to attempt to reverse HF/HS induced damage to oocytes and the mitochondria within them. For example, when mice return to a normal diet, their weight and glucose tolerance returned to levels of control counterparts. However, oocyte mitochondrial damage and spindle abnormalities persisted, suggesting damage to the oocyte is permanent (Reynolds et al., 2015). Attempts to use antioxidants as pharmacological interventions, such as administration of the antioxidant CoQ10, proved unsuccessful in complete reversal of HF/HS induced oocyte damage as well (Boots et al., 2016). The antioxidant resveratrol was able to increase the number of oocytes ovulated and fertilized in the genetically obese ob/ob mice. However, the study did not determine if resveratrol improved the quality of these oocytes (Cabello et al., 2015). Therefore, simply improving an individual's health may not be sufficient to improve the oocytes and prevent offspring predisposition to poor health.

1.3   Autophagy and Mitophagy in Oocytes and Embryos
Potentially, oocytes cannot repair damage because of a lack of macroautophagy (hereafter autophagy), a repair mechanism that somatic cells use to recycle damaged contents. Multiple forms of stress activate autophagy, which results in the formation of a double membrane structure that engulfs the damaged contents (proteins and organelles). The structure, the autophagosome, will then fuse with a lysosome for degradation and recycling of the macromolecular contents (Lamb et al., 2013; Stolz et al., 2014). The first study demonstrating oocytes do not undergo autophagy was published in 2008, when Tsukamoto et al. elegantly displayed oocyte knockout of the essential autophagy protein Atg5 (Autophagy gene 5) did not inhibit oocyte maturation or fertilization. However, shortly after fertilization, embryos died at the

7

4-8 cell stage (Tsukamoto et al., 2008a; Tsukamoto et al., 2008b). More recently, groups have shown that autophagy proteins have roles outside of autophagy in oocytes. For example, Beclin-1, a key protein involved in the formation of the autophagosome, is required for cytokinesis. However, the autophagy-activating functions of Beclin-1 are dispensable and unchanged when Beclin-1 activity is blocked (You et al., 2016). Additionally, studies in *Drosophila* oocytes demonstrate that autophagy may be blocked by degradation of autophagy transcripts prior to translation (Rojas-Rios et al., 2015). Autophagy is dispensable later in embryonic development, suggesting the embryo utilizes autophagy to complete the maternal to zygotic transition but can activate alternate stress response mechanisms later in development (Tsukamoto et al., 2008a). These data strongly suggest that oocytes are programmed to inhibit autophagy until fertilization.

Recent research has demonstrated that autophagy has specialized subsets. One of the most well studied of these pathways is mitophagy, the specific targeting and removal of damaged mitochondria by the autophagy pathway. Pten-inducible kinase 1 (Pink1) stabilizes on depolarized mitochondrial membranes (Jin et al., 2010). Pink1 then phosphorylates outer mitochondrial membrane proteins, which recruits the ubiquitin ligase Parkin (Narendra et al., 2010b; Ziviani et al., 2010). Parkin subsequently ubiquitinates proteins on the mitochondria which triggers recruitment of the autophagosome (Narendra et al., 2010a; Tanaka et al., 2010). At this point, the pathway proceeds in the same manner as autophagy (Gegg et al., 2010; Narendra et al., 2010a; Okatsu et al., 2010; Palikaras and Tavernarakis, 2014). Mitophagy is critical in the removal of sperm mitochondria after fertilization. This process is highly conserved across species in order to prevent inheritance of the paternal mitochondrial genome. Mitophagy occurs rapidly after fertilization. In *C. elegans* mitophagy occurs within 15 minutes of fertilization (Al Rawi et al., 2011). In mice, the process occurs more slowly and relies on

multiple mechanisms, not only mitophagy (Cummins et al., 1997; Song et al., 2016). However, no research to date has investigated the role of mitophagy in oocytes.

1.4   Conclusion

The research in this dissertation addresses three unique but interrelated mechanisms by which obesity influences both fertility and offspring health. The chapters will discuss: (1) how oocytes are unable to reverse oocyte damage when mice are allowed to engage in moderate voluntary exercise to improve their physical health; (2) a mechanism for why oocytes cannot repair obesity induced damage to mitochondria; and (3) the effects of maternal obesity and inheritance of damaged mitochondria on the development of cardiovascular disease.

First, exercise has been shown to positively affect an individual. In skeletal muscle, exercise training influences mitochondrial structure and increases mtDNA in order to improve skeletal muscle function (Lira et al., 2013; Yan et al., 2012). The exercise-induced changes in mitochondrial structure impart physiological benefit by improving insulin sensitivity (Bradley et al., 2008; Yan et al., 2012). Additionally, moderate exercise during pregnancy has been shown to be beneficial to offspring from obese mothers by improving insulin sensitivity and decreasing rates of congenital septal defects in the heart (Carter et al., 2012; Carter et al., 2013; Schulkey et al., 2015). However, no research had addressed if these benefits were due to preconception exposure to exercise which improved oocyte quality. Therefore, the first chapter of this dissertation will address the effects of maternal exercise on oocyte quality.

Second, obesity has been shown to damage the mitochondria in oocytes. However, no studies to date have addressed why this damage persists in oocytes. In somatic cells, mitophagy is employed to detect and remove damaged mitochondria (Friedman and Nunnari, 2014).

9

However, a growing body of literature demonstrates that oocytes do not activate autophagy until after fertilization (Rojas-Rios et al., 2015; Tsukamoto et al., 2008b; You et al., 2016). Because mitophagy is a specialized form of autophagy, we test if mitophagy can be activated after supraphysiological mitochondrial damage in the oocytes in the second chapter of this dissertation.

Finally, in line with David Barker's DoHAD hypothesis, offspring from obese mothers are more likely to develop cardiovascular disease (Blackmore et al., 2014; Fernandez-Twinn et al., 2012; Gaillard et al., 2014; Godfrey et al., 2016). Mitochondrial dynamics, the mechanisms which maintain a healthy population of mitochondria in somatic cells, as well as mitophagy, are both important in cardiomyocytes for protecting the heart from the development of cardiovascular disease which can progress to heart failure (Hall et al., 2014). In skeletal muscle, a cell type which relies on mitochondrial metabolism for normal cell function, mitochondrial dynamics are significantly perturbed by maternal obesity (Saben et al., 2016). Based on the evidence that mitochondria are inherited directly from the oocyte without a paternal contribution (Cummins, 2000; Piko and Taylor, 1987; Song et al., 2016; Sutovsky et al., 1999), and that maternal obesity damages this pool of mitochondria (Boots et al., 2016; Boudoures et al., 2016; Igosheva et al., 2010; Jungheim et al., 2010; Luzzo et al., 2012; Wu et al., 2010; Wu et al., 2015), the third chapter of this dissertation presents ongoing research that addresses the effects maternal obesity has on cardiovascular mitochondrial dynamics and metabolism.

Taken together, this research contributes to the understanding of obesity on reproductive health, embryo development, and cardiovascular disease. It deepens our understanding of basic oocyte biology while also demonstrating a mechanism by which obesity imparts heritable traits on offspring.

10

1.5　References

Al Rawi, S., Louvet-Vallee, S., Djeddi, A., Sachse, M., Culetto, E., Hajjar, C., Boyd, L., Legouis, R., Galy, V., 2011. Postfertilization autophagy of sperm organelles prevents paternal mitochondrial DNA transmission. Science (New York, N.Y.) 334, 1144-1147.

Association, A.D., 2010. Diagnosis and classification of diabetes mellitus. Diabetes care 33, S62-S69.

Barker, D.J., 2004. Developmental origins of adult health and disease. Journal of epidemiology and community health 58, 114-115.

Biggers JD, W.D., Dnoahue RP, 1967. The pattern of energy metabolism in the mouse oocyte and zygote. Proceedings of the National Academy of Sciences of the United State of America 58, 560-567.

Binder, N.K., Mitchell, M., Gardner, D.K., 2012. Parental diet-induced obesity leads to retarded early mouse embryo development and altered carbohydrate utilisation by the blastocyst. Reproduction, fertility, and development 24, 804-812.

Blackmore, H.L., Niu, Y., Fernandez-Twinn, D.S., Tarry-Adkins, J.L., Giussani, D.A., Ozanne, S.E., 2014. Maternal diet-induced obesity programs cardiovascular dysfunction in adult male mouse offspring independent of current body weight. Endocrinology 155, 3970-3980.

Boots, C.E., Boudoures, A., Zhang, W., Drury, A., Moley, K.H., 2016. Obesity-induced oocyte mitochondrial defects are partially prevented and rescued by supplementation with co-enzyme Q10 in a mouse model. Human reproduction (Oxford, England) 31, 2090-2097.

Boudoures, A.L., Chi, M., Thompson, A., Zhang, W., Moley, K.H., 2016. The effects of voluntary exercise on oocyte quality in a diet-induced obese murine model. Reproduction (Cambridge, England) 151, 261-270.

Bradley, R.L., Jeon, J.Y., Liu, F.F., Maratos-Flier, E., 2008. Voluntary exercise improves insulin sensitivity and adipose tissue inflammation in diet-induced obese mice. American journal of physiology. Endocrinology and metabolism 295, E586-594.

Cabello, E., Garrido, P., Moran, J., Gonzalez del Rey, C., Llaneza, P., Llaneza-Suarez, D., Alonso, A., Gonzalez, C., 2015. Effects of resveratrol on ovarian response to controlled ovarian hyperstimulation in ob/ob mice. Fertil Steril 103, 570-579.e571.

Carter, L.G., Lewis, K.N., Wilkerson, D.C., Tobia, C.M., Ngo Tenlep, S.Y., Shridas, P., Garcia-Cazarin, M.L., Wolff, G., Andrade, F.H., Charnigo, R.J., Esser, K.A., Egan, J.M., de Cabo, R., Pearson, K.J., 2012. Perinatal exercise improves glucose homeostasis in adult offspring. American journal of physiology. Endocrinology and metabolism 303, E1061-1068.

Carter, L.G., Qi, N.R., De Cabo, R., Pearson, K.J., 2013. Maternal exercise improves insulin sensitivity in mature rat offspring. Medicine and science in sports and exercise 45, 832-840.

Catalano, P.M., Farrell, K., Thomas, A., Huston-Presley, L., Mencin, P., de Mouzon, S.H., Amini, S.B., 2009a. Perinatal risk factors for childhood obesity and metabolic dysregulation. The American journal of clinical nutrition 90, 1303-1313.

Catalano, P.M., Presley, L., Minium, J., Hauguel-de Mouzon, S., 2009b. Fetuses of obese mothers develop insulin resistance in utero. Diabetes care 32, 1076-1080.

Clancy, B., Darlington, R.B., Finlay, B.L., 2001. Translating developmental time across mammalian species. Neuroscience 105, 7-17.

Cummins, J.M., 2000. Fertilization and elimination of the paternal mitochondrial genome. Human reproduction (Oxford, England) 15 Suppl 2, 92-101.

Cummins, J.M., 2004. The role of mitochondria in the establishment of oocyte functional competence. European journal of obstetrics, gynecology, and reproductive biology 115 Suppl 1, S23-29.

Cummins, J.M., Wakayama, T., Yanagimachi, R., 1997. Fate of microinjected sperm components in the mouse oocyte and embryo. Zygote (Cambridge, England) 5, 301-308.

Desmet, K.L., Van Hoeck, V., Gagne, D., Fournier, E., Thakur, A., O'Doherty, A.M., Walsh, C.P., Sirard, M.A., Bols, P.E., Leroy, J.L., 2016. Exposure of bovine oocytes and embryos to elevated non-esterified fatty acid concentrations: integration of epigenetic and transcriptomic signatures in resultant blastocysts. BMC genomics 17, 1004.

Dumollard, R., Carroll, J., Duchen, M.R., Campbell, K., Swann, K., 2009. Mitochondrial function and redox state in mammalian embryos. Seminars in cell & developmental biology 20, 346-353.

Dunning, K.R., Akison, L.K., Russell, D.L., Norman, R.J., Robker, R.L., 2011. Increased beta-oxidation and improved oocyte developmental competence in response to l-carnitine during ovarian in vitro follicle development in mice. Biology of reproduction 85, 548-555.

Fernandez-Twinn, D.S., Blackmore, H.L., Siggens, L., Giussani, D.A., Cross, C.M., Foo, R., Ozanne, S.E., 2012. The programming of cardiac hypertrophy in the offspring by maternal obesity is associated with hyperinsulinemia, AKT, ERK, and mTOR activation. Endocrinology 153, 5961-5971.

Flegal, K.M., Kruszon-Moran, D., Carroll, M.D., Fryar, C.D., Ogden, C.L., 2016. Trends in Obesity Among Adults in the United States, 2005 to 2014. JAMA : the journal of the American Medical Association 315, 2284-2291.

Fowden, A.L., Giussani, D.A., Forhead, A.J., 2005. Endocrine and metabolic programming during intrauterine development. Early human development 81, 723-734.

Friedman, J.R., Nunnari, J., 2014. Mitochondrial form and function. Nature 505, 335-343.

Gaillard, R., Steegers, E.A., Duijts, L., Felix, J.F., Hofman, A., Franco, O.H., Jaddoe, V.W., 2014. Childhood cardiometabolic outcomes of maternal obesity during pregnancy: the Generation R Study. Hypertension (Dallas, Tex. : 1979) 63, 683-691.

Ge, H., Tollner, T.L., Hu, Z., Dai, M., Li, X., Guan, H., Shan, D., Zhang, X., Lv, J., Huang, C., Dong, Q., 2012. The importance of mitochondrial metabolic activity and mitochondrial DNA replication during oocyte maturation in vitro on oocyte quality and subsequent embryo developmental competence. Molecular reproduction and development 79, 392-401.

Gegg, M.E., Cooper, J.M., Chau, K.Y., Rojo, M., Schapira, A.H., Taanman, J.W., 2010. Mitofusin 1 and mitofusin 2 are ubiquitinated in a PINK1/parkin-dependent manner upon induction of mitophagy. Human molecular genetics 19, 4861-4870.

Godfrey, K.M., Reynolds, R.M., Prescott, S.L., Nyirenda, M., Jaddoe, V.W., Eriksson, J.G., Broekman, B.F., 2016. Influence of maternal obesity on the long-term health of offspring. The lancet. Diabetes & endocrinology.

Hall, A.R., Burke, N., Dongworth, R.K., Hausenloy, D.J., 2014. Mitochondrial fusion and fission proteins: novel therapeutic targets for combating cardiovascular disease. British journal of pharmacology 171, 1890-1906.

Hauck, A.K., Bernlohr, D.A., 2016. Oxidative stress and lipotoxicity. Journal of lipid research 57, 1976-1986.

Hou, Y.J., Zhu, C.C., Duan, X., Liu, H.L., Wang, Q., Sun, S.C., 2016. Both diet and gene mutation induced obesity affect oocyte quality in mice. Scientific reports 6, 18858.

Huypens, P., Sass, S., Wu, M., Dyckhoff, D., Tschop, M., Theis, F., Marschall, S., Hrabe de Angelis, M., Beckers, J., 2016. Epigenetic germline inheritance of diet-induced obesity and insulin resistance. Nature genetics 48, 497-499.

Igosheva, N., Abramov, A.Y., Poston, L., Eckert, J.J., Fleming, T.P., Duchen, M.R., McConnell, J., 2010. Maternal diet-induced obesity alters mitochondrial activity and redox status in mouse oocytes and zygotes. PloS one 5, e10074.

Jacobs, L.J., de Wert, G., Geraedts, J.P., de Coo, I.F., Smeets, H.J., 2006. The transmission of OXPHOS disease and methods to prevent this. Human reproduction update 12, 119-136.

Jin, S.M., Lazarou, M., Wang, C., Kane, L.A., Narendra, D.P., Youle, R.J., 2010. Mitochondrial membrane potential regulates PINK1 import and proteolytic destabilization by PARL. The Journal of cell biology 191, 933-942.

Jungheim, E.S., Schoeller, E.L., Marquard, K.L., Louden, E.D., Schaffer, J.E., Moley, K.H., 2010. Diet-induced obesity model: abnormal oocytes and persistent growth abnormalities in the offspring. Endocrinology 151, 4039-4046.

Jungheim, E.S., Schon, S.B., Schulte, M.B., DeUgarte, D.A., Fowler, S.A., Tuuli, M.G., 2013. IVF outcomes in obese donor oocyte recipients: a systematic review and meta-analysis. Human reproduction (Oxford, England) 28, 2720-2727.

Lamb, C.A., Dooley, H.C., Tooze, S.A., 2013. Endocytosis and autophagy: Shared machinery for degradation. BioEssays : news and reviews in molecular, cellular and developmental biology 35, 34-45.

Lira, V.A., Okutsu, M., Zhang, M., Greene, N.P., Laker, R.C., Breen, D.S., Hoehn, K.L., Yan, Z., 2013. Autophagy is required for exercise training-induced skeletal muscle adaptation and improvement of physical performance. FASEB journal : official publication of the Federation of American Societies for Experimental Biology.

Luke, B., Brown, M.B., Stern, J.E., Missmer, S.A., Fujimoto, V.Y., Leach, R., 2011. Female obesity adversely affects assisted reproductive technology (ART) pregnancy and live birth rates. Human reproduction (Oxford, England) 26, 245-252.

Luzzo, K.M., Wang, Q., Purcell, S.H., Chi, M., Jimenez, P.T., Grindler, N., Schedl, T., Moley, K.H., 2012. High fat diet induced developmental defects in the mouse: oocyte meiotic aneuploidy and fetal growth retardation/brain defects. PloS one 7, e49217.

Mann, J.R., McDermott, S.W., Hardin, J., Pan, C., Zhang, Z., 2013. Pre-pregnancy body mass index, weight change during pregnancy, and risk of intellectual disability in children. BJOG: An International Journal of Obstetrics & Gynaecology 120, 309-319.

Marquard, K.L., Stephens, S.M., Jungheim, E.S., Ratts, V.S., Odem, R.R., Lanzendorf, S., Moley, K.H., 2011. Polycystic ovary syndrome and maternal obesity affect oocyte size in in vitro fertilization/intracytoplasmic sperm injection cycles. Fertil Steril 95, 2146-2149, 2149.e2141.

Metwally, M., Cutting, R., Tipton, A., Skull, J., Ledger, W.L., Li, T.C., 2007. Effect of increased body mass index on oocyte and embryo quality in IVF patients. Reproductive biomedicine online 15, 532-538.

Minge, C.E., Bennett, B.D., Norman, R.J., Robker, R.L., 2008. Peroxisome proliferator-activated receptor-gamma agonist rosiglitazone reverses the adverse effects of diet-induced obesity on oocyte quality. Endocrinology 149, 2646-2656.

Narendra, D., Kane, L.A., Hauser, D.N., Fearnley, I.M., Youle, R.J., 2010a. p62/SQSTM1 is required for Parkin-induced mitochondrial clustering but not mitophagy; VDAC1 is dispensable for both. Autophagy 6, 1090-1106.

Narendra, D.P., Jin, S.M., Tanaka, A., Suen, D.F., Gautier, C.A., Shen, J., Cookson, M.R., Youle, R.J., 2010b. PINK1 is selectively stabilized on impaired mitochondria to activate Parkin. PLoS biology 8, e1000298.

Okatsu, K., Saisho, K., Shimanuki, M., Nakada, K., Shitara, H., Sou, Y.S., Kimura, M., Sato, S., Hattori, N., Komatsu, M., Tanaka, K., Matsuda, N., 2010. p62/SQSTM1 cooperates with Parkin for perinuclear clustering of depolarized mitochondria. Genes to cells : devoted to molecular & cellular mechanisms 15, 887-900.

Palikaras, K., Tavernarakis, N., 2014. Mitochondrial homeostasis: The interplay between mitophagy and mitochondrial biogenesis. Experimental gerontology.

Patterson, R.E., Frank, L.L., Kristal, A.R., White, E., 2004. A comprehensive examination of health conditions associated with obesity in older adults. American journal of preventive medicine 27, 385-390.

Piko, L., Taylor, K.D., 1987. Amounts of mitochondrial DNA and abundance of some mitochondrial gene transcripts in early mouse embryos. Developmental biology 123, 364-374.

Poston, L., Caleyachetty, R., Cnattingius, S., Corvalan, C., Uauy, R., Herring, S., Gillman, M.W., 2016. Preconceptional and maternal obesity: epidemiology and health consequences. The lancet. Diabetes & endocrinology 4, 1025-1036.

Pulgaron, E.R., Delamater, A.M., 2014. Obesity and type 2 diabetes in children: epidemiology and treatment. Current diabetes reports 14, 508.

Ramalho-Santos, J., Varum, S., Amaral, S., Mota, P.C., Sousa, A.P., Amaral, A., 2009. Mitochondrial functionality in reproduction: from gonads and gametes to embryos and embryonic stem cells. Human reproduction update 15, 553-572.

Reynier, P., May-Panloup, P., Chretien, M.F., Morgan, C.J., Jean, M., Savagner, F., Barriere, P., Malthiery, Y., 2001. Mitochondrial DNA content affects the fertilizability of human oocytes. Molecular human reproduction 7, 425-429.

Reynolds, K.A., Boudoures, A.L., Chi, M.M., Wang, Q., Moley, K.H., 2015. Adverse effects of obesity and/or high-fat diet on oocyte quality and metabolism are not reversible with resumption of regular diet in mice. Reproduction, fertility, and development.

Rojas-Rios, P., Chartier, A., Pierson, S., Severac, D., Dantec, C., Busseau, I., Simonelig, M., 2015. Translational Control of Autophagy by Orb in the Drosophila Germline. Developmental cell 35, 622-631.

Santos, T.A., El Shourbagy, S., St John, J.C., 2006. Mitochondrial content reflects oocyte variability and fertilization outcome. Fertil Steril 85, 584-591.

Sasson, I.E., Vitins, A.P., Mainigi, M.A., Moley, K.H., Simmons, R.A., 2015. Pre-gestational vs gestational exposure to maternal obesity differentially programs the offspring in mice. Diabetologia 58, 615-624.

Schulkey, C.E., Regmi, S.D., Magnan, R.A., Danzo, M.T., Luther, H., Hutchinson, A.K., Panzer, A.A., Grady, M.M., Wilson, D.B., Jay, P.Y., 2015. The maternal-age-associated risk of congenital heart disease is modifiable. Nature 520, 230-233.

Song, W.H., Yi, Y.J., Sutovsky, M., Meyers, S., Sutovsky, P., 2016. Autophagy and ubiquitin-proteasome system contribute to sperm mitophagy after mammalian fertilization. Proceedings of the National Academy of Sciences of the United States of America.

Stolz, A., Ernst, A., Dikic, I., 2014. Cargo recognition and trafficking in selective autophagy. Nature cell biology 16, 495-501.

Stothard, K.J., Tennant, P.W., Bell, R., Rankin, J., 2009. Maternal overweight and obesity and the risk of congenital anomalies: a systematic review and meta-analysis. JAMA : the journal of the American Medical Association 301, 636-650.

Sutovsky, P., Moreno, R.D., Ramalho-Santos, J., Dominko, T., Simerly, C., Schatten, G., 1999. Ubiquitin tag for sperm mitochondria. Nature 402, 371-372.

Tanaka, A., Cleland, M.M., Xu, S., Narendra, D.P., Suen, D.F., Karbowski, M., Youle, R.J., 2010. Proteasome and p97 mediate mitophagy and degradation of mitofusins induced by Parkin. The Journal of cell biology 191, 1367-1380.

Thouas, G.A., Trounson, A.O., Wolvetang, E.J., Jones, G.M., 2004. Mitochondrial dysfunction in mouse oocytes results in preimplantation embryo arrest in vitro. Biology of reproduction 71, 1936-1942.

Tsukamoto, S., Kuma, A., Mizushima, N., 2008a. The role of autophagy during the oocyte-to-embryo transition. Autophagy 4, 1076-1078.

Tsukamoto, S., Kuma, A., Murakami, M., Kishi, C., Yamamoto, A., Mizushima, N., 2008b. Autophagy is essential for preimplantation development of mouse embryos. Science (New York, N.Y.) 321, 117-120.

Van Hoeck, V., Sturmey, R.G., Bermejo-Alvarez, P., Rizos, D., Gutierrez-Adan, A., Leese, H.J., Bols, P.E., Leroy, J.L., 2011. Elevated non-esterified fatty acid concentrations during bovine oocyte maturation compromise early embryo physiology. PloS one 6, e23183.

Wakefield, S.L., Lane, M., Mitchell, M., 2011. Impaired mitochondrial function in the preimplantation embryo perturbs fetal and placental development in the mouse. Biology of reproduction 84, 572-580.

Wittemer, C., Ohl, J., Bailly, M., Bettahar-Lebugle, K., Nisand, I., 2000. Does body mass index of infertile women have an impact on IVF procedure and outcome? Journal of assisted reproduction and genetics 17, 547-552.

Wu, L.L., Dunning, K.R., Yang, X., Russell, D.L., Lane, M., Norman, R.J., Robker, R.L., 2010. High-fat diet causes lipotoxicity responses in cumulus-oocyte complexes and decreased fertilization rates. Endocrinology 151, 5438-5445.

Wu, L.L., Russell, D.L., Norman, R.J., Robker, R.L., 2012. Endoplasmic reticulum (ER) stress in cumulus-oocyte complexes impairs pentraxin-3 secretion, mitochondrial membrane potential (DeltaPsi m), and embryo development. Molecular endocrinology (Baltimore, Md.) 26, 562-573.

Wu, L.L., Russell, D.L., Wong, S.L., Chen, M., Tsai, T.S., St John, J.C., Norman, R.J., Febbraio, M.A., Carroll, J., Robker, R.L., 2015. Mitochondrial dysfunction in oocytes of obese mothers: transmission to offspring and reversal by pharmacological endoplasmic reticulum stress inhibitors. Development (Cambridge, England) 142, 681-691.

Yan, Z., Lira, V.A., Greene, N.P., 2012. Exercise training-induced regulation of mitochondrial quality. Exercise and sport sciences reviews 40, 159-164.

You, S.Y., Park, Y.S., Jeon, H.J., Cho, D.H., Jeon, H.B., Kim, S.H., Chang, J.W., Kim, J.S., Oh, J.S., 2016. Beclin-1 knockdown shows abscission failure but not autophagy defect during oocyte meiotic maturation. Cell cycle (Georgetown, Tex.) 15, 1611-1619.

Ziviani, E., Tao, R.N., Whitworth, A.J., 2010. Drosophila parkin requires PINK1 for mitochondrial translocation and ubiquitinates mitofusin. Proceedings of the National Academy of Sciences of the United States of America 107, 5018-5023.

Chapter 2: The Effects of Voluntary Exercise on Oocyte Quality in a Diet-Induced Obese Murine Model

Anna L Boudoures, Maggie Chi, Alysha Thompson, Wendy Zhang and Kelle H Moley

Department of Obstetrics and Gynecology, Center for Reproductive Health Sciences,

Washington University in St. Louis School of Medicine, St. Louis, MO 63110 USA

2.1   Abstract

Obesity negatively affects many aspects of the human body, including reproductive function. In females, the root of the decline in fertility is linked to problems in the oocyte. Problems seen in oocytes that positively correlate with increasing BMI include changes to the metabolism, lipid accumulation, meiosis, and metaphase II (MII) spindle structure. Studies in mice indicate dietary interventions fail to reverse these problems. How exercise affects the oocytes has not been addressed. Therefore, we hypothesized an exercise intervention would improve oocyte quality. Here we show in a mouse model of an exercise intervention can improve lipid metabolism in germinal vesicle (GV) stage oocytes. Oocytes significantly increased activity and transcription of the β-oxidation enzyme Hadha (Hydroxyacyl-CoA-dehydrogenase) in response to exercise training only if the mice had been fed a high fat diet (HFD). An exercise intervention also reversed the lipid accumulation seen in GV stage oocytes of HFD females. However, delays in meiosis and disorganized MII spindles remained present. Therefore, exercise is able to improve, but not reverse, damage imparted on oocytes as a result of a high fat diet and obesity. By utilizing an exercise intervention on a HFD, we determined only lipid content and lipid metabolism is changed in GV oocytes. Moving forward, interventions to improve oocyte quality may need to be more targeted to the oocyte specifically. Because of the HFD induced deficiency in β-oxidation, dietary supplementation with substrates to improve lipid utilization may be more beneficial.

2.2   Introduction

Approximately 25% of individuals in the western world are obese, and the worldwide prevalence of obesity is predicted to continue increasing (Kelly et al., 2008). Obesity predisposes individuals to many diseases including type 2 diabetes, cardiovascular disease, and stroke (Swift et al., 2014). In addition to impairing overall health, obesity has been linked to subfertility (Bellver et al., 2010). This subfertility can likely be traced to the oocyte, as studies of oocytes obtained from women undergoing *in vitro* fertilization demonstrated that oocytes from obese women are often apoptotic and meiotically delayed (Metwally et al., 2007; Wittemer et al., 2000).

To better understand the mechanisms causing decreased oocyte quality, many labs have modeled diet induced obesity in mice by feeding a high fat diet (HFD). These studies have shown that HFD affects oocyte meiotic maturation, ovulation, and fertilization and leads to embryos with restricted growth and brain abnormalities (Luzzo et al., 2012; Minge et al., 2008) (Jungheim et al., 2010). Additionally, when blastocysts or two-cell embryos fertilized in HFD mice were transferred to control recipients, the resulting fetuses still had restricted growth and brain abnormalities, confirming that the defects arose from the oocytes and not the uterine environment (Sasson et al., 2014). Several papers have detailed the negative effects of HFD on oocyte quality in mice. After exposure to a high-fat diet for only four weeks, oocytes of HFD mice show increased lipid accumulation, lipotoxicity, and endoplasmic reticulum stress (Wu et al., 2010). Additionally, compared to controls, HFD mice ovulate a significantly higher proportion of oocytes with disorganized meiosis II spindles (Luzzo et al., 2012). Finally, HFD oocytes have a significant increase in mitochondrial damage, including the appearance of large vacuoles and ruptured membranes, and a significant decrease in citrate production, suggesting defects in citric acid cycle metabolism (Luzzo et al., 2012).

20

Previously, our lab attempted to ameliorate HFD-induced oocyte damage by returning the mice to a control diet. Although overall physiology improved, including weight loss and return to normal glucose tolerance, the benefits were not paralleled in the oocytes (Reynolds et al., 2014). In humans, exercise confers many physiological benefits, including decreased risk of developing cardiovascular disease, type 2 diabetes, and stroke, even in the absence of weight loss (Swift et al., 2014). Additionally, several rodent studies revealed that offspring of exercised dams were significantly healthier than offspring of sedentary dams (Bradley et al., 2008; Carter et al., 2013; Vega et al., 2013; Wagener et al., 2012). Finally, HFD female rats that were allowed to exercise had significant fertility improvements despite the lack of other physiological improvements (Vega et al., 2013).

Because the reproductive consequences of obesity are likely rooted at the oocyte level, and exercise is beneficial to both mother and offspring, we hypothesized that even without at change in diet, the physiological benefits of exercise would be reflected in oocytes. To test this hypothesis, we allowed HFD females to voluntarily exercise for six weeks and compared their oocytes to those of sedentary HFD mice and exercised and sedentary mice on a control diet. We assayed oocytes for changes in lipid accumulation, mitochondrial damage, and hydroxyacyl Co-A dehydrogenase activity (a fatty acid oxidation enzyme) and recorded the percentage of oocytes ovulated either prior to meiosis II arrest or with deformed spindles. Our data revealed that exercise was able to improve, but not entirely reverse, the negative effects of HFD on oocytes.

21

2.3   Materials and Methods

Animals and Diet

This study was carried out in strict accordance with the recommendations in the Guide

for the Care and Use of Laboratory Animals of the National Institutes of Health. The protocol

was approved by the IACUC-accredited Animal Studies Committee of Washington University

School of Medicine (Study #20120051). Female C57Bl/6J mice (Jackson Laboratories, Bar

Harbor, ME) were fed either a high-fat diet (HFD; Test Diet 58R3, 58% fat energy) or a standard

mouse chow diet (CD; Lab Diet 5053, 13% fat energy) *ad libitum* from four weeks of age.

Exercise Exposure

For the first six weeks of the study (age 4 weeks to 10 weeks), mice were housed four per

cage (feeding period). Mice were then moved to standard rat cages and housed eight mice per

cage either with or without *ad libitum* exposure to exercise wheels (exercise exposure period) for

six weeks. Mice remained on their respective HFD or CD during this period.

Body Composition Analysis

No more than 12 hours before sacrifice, eight mice from each experimental group were

subjected to body composition analysis to determine absolute fat and lean tissue mass by

magnetic resonance imaging (EchoMRI 3-in-1, Echo Medical Systems, Houston, TX). Two or

three measurements were taken per mouse to ensure instrument precision, and values for

individual mice were averaged for statistical analyses.

Glucose Tolerance Test

Eight to nine mice per experimental group were fasted for 12 hours and then administered

an intraperitoneal (IP) injection of glucose (2 mg/g body weight) with a 30 x ½ gauge needle.

Blood glucose was monitored by readings of a small (2-3 µl) drop of tail vein blood with a One

Touch Ultra Glucose Monitoring glucometer and test strips (Johnson and Johnson, New

Brunswick, NJ) at 15, 30, 60, 90, and 120 min after injection. Mice were then returned to their respective diets.

Serum Triglyceride, Glucose and Insulin Levels

Eight mice in each experimental group were fasted for four hours before blood was collected by puncturing the facial vein with a 25 x 5/8 gauge needle. Approximately 50 µL of blood was collected in BD Microtainer Serum Separator Tubes (Franklin Lakes, NJ). At the same time as facial vein bleed, fasting blood glucose was measured by readings of a small (2-3 µl) drop of tail vein blood with a One Touch Ultra Glucose Monitoring glucometer and test strips (Johnson and Johnson). After blood collection, mice were returned to their respective diets. Tubes were incubated for 30 min at room temperature (RT) and spun at 12,000 rpm for 10 min at RT. Serum was collected on ice and stored at -20°C until analysis. The Infinity Triglycerides Liquid Stable Reagent Kit (Thermo Scientific, Waltham, MA) was used according to the manufacturer's protocol to measure triglycerides. The Ultra Sensitive Mouse Insulin ELISA kit (Crystal Chem, Downers Grove, IL) was used according to the manufacturer's protocol to measure serum insulin levels. Each serum sample was tested in duplicate for precision, and values were averaged prior to statistical analysis.

The Homeostatic Model Assesment (HOMA1-IR) is a validated measure of insulin resistance that is calculated using the values listed in Table 1 using the following formula:

$HOMA1 - IR = \frac{(FSI \times FSG)}{22.5}$, where FSI is fasting serum insulin in mU/L and FSG is fasting serum glucose in mmol/l (Matthews et al., 1985).

BODIPY Staining of Germinal Vesicle (GV) Stage Oocytes

Three mice from each experimental condition were administered an IP injection of 10 IU PMSG 46-48 hours prior to sacrifice. Ovaries were removed and placed in M2 media + 4 mM hypoxanthine (Sigma-Aldrich, St. Louis, MO). Large antral follicles were punctured with a 29 x

23

½ gauge needle, and cumulus cells were removed by multiple passes through a glass pipette.

Oocytes were then fixed in 4% paraformaldehyde (Sigma-Aldrich) diluted in PBS +1%

Polyvinylpyrrolidone (PVP; Sigma-Aldrich), washed twice, and transferred to a 1 µg/ml solution

of 4,4-difluoro-4-bora-3a,4a-diaza-s-indacene 493/503 (BODIPY; Invitrogen, Carlsbad, CA)

+1% PVP for 1 hr at room temperature in the dark. After two washes in PBS + 1% PVP, oocytes

were mounted in VectaShield (Vector Labs, Burlingame, CA) and visualized by using an

Olympus Laser scanning confocal microscope at 20X magnification. All images were taken as a

single optical section through the plane containing the germinal vesicle at the same laser power

and gain settings and adjusted by using the same gain and contrast adjustments in Adobe

Photoshop CS6. For analysis, the mean gray value of pixels in an individual oocyte was

measured in a minimum of 25 oocytes per group.

Transmission Electron Microscopy

Denuded GV stage oocytes from three mice per experimental group were collected as

described for BODIPY staining and fixed in 2% paraformaldehyde plus 2.5% glutaraldehyde

(Polysciences) in 100 mM cacodylate buffer (Sigma-Aldrich), pH 7-7.2, for 1 hr at RT. Oocytes

were embedded in 2% agarose and washed 3 x 30 min in 100 mM cacodylate buffer at RT.

Agarose-embedded oocytes were then fixed in 1% OsO_4 (Electron Microscopy Sciences,

Hartfield, PA) in 100 mM cacodylate buffer for 1 hr at RT. Oocytes were washed thoroughly in

distilled water, stained in 1% uranyl acetate in dH_2O for 1 hr at RT, dehydrated in a series of

ethanol washes, and then washed in 100% ethanol at RT. Next, oocytes were washed twice in

propylene oxide (Electron Microscopy Science) and then infiltrated with resin by using the

Eponate 12 Kit (Ted Pella, Redding, CA). After infiltration, blocks were embedded, cured, and

then sectioned with a Leica Ultracut UCT ultramicrotome (Leica Microsystems Inc.,

Bannockburn, IL). Sections (90 nm) were stained with uranyl acetate and Reynolds' lead citrate

before viewing at 2,000x - 15,000x magnification with a JEOL 1200 EX transmission electron microscope (JEOL USA Inc., Peabody, MA) equipped with an AMT 8-megapixel digital camera (Advanced Microscopy Techniques, Woburn, MA). Images taken at 15,000x magnification were blinded and analyzed by three independent observers for mitochondrial shape, the number of lipid droplets in each image, and the number of rose petal mitochondria in each image.

Hydroxyacyl-coenzyme A dehydrogenase, type II (HADHA) Enzymatic Activity
Denuded GV stage oocytes were collected from three mice per group as described for BODIPY staining. Individual oocytes were frozen on glass slides in isopentane equilibrated with liquid nitrogen and freeze-dried overnight under vacuum at -35°C. 15 individual oocytes were extracted under nanoliter volume and used for analysis of levels of HADHA activity by enzyme-linked cycling assays as previously described (Chi et al., 2002).

Quantitative Real-Time PCR
Three GV oocytes per mouse were collected from six mice per experimental group as described for BODIPY staining. Oocytes were denuded and washed in 50 mg/mL nuclease-free bovine serum albumin (BSA; Invitrogen) on ice. Oocytes were then transferred to the Single Cell Lysis Solution with Single Cell DNase I solution (both parts of the Single Cell-To-Ct Kit [Ambion, Austin, TX]). All steps of RNA isolation and reverse transcription followed the manufacturer's protocol. Real-time PCR reactions were carried out on a 7500 Fast Real-Time PCR system. Expression of *Cpt2, Hadh*, *Aco2, Idh3b* and *Actb* were measured by using the inventoried TaqMan Gene Expression assays (Cpt2: Mm00487205_m1, Hadh: Mm00492535_m1, Actb: Mm00607939_s1, Life Technologies, Carlsbad, CA). Expression of genes for each diet were normalized to *Actb* based on its utilization in prior publications as a reference gene in oocytes and the because its expression remains stable throughout meiosis (Bachvarova et al., 1985).

Spindle and Chromosome Imaging of Metaphase II Stage Oocytes

Four to five mice from each of the four experimental conditions were IP injected with 10

IU of pregnant mare serum gonadotropin (PMSG; Sigma-Aldrich) and then with 5 IU of human

chronic gonadotropin (hCG; Sigma-Aldrich) 48 hours after PMSG. Mice were sacrificed by

cervical dislocation 12-14 hours after hCG administration, and the cumulus-oocyte complexes

were collected from the ampullae. Cumulus cells were removed with a brief wash in 1 mg/ml of

hyaluronidase in M2 media (Sigma-Aldrich). Oocytes were then fixed for 30 min in 4%

paraformaldehyde in PBS + 1% BSA (Sigma-Aldrich). Oocytes were transferred to a

permeabilization solution (0.5% Triton X-100 in PBS) for 20 min and then blocked with PBS +

0.1% Tween-20 + 0.01% Triton X-100 + 1% BSA for 1 hr. Oocytes were stained with FITC-

conjugated anti-tubulin antibody (1:500; Sigma-Aldrich) overnight at 4°C, washed three times,

and then co-stained with TOPRO-3 iodide (1:500; Invitrogen) for 10 min. Oocytes were washed

twice in PBS + 0.1% Tween-20 + 0.01% Triton X-100, mounted in VectaShield, and visualized

by using an Olympus Laser scanning confocal microscope at 20X magnification. Images were

blinded and analyzed by three independent observers for meiotic stage (metaphase II vs.

prophase or anaphase), spindle shape (normal, barrel shaped vs. deformed) and apoptosis.

2.4   Results

Exercise training improves some aspects of whole-body physiology

Previously, our lab and others have shown that mice maintained on a high-fat diet (HFD)

became obese and had damaged oocytes. To determine whether exposure to voluntary exercise

could reverse any of the defects, we exposed mice to either HFD or control chow diet (CD) for

12 weeks beginning at 4 weeks of age. During the last six weeks, half of each diet cohort had

access to an exercise wheel 24 hours a day, based on the experimental design of Schulkey et al. (exercise exposure period). Mice were filmed for a 24h period to confirm frequent use of wheels (data not shown). We found that HFD exposure caused significant weight gain that was not reversible by exercise (n=32/group, Figure 2-1A). However, compared to their sedentary counterparts of the same age, the cohort of HFD exercising mice had significantly less fat mass and unchanged lean mass (n=8 per group, Figure 2-1B-C). This significant change in fat mass was likely not reflected in total body mass because of the differences in sample size. HFD mice had significantly higher insulin resistance as measured by the homeostatic assessment of insulin resistance (HOMA-IR), which was not reversed by exercise (Figure 2-1D). Additionally, the range of insulin sensitivity was much greater in HFD mice than CD mice. Allowing mice to exercise while maintaining a HFD was able to cause a trend towards a restoration of glucose tolerance, especially at earlier time points (see 15-minute time point in Figure 2-1E). Exercise was able to significantly decrease triglyceride levels in HFD females, but triglyceride levels were still higher than in CD mice; exercise did not significantly change triglyceride levels in CD mice (Figure 2-1F). Therefore, our results confirm previously published findings that exercise alone cannot improve body weight, but some physiological parameters are improved by exercise (Carter et al., 2013; Kelly et al., 2011; Stanford et al., 2014; Vega et al., 2013).

Changes in Oocyte Lipid Accumulation

Human obesity causes an increased accumulation of triglycerides in the follicular fluid surrounding the oocyte in a maturing ovarian follicle, and mouse oocytes exposed to this lipid-rich environment also contain excess lipids (Dunning et al., 2014a; Dunning et al., 2014b; Jungheim et al., 2011; Valckx et al., 2014a; Valckx et al., 2014b; Yang et al., 2012). Thus, given that exercising HFD mice had lower serum triglycerides than their sedentary peers, we

27

hypothesized that these mice would also have decreased lipid accumulation in their maturing

oocytes. To test this, oocytes were collected from superovulated females at the germinal vesicle

(GV) stage, stained with the fluorescent neutral lipid dye BODIPY 493/503, and imaged by

confocal microscopy (Figure 2-2A). Measurements of the mean gray value of the fluorescence of

individual oocytes revealed that, as expected, oocytes from sedentary HFD females contained

more lipid than oocytes from CD females. However, oocytes from exercised HFD females

contained the same amount of lipid as those from sedentary CD females. Surprisingly, oocytes

from exercised CD mice contained the most lipid of any of the groups (Figure 2-2A-B).

We also examined lipid accumulation by counting lipid droplets in transmission electron

microscopy (TEM) images of GV oocytes. Consistent with the BODIPY results, oocytes from

sedentary HFD females contained more lipid droplets than those from exercised HFD mice or

either of the CD groups (Figure 2-2C-D). From these data, we conclude that exercise is able to

reverse the lipid accumulation phenotype induced by exposure to HFD.

Oocyte metabolism is affected by changes in diet and exercise

Oocytes rely heavily on carbohydrates supplied by cumulus cells to generate ATP and

fuel maturation and fertilization (Rieger D, 1994). In addition, maturing oocytes metabolize

lipids by the fatty acid oxidation pathway within the mitochondria (Dunning et al., 2014b;

Dunning et al., 2010). Thus, the significant increase of lipids in the GV oocytes of sedentary

HFD females led us to ask whether these oocytes have changes in their mitochondrial

metabolism. First, the significant changes in lipid accumulation after exercise exposure led us to

hypothesize there may be changes to fatty acid metabolism. To test this, we used enzymatic

cycling to measure activity of Hydroxyacyl-CoA dehydrogenase (HADHA) in individual GV

stage oocytes. HADHA is a key enzymatic subunit of the mitochondrial trifunctional protein,

which catalyzes three steps of fatty acid beta oxidation (Houten and Wanders, 2010). We found that oocytes from both cohorts of HFD females had significantly lower HADHA activity than oocytes from both cohorts of CD females. Although exercise was not able to increase the level of HADHA activity in HFD oocytes to the levels observed in CD oocytes, oocytes from exercised HFD and CD mice had significantly higher HADHA activity than those of their sedentary counterparts (Figure 2-3A).

To determine if this activity change was reflected in ATP production, we next measured ATP content of individual GV oocytes using enzymatic cycling assays. However, we observed significantly lower ATP only in HFD exercising mice (Figure 2-3B). Lower ATP levels contradicts the positive effects of exercise on *Hadha* activity. Fatty acid oxidation produces 14 molecules of ATP for every 2 carbons in a carbon chain (e.g. 104 molecules of ATP for a single molecule of palmitate). Given the efficiency of this reaction, increased *Hadha* activity would be expected to increase ATP (Garrett, 2013). To decide if the contradiction of *Hadha* activity and ATP production could be explained by changes to other metabolic pathways, we measured citrate levels in oocytes (Figure 2-3C). Citrate was significantly higher only in oocytes from HFD sedentary females. These results are both surprising and conflicting to both the activity of *Hadha* and ATP levels of oocytes.

Although the data are conflicting, these data agree with transcript abundance of TCA cycle enzymes and Hadha; HFD sedentary mice have significantly higher levels Isocitrate Dehydrogenase 3 (Idh3b) and levels of aconitase (Aco2) are increased, but the results did not reach statistical significance (p=0.15), two enzymes involved in the TCA cycle (Figure 2-3D). This is likely due to increased citrate abundance. Similarly, the transcript abundance of fatty acid oxidation enzyme Hydroxyacyl CoA dehydrogenase is significantly decreased only in HFD

sedentary oocytes. This is reflected in the significant decrease in Hadha activity and lipid droplet accumulation also observed in HFD sedentary oocytes (Figure 2-3A and Figure 2-2, respectively).

Mitochondrial ultrastructure is changed by exercise exposure

Because metabolite and qPCR data indicated changes to mitochondrial pathways, but could not fully explain the changes to lipid accumulation observed in oocytes form HFD sedentary and exercise mice, we wondered whether mitochondrial damage previously reported persisted or was changed by exercise (Luzzo et al., 2012; Wu et al., 2010). To address this question, we used TEM to examine mitochondrial ultrastructure in GV stage oocytes. Whereas oocyte mitochondria are normally round, the appearance of elliptical and dumbbell-shaped mitochondria suggests the occurrence of fission and fusion (Friedman and Nunnari, 2014). We found that oocytes from sedentary HFD females had a higher proportion of elliptical and dumbbell-shaped mitochondria than did oocytes from exercising HFD mice or CD mice (Figure 2-4A-B).

Another morphological measure of mitochondrial health is the appearance of so-called "rose petal" mitochondria (see examples in Figure 2-4C). These occur when there are deficiencies in oligomerization of the F_1F_0-ATP synthase in the mitochondrial inner membrane (Arselin et al., 2003). To assess presence of rose petal mitochondria in the four cohorts of mice, we collected GV oocytes from three mice from each group and subjected them to TEM. Images were coded and scored by three independent blinded observers. We found that oocytes from sedentary HFD mice had significantly more rose petal mitochondria than did oocytes from CD mice. However, oocytes from exercised HFD mice had similar numbers of rose petal

mitochondria as CD mice (Figure 2-4D). These results suggest that oocyte mitochondrial damage that occurs as a result of HFD exposure can be compensate for by exercise.

MII spindle structure is unchanged by exercise

Exposure to a high-fat diet causes multiple abnormalities in oocytes, including disorganized spindle structure in the metaphase II (MII) oocyte, aberrant segregation of chromosomes, and delayed meiotic maturation (Luzzo et al., 2012). Lipid accumulation was also linked to delayed oocyte maturation and increased apoptosis at the MII stage (Wu et al., 2010). Consistent with these reports, we observed a greater proportion of delayed oocytes in HFD mice than in CD mice (CDS = 15%, CDE = 7% vs. HFDS = 38%, HFDE = 32%; Figure 2-5). However, the proportion of normal, meiotically mature oocytes from exercised HFD mice did not differ greatly from those of sedentary HFD mice (HFDE = 40%, HFDS = 32%; Figure 2-5).

2.5   Discussion

Here, we report that exercise brought about moderate change to female physiology and a significant decrease in lipid accumulation in the oocytes of HFD females. This may be due, in part, to increased activity of the fatty acid oxidation enzyme HADHA. However, these positive changes did not negate the effects of HFD on spindle morphology and meiotic maturation at ovulation.

We found that, in female mice, voluntary exercise resulted in moderate physiological benefits and no significant total body weight loss. This is not surprising for three reasons. First, in a study of mice that were forced to exercise, female mice had a much smaller decrease in total body mass and fat mass than their male counterparts (Kelly et al., 2010). Second, the mice in our

31

study voluntarily exercised, likely at lower levels than those in the forced-exercise study. Although we did not control for the exact amounts of exercise each female received, our experimental design was based off of a study that showed moderate voluntary exercise in HFD females was beneficial in the reversal of congenital heart disease in their offspring (Schulkey et al., 2015). Finally, a weak relationship between exercise and weight loss has also been reported in humans (Swift et al., 2014).

Although body weight was largely unchanged by exposure to exercise, the lipid content of oocytes from HFD females was decreased, as shown by both our BODIPY and EM data. Although we saw more lipid in the oocytes of exercising CD mice than in their sedentary counterparts, our contrasting EM data suggest that this was due to experimental error. Oocytes were used from three mice and pooled prior to staining, thus contribution from any one mouse is not possible to determine. Our data are consistent with previous findings that lipid accumulates in oocytes in the presence of increased substrate availability both *in vivo* (Luzzo et al., 2012; Wu et al., 2010) and *in vitro* (Jungheim et al., 2011), but the mechanism of lipid uptake by oocytes is still under investigation.

The exercise-induced reductions in lipid content of oocytes we observed in HFD mice might, in part, be explained by the significant decrease in circulating serum triglycerides in the mice. Previous research in both mice and humans has shown that serum levels of triglycerides correlate with triglyceride levels in both the ovarian follicle and the oocyte (Wu et al., 2012; Yang et al., 2012).

The accumulation of lipids within oocytes of HFD females and the reductions we recorded after exercise exposure may also be partially explained by changes to expression of TCA cycle enzymes and fatty acid beta-oxidation. We found that the transcript abundance and activity level

of the fatty acid beta-oxidation enzyme HADHA was lower in oocytes of sedentary HFD mice than in all other groups of mice. Additionally, HFD sedentary mice had at significant increase in TCA cycle enzyme isocitrate dehydrogenase, and transcript levels of aconitase were increased, but the difference was not statistically significant. However, exercise exposure significantly increased HADHA activity and decreased isocitrate dehydrogenase gene expression changes in oocytes from both the HFD mice. One explanation for the increase in TCA cycle gene expression and decrease fatty acid oxidation gene expression genes is that there is chronic utilization of the TCA cycle due to the high glucose levels in the blood. In a study of patients with non-alcoholic fatty liver disease, investigators showed that there is a chronic utilization of the TCA cycle due to increased blood glucose, which results in no utilization of lipid and causes the trigylcerides to accumulate in hepatocytes (Sunny et al., 2011). Our qPCR, metabolite and, HADHA activity assays, in combination with the rescue of the HFD sedentary increase lipid, suggests a similar mechanism could be occurring in the oocytes. However, further functional assays not conducted here must be conducted to confirm this.

This finding is in agreement with previous demonstrations that exercise increases fatty acid oxidation in mitochondria of other tissue types (Houten and Wanders, 2010). Additionally, mitochondrial biogenesis is stimulated in the skeletal muscle of exercised animals (Russell et al., 2014), but we have not explored that possibility here.

Fatty acid beta-oxidation is necessary for proper oocyte maturation and ovulation and embryo development (Dunning et al., 2010). For example, inhibition of beta-oxidation in cumulus-enclosed oocytes prevents the oocytes from eliciting the appropriate hormone-induced meiotic activation and maturation *in vitro* (Valsangkar and Downs, 2013). Additionally, defects in beta-oxidation cause fertility defects in mice and humans (Dunning et al., 2014a). Finally,

enhancing fatty acid oxidation by exposure of oocytes to L-carnitine improves the blastocyst development rate after fertilization (Paczkowski et al., 2014). Thus, an important question for the future is whether or not the increase in fatty acid oxidation activity induced by exercise can improve fertility.

The increased HADHA activity correlated with improvements to two aspects of mitochondrial ultrastructure: fewer rose-petal mitochondria and fewer elliptical mitochondria. In oocytes, mitochondrial ultrastructure is generally round with cristae that wrap the periphery (Sathananthan and Trounson, 2000). In other tissue types, particularly skeletal muscle, both exercise training and insulin resistance cause changes to mitochondrial ultrastructure and activity (Russell et al., 2014; Yan et al., 2012). Here, our data indicate that exercise may be able to induce changes to mitochondrial morphology independent of insulin resistance. HOMA-IR was unaffected by moderate exercise, yet exercise reduced the prevalence of abnormal elliptical shaped mitochondria by EM analysis. A direct relationship between glucose tolerance, insulin resistance, and mitochondrial shape was not addressed here. Still, previous research suggests impaired glucose tolerance and insulin responsiveness can affect mitochondrial morphology (Luzzo et al., 2012; Wang et al., 2012; Wang et al., 2009). While the mechanism underlying the changes in mitochondrial morphology remains to be determined, we demonstrate here exercise is clearly beneficial and may be able to override the previously observed negative effects of insulin resistance on oocyte mitochondria morphology (Wang et al., 2009).

Despite the benefits of moderate exercise on lipid accumulation and mitochondrial structure in the oocytes of HFD mice, exercise did not change the proportion of oocytes ovulated with deformed spindles. One possibility is that glucose tolerance is not completely normalized by exercise and insulin resistance is unchanged by exercise. Glucose intolerance due to insulin

34

resistance could lead to decreased glucose uptake within the cumulus oocyte complexes (COC) during maturation. Previously, it has been shown glucose uptake by COCs is an insulin stimulated response, meaning it is less sensitive in situations in cases of insulin resistance and decreased glucose tolerance (Purcell et al., 2012). Additionally, insulin resistance and glucose intolerance in mice attenuates insulin-stimulated glucose uptake in oocytes (Wang et al., 2012). Importantly, the decreased glucose uptake correlated with deformed spindles. Therefore, a possible explanation for unchanged spindle morphology is persistent impaired glucose tolerance and insulin resistance in HFD mice after exercise exposure.

In conclusion, we showed that exercise was able to improve some aspects of oocyte quality in HFD-exposed mice. Whether these improvements to oocyte quality are beneficial to fertility remains to be investigated. Likewise, it will be important to determine whether exercise can improve oocyte quality in obese women who are attempting to conceive.

2.6   Figure Legends

Figure 2-1: Body weights and body composition and metabolic parameters of mice. A) Average body weights; B) Fat Mass and C) Lean Mass as measured by magnetic resonance imaging. D) Homeostatic Model Assessment Indexes (HOMA1-IR) calculated as described in *Materials and Methods*. E) Glucose Tolerance Test, F) Fasting serum triglycerides different letters designate statistical significance, same letter indicates no significance between groups, $p < 0.05$. . In A-D and F) different letters designate statistical significance between groups whereas same letter indicates no significance between groups, $p < 0.05$. In E) letters above each time point represent statistical significance between groups at that time as follows; a) CD Exercise vs HFD exercise, b) CD Exercise vs HFD Sedentary, c) CD Sedentary vs. HFD Exercise, d) CD Sedentary vs. HFD Sedentary, e) HFD Exercise vs. HFD Sedentary, $P<0.05$. All Data was analyzed by two-way ANOVA with Tukey-Kramer correction for multiple comparisons. CD: Control Diet, HFD: High Fat Diet.

Figure 2-2: Lipid droplet accumulation in germinal vesicle stage oocytes in response to diet and exercise training. A) Representative images of oocytes from BODIPY 493/503 staining. All images were taken at the same keeping confocal settings identical, scale bars: 25 µm B) Mean relative gray value of fluorescence of individual oocyte area measured using ImageJ. C) Representative images of sections of oocytes taken by transmission electron microscopy at 2,000x magnification, scale bars: 2µm. Black arrowheads indicate lipid droplets. D) Total number of lipid droplets counted in images from each group. Different letters designate statistical significance, same letter indicates no significance between groups, $p < 0.05$; two-way ANOVA with Tukey-Kramer correction for multiple comparisons.

36

Figure 2-3: Metabolic enzyme activity, metabolite levels, and transcript levels are altered by diet and exercise. A) *Hadha* enzymatic activity was measured in individual GV-stage oocytes , (n=15 oocytes/group). Two-way ANOVA with multiple comparisons; different letters represent statistical significance between groups, p<0.001 B) ATP and C) citrate content of GV-stage oocytes as measured by enzymatic cycling assay (n=45 oocytes/group). Two way ANOVA with multiple comparisons; * P<0.05, **P<0.01 D)Relative abundance of *Cpt2, Hadh, Idh3b,* and *Aco2* transcripts. 3 oocytes per mouse were collected from 6 individual mice per experimental condition and relative abundance of transcripts was calculated using the $\Delta\Delta C_T$ method, with *Actb* as the reference gene. Two-way ANOVA with multiple-comparisons; For *Idh3b,* a – no change between groups; b – P<0.001for *Hadh* Sedentary vs. Exercise. For *Aco2*, the difference was not statistically significant but is trending towards significance (p=0.015).

Figure 2-4: Transmission electron microscopy of GV stage oocytes. A) Representative image of round (normal), elliptical and dumbbell shaped oocyte mitochondria. B) Percentages of shape of mitochondria from each cohort of mice (n=7-9 oocytes/cohort). C) Representative image of normal oocyte mitochondria and rose petal mitochondria. D) Comparison of the number of rose petal mitochondria counted in oocytes from each cohort (n=7-9 oocytes/cohort); two-way ANOVA with multiple comparisons; different letters designate statistical significance, same letter indicates no significance between groups, p < 0.05. All images are at 15,000x magnification, scale bars: 500 nm.

Figure 2-5: Meiotic progression and spindle structure of meiosis-II stage (MII) oocytes. A) Representative images of each classification category of meiotic anomalies. Arrow indicates polar body. Apoptotic indicates and apoptotic oocyte contained within the zona pellucida, scale

bars: 25 µm. B) Graph depicting percentage of oocyte in each category from each of the four

experimental conditions. CD: Control Diet, HFD: High Fat Diet

2.7 Tables

Table 2- 1: Serum Insulin and Blood Glucose levels for 12 week old mice.

	Serum Insulin (ng/mL)					mmol/L glucose			
Mouse	CD Ex	CD Sed	HFD Ex	HFD Sed	Mouse	CD Ex	CD Sed	HFD Ex	HFD Sed
1	0.48	0.33	0.74	0.72	1	9.55	5.83	7.22	7.10
2	0.46	0.42	1.06	1.73	2	6.05	5.83	6.16	8.49
3	0.76		1.53	0.28	3	5.83	5.94	5.99	8.44
4	0.53	0.55	1.07	0.87	4	6.27	4.72	8.49	8.55
5	0.53	0.41	2.05	0.91	5	5.38	5.72	8.88	7.83
6	0.50		1.05	1.52	6	5.99	5.88	6.66	8.66
7	0.50	0.41	0.69	1.17	7	6.11	4.33	9.55	7.44
8	0.78	0.33	0.62	1.06	8	6.66	5.11	8.44	9.82
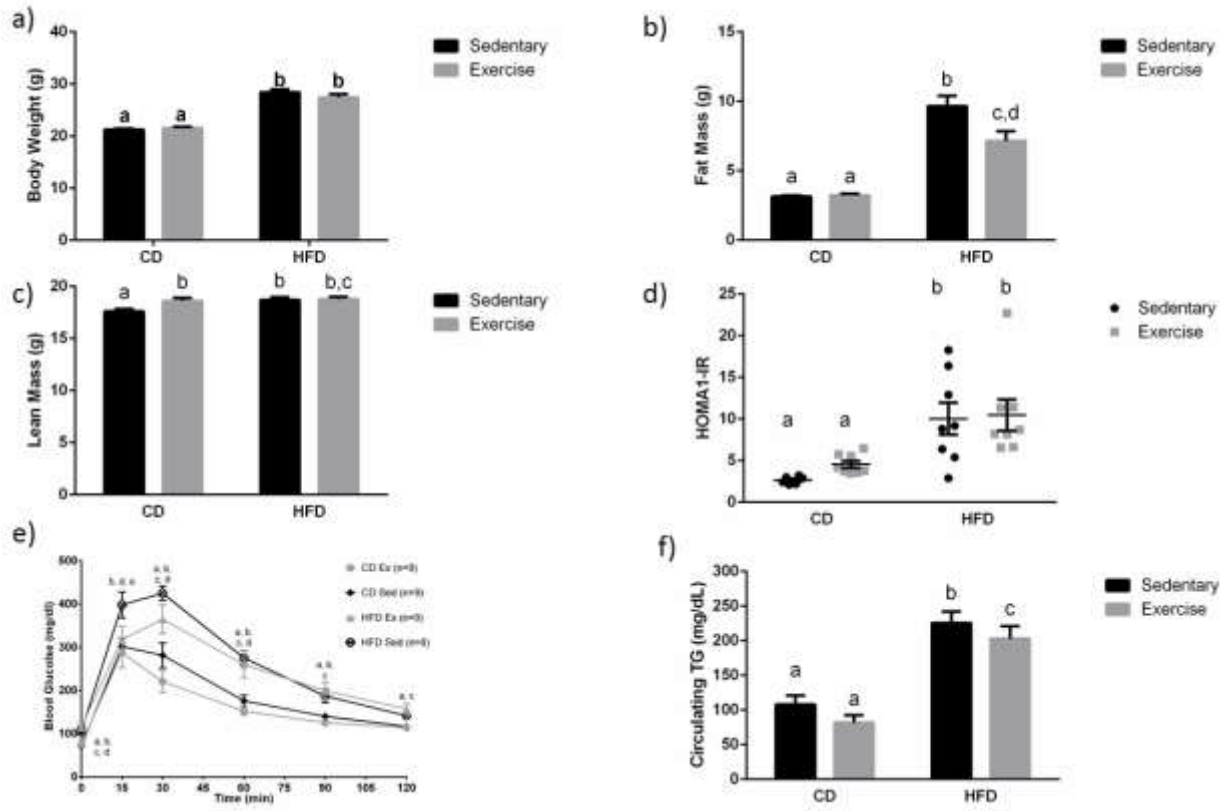
Figure 2- 1: Body weights and body composition and metabolic parameters of mice
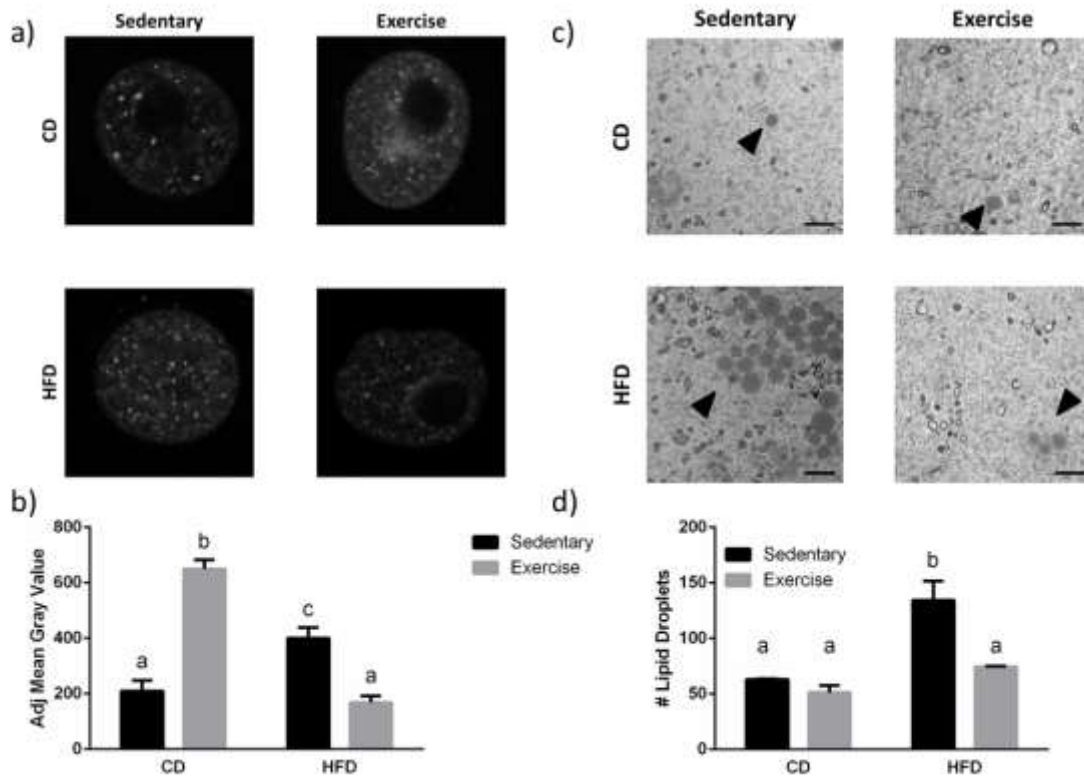
Figure 2- 2: Lipid droplet accumulation in germinal vesicle stage oocytes in response to diet and exercise training
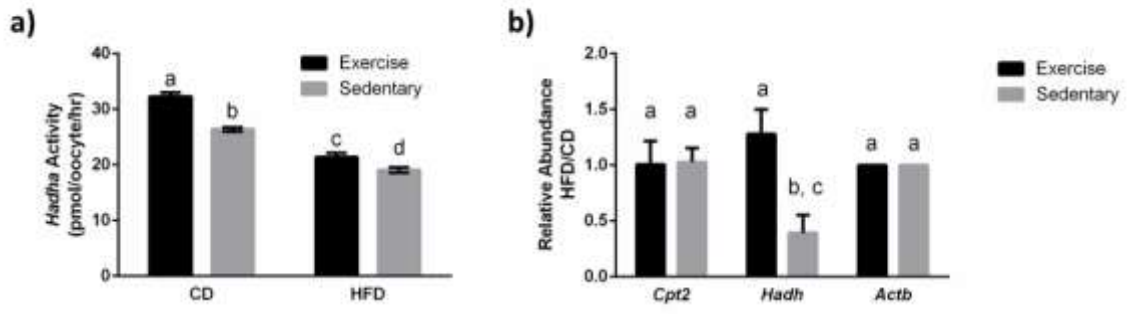
Figure 2- 3: Metabolic enzyme activity, metabolite levels, and transcript levels are altered by diet and exercise
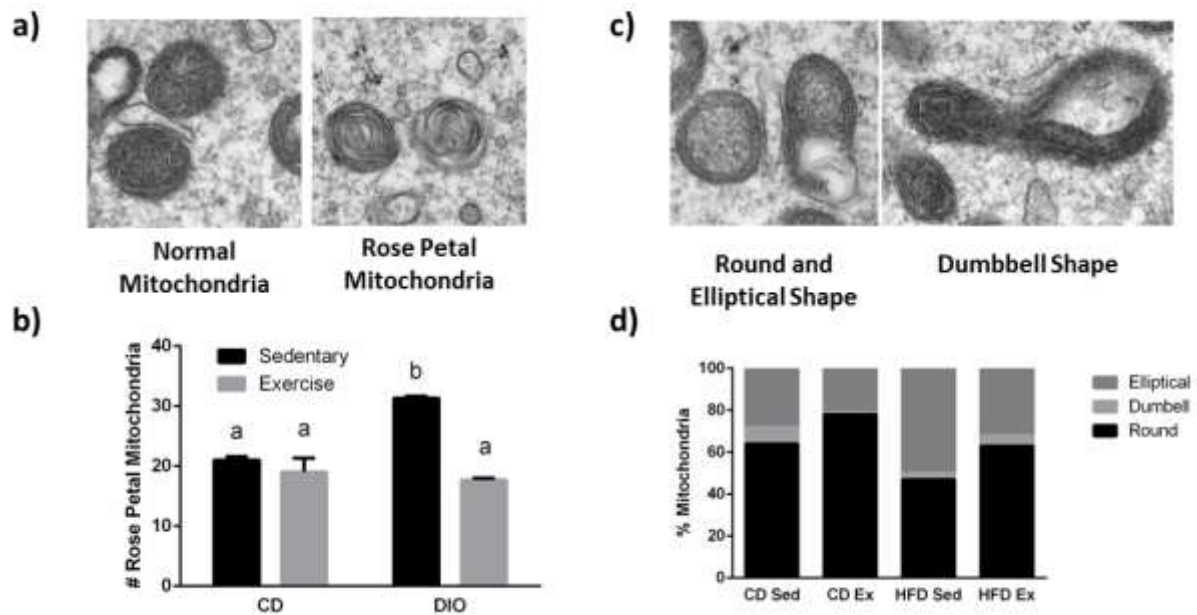
Figure 2- 4: Transmission electron microscopy of GV stage oocytes
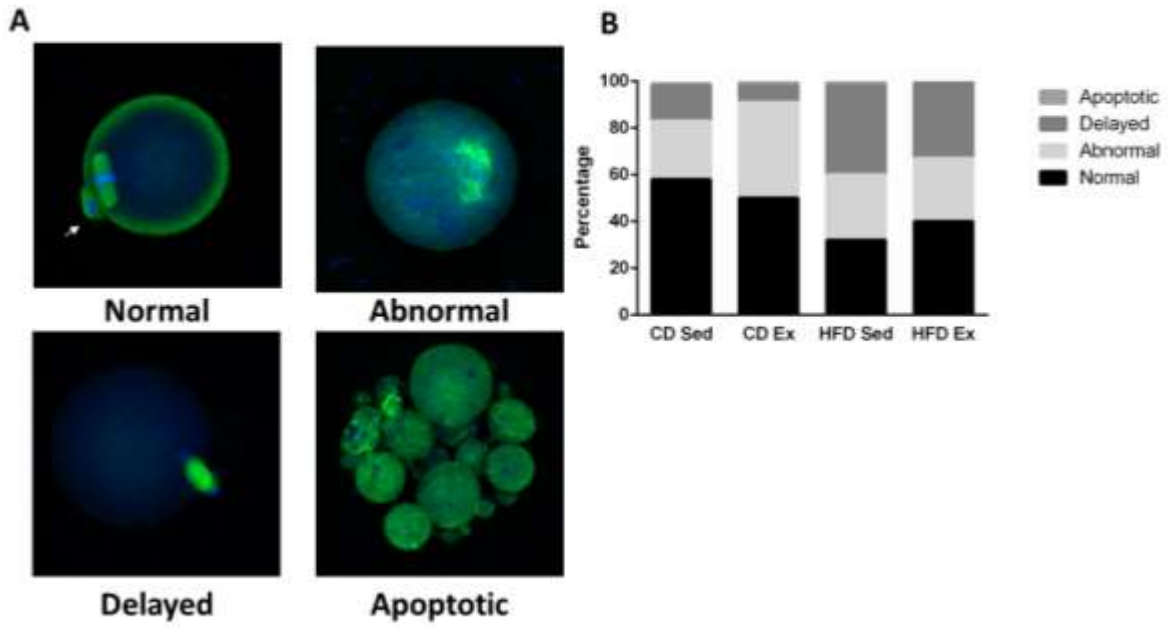
Figure 2- 5: Meiotic progression and spindle structure of meiosis-II stage (MII) oocytes.

Chapter 3: Obesity-exposed oocytes accumulate and transmit damaged mitochondria due to an inability to activate mitophagy.

Anna L. Boudoures, Jessica Saben, PhD, Alysha Thompson, Andrea Drury, Wendy Zhang and

Kelle H. Moley, MD.

Center for Reproductive and Health Sciences, Washington University in St. Louis, St. Louis, MO

3.1 Abstract

Maternal obesity predisposes offspring to cardiometabolic syndrome, obesity, and type 2 diabetes. Recent data suggest oocyte mitochondrial dysfunction mediates the deleterious consequences of maternal obesity on subsequent generations. However, the mechanisms underlying maternal transmission of defective mitochondria remains unclear. Here we test the hypothesis that inactive macroautophagic mitochondrial clearance (e.g. "mitophagy") in the oocyte underlies maternal transmission of dysfunctional mitochondria. We demonstrate that high fat/high sugar (HF/HS) diet exposure induces mitochondrial dysfunction in oocytes as indicated by decreased oocyte mitochondrial membrane potential and phospho-creatine content in HF/HS exposed oocytes. Moreover, oocytes cannot induce mitophagy. In vitro fertilization of HF/HS-exposed oocytes generated blastocysts with lower citrate, lower phospho-creatine, and accumulation of PINK1, a mitophagy marker protein. These phenotypes mirror effects in HF/HS-exposed oocytes. Taken together, these data suggest that the mechanisms governing oocyte mitophagy are fundamentally distinct from those governing somatic cell mitophagy and that absence of mitophagy in the setting of HF/HS exposure underlies the oocyte-to-blastocyst transmission of dysfunctional mitochondria.

3.2 Introduction

Obesity, an epidemic in first world countries, causes a variety of health conditions in children and adults. Additionally, epidemiological studies have demonstrated that maternal obesity puts children at increased risk of developing cardiometabolic syndrome and obesity (Margaret J. R. Heerwagen, 2010). Several pieces of evidence support the idea that obesity impairs offspring health, in part, by impairing oocyte quality. First, obese women undergoing *in*

46

vitro fertilization have lower fertilization success rates than lean women (Shah et al., 2011).

Second, a metaanalysis showed that obese women who used donor oocytes from lean women

had higher live birth rates than those who used their own oocytes (Jungheim et al., 2013). Third,

multiple labs have shown in mice that exposure to a high-fat/high-sugar, obesogenic diet

damages oocytes and leads to defects in embryo development (Boots et al., 2016; Boudoures et

al., 2016; Igosheva et al., 2010; Luzzo et al., 2012; Wu et al., 2010; Wu et al., 2015). For

example, embryos in obese mice showed delayed progression as early as the 4–8-cell stage

(Minge et al., 2008). Fourth, when oocytes from obese mice were transferred to lean recipients at

the two-cell stage, the resulting fetuses had decreased fetal/placental ratios (indicative of

placental insufficiency) and changes in expression of lipid metabolism genes and developmental

regulators (Sasson et al., 2015). Similarly, when oocytes from obese mice were fertilized *in vitro*

and transferred to lean recipient dams at the 2-cell stage, the resulting 12-week-old offspring had

peripheral glucose intolerance and were significantly heavier than controls, despite eating a

normal diet throughout their lives (Huypens et al., 2016).

Multiple groups, including ours, have sought to determine the mechanism by which

exposure to an obesogenic diet affects oocytes and offspring. The most significant effects that

occur are endoplasmic reticulum stress (Wu et al., 2012; Wu et al., 2015), accumulation of

reactive oxygen species (Boots et al., 2016; Igosheva et al., 2010; Luzzo et al., 2012), and

accumulation of damaged and defective mitochondria (Boudoures et al., 2016; Igosheva et al.,

2010; Luzzo et al., 2012; Wu et al., 2015). Because all mitochondria are inherited from the

oocyte (sperm mitochondria are degraded upon fertilization (Song et al., 2016; Sutovsky et al.,

1999)) and mitochondria play critical roles in cellular metabolism, gene expression, and cell

47

signaling, inheriting damaged oocyte mitochondria can greatly influence offspring development and health.

In numerous somatic cell types, mitochondrial health is maintained by removing damaged mitochondria through a specialized version of the intracellular recycling pathway autophagy (Palikaras and Tavernarakis, 2014). This process, termed mitophagy, is initiated by depolarization of the mitochondrial membrane. Mitochondrial depolarization stabalizes the protein Pink1, which ultimately recruites Microtubule-associated proteins 1A/1B light chain 3B (LC3-B) to initiate the formation the autophagosome around the damaged, depolarized mitochondria. After the autophagosome is formed, it fuses with a lysosome and becomes acidified. The autolysosome contents are then degraded, and the resulting macromolecules are reused by the cell (Tanida et al., 2008).

Although mitophagy is an effective means of eliminating damaged mitochondria, this process may not function in oocytes. Evidence for this idea comes from the finding that autophagy does not become active in mouse oocytes until fertilization (Tsukamoto et al., 2008). This idea could also help explain our finding that the mitochondrial damage caused by diet-induced obesity was not reversed by return to a normal diet or exercise, both of which improved the overall health of the mothers (Boudoures et al., 2016; Reynolds et al., 2015). Here, we tested the hypothesis that oocytes cannot activate mitophagy, so oocyte mitochondria that are damaged by exposure to a high fat/high sugar (HF/HS) diet are not eliminated, are transmitted to offspring, and thus impair offspring mitochondrial function and metabolism in the embryo.

3.3   Materials and Methods
Animals and Diet

This study was carried out in strict accordance with the recommendations in the Guide for the Care and Use of Laboratory Animals of the National Institutes of Health. The protocol

was approved by the IACUC-accredited Animal Studies Committee of Washington University School of Medicine (Study #20150034). Four-week-old female C57Bl/6J mice (Jackson Laboratories, Bar Harbor, ME) were fed either a high-fat/high-sugar (HF/HS; Test Diet 58R3, 35.8% hydrogenated coconut oil/17.5% sucrose) diet or a diet of standard mouse chow (Lab Diet 5053, 13% Fat/3.25% sucrose) *ad libitum* for six to eight weeks. Mice constitutively and ubiquitously expressing green fluorescent protein-tagged version myosin light chain 3 protein (GFP-LC3) were a gift from Dr. Conrad Wiehl and were initially described in (Mizushima et al., 2004).

Oocyte collection

To collect germinal vesicle (GV) stage oocytes and cumulus oocyte complexes (COCs), mice were intraperitoneally injected with 5 IU pregnant mare serum gonadotropin (PMSG; EMD Millipore, Billerica, MA). Mice were sacrificed by cervical dislocation 46-48 hours later, and ovaries were removed and placed in pre-warmed M2 media (Sigma-Aldrich, St. Louis, MO) supplemented with 5 µM milrinone (EMD Millipore) to maintain GV arrest and 10% fetal bovine serum (FBS; Sigma-Aldrich, St. Louis, MO). Large antral follicles were punctured with a 29 x ½ gauge needle, and cumulus cells were removed by multiple passes through a glass pipette to isolate GV oocytes. To collect metaphase II (MII) stage oocytes, mice were administered 5 IU PMSG. After 46–48 hours, they were administered 5 IU human chorionic gonadotropin (Sigma Aldrich), and 13 hours later, they were sacrificed as above, and ampullae were removed and placed in M2 media + 1 µg/ml hyaluronidase (Sigma Aldrich) + 10% FBS (Sigma Aldrich). Ampullae were nicked with a 29 x ½ gauge needle and incubated for 10 min to remove cumulus cells. Oocytes were washed once in fresh M2 media +10% FBS and used for assays.

Cell Culture

Murine embryonic fibroblasts (MEF) cells were cultured in Dulbecco's Modified Eagle's Medium (DMEM; Sigma D579) with 2 mM L-glutamine, 100 U/ml Penicillin and Streptozocin, and 10% FBS. MEFs were a gift of Dr. Jason Weber.

Mitochondrial membrane potential

For JC-1 staining of oocytes, the MitoPT™ JC-1 Assay Kit (Immunochemistry Technologies, Bloomington, MN) was used according to the manufacturer's protocol with the following modification. Oocytes were stained for 20 min in 200 µl of JC-1 diluted in M2 media instead of assay buffer followed by a single manufacturer prescribed wash once for 5 min in pre-warmed EmbryoMax FHM with HEPES without phenol red (MR-025-D; EMD Millipore) with 5 µM milrinone and 10% FBS. Oocytes were immediately imaged live at 37°C, 5% CO_2 in a glass-bottomed culture dish on a Leica LASX scanning confocal microscope using a 63X oil immersion lens. To detect green and red J-aggregates, images were acquired with sequential scanning using a 488 nm laser with a 510nm-540nm bandpass filter followed by a 532nm laser with a 580-610 nm bandpass filter (Perelman et al., 2012). Fluorescent analysis was done by measuring the total fluorescence of the entire oocyte in each channel. Mean gray value for each channel was normalized to area of measurement using the corrected total cell fluorescence (CTCF) method (Parry and Hemstreet, 1988). Values are expressed as total red CTCF divided by total green CTCF for individual oocytes from three different mice in each diet group.

Oocytes and blastocysts were stained with 500 nM MitoTracker CMXRosamine (CMX Ros, Invitrogen, Carlsbad, CA) diluted in M2 media for 30 min at 32°C, 5% CO_2. After staining, oocytes and blastocysts were fixed for 30 min in 4% paraformaldehyde, 1% bovine serum albumin and either mounted in VectaShield (Vector Labs, Burlingame, CA) or used for immunofluorescent staining. Oocytes and blastocysts were visualized on an Olympus Laser scanning confocal microscope with a 532 nm laser and a 60X oil immersion lens.

Metabolic Assays

Fifteen denuded germinal vesicle (GV) stage oocytes or blastocysts were collected from 6-8 mice per diet. Individual oocytes or blastocysts were frozen on glass slides in isopentane equilibrated with liquid nitrogen and freeze dried overnight under vacuum at -35°C. Individual oocytes or blastocysts were extracted under nanoliter volume and used for analysis of levels of citrate, ATP, or phosphocreatine (pCr) by enzyme-linked cycling assays as previously described (Chi et al., 2002; Chi et al., 1988).

Western Blots

For MEF protein, cells were lysed in RIPA buffer with three 15-second sonication pulses. BCA analysis was used to assess protein level. Protein was diluted in 4x NuPage LDS sample buffer (Invitrogen, Carlsbad, CA) and 10 µg was used in each lane. Three hundred denuded GV oocytes from at least 15 mice or 35 blastocysts from 6-8 mice were washed twice with cOmplete protease and phosphatase inhibitors (Roche, Indianapolis, IN) and added directly to Laemmli sample buffer, boiled for 5 min. Samples were subjected to SDS-PAGE on 10% acrylamide gels, and transferred to nitrocellulose by using the iBlot® 2 Dry Blotting System (Thermo Fischer Scientific, Waltham, MA) at 20 V for 7 min. Blots were processed according to standard Western blot procedures and probed with primary antibodies specific to Pink1 (1:1000, Abcam, Cambrige, United Kingdom, ab23707) Tom20 (1:1000, Santa Cruz Biotechnologies, Santa Cruz, CA, FL-145) and Gapdh (1:1000, Cell Signaling Technologies, Clone 14C10, catalog # 2118L). Anti-rabbit or anti-mouse secondary antibodies (1:10,000, Cell Signaling Technologies) were used as appropriate, and signal was detected with SuperSignal™ West Pico Chemiluminescent Substrate (Thermo Fischer Scientific). All experiments were performed three times. Relative protein levels were quantified in Image J and normalized to Tom20 levels.

CCCP exposure

GV oocytes were cultured for 2 hours in 10 µM Carbonyl cyanide 3-chlorophenylhydrazone (CCCP; Sigma-Aldrich, C2759-100MG) reconstituted in dimethyl sulfoxide (DMSO, Sigma-Aldrich) and diluted in M2 media (Sigma-Aldrich) supplemented with 10% FBS and 10 µM milrinone in organ dishes overlain with mineral oil. MEFs were treated for up to 24 hours with 20 µM CCCP in previously defined culture media. Vehicle-only controls omitted the CCCP.

Lysosome Quantification

To quantify lysosomal puncta, COCs from transgenic GFP-LC3 mice were collected as described above. COCs were cultured for two hours in 10 µM CCCP alone, 5nm Bafilomycin A1 (Cayman Chemical Company, Ann Arbor, MI) alone, or the two in combination. After CCCP exposure, COCs were stained with 500 nM MitoTracker CMXRosamine (Invitrogen) diluted in M2 media + 5 µM milrinone with or without the above agents for 30 min at 37°C, 5% CO_2 to confirm mitochondrial membrane depolarization. After staining, COCs were fixed in 4% PFA and stained for immunofluorescence as described below. COCs were visualized on a Leica LASX scanning confocal microscope with a 63X oil immersion lens, and 15 images of a 10 µm section of each oocyte were collected. Lysosome puncta in oocytes were quantified with LASX Analysis software, version 1.9, from at least 12 oocytes/animal/treatment. Specifically, images were first processed with background subtraction and median noise removal before setting a threshold of accepted fluorescence to reject further background noise. Next, the edge removal algorithm was applied. Finally, to count objects, only puncta greater than 0.68 µm (the lower limit of autophagosome size; Martin et al, 2013) within the user-defined oocyte region were accepted by the pipeline. The averages of the sum of puncta from each 10 µm oocyte section in each treatment group were compared by using GraphPad Prism software to perform a two-way ANOVA with Tukey-Kramer correction for multiple comparisons. Lysosome puncta in cumulus

cells were counted by a blinded observer and normalized to the total number of cumulus cells in that image. The biological assay was performed four times using 2-3 mice per assay.

Immunofluorescence

Oocytes were fixed for 15 min in 4% paraformaldehyde (Sigma-Aldrich, St. Louis, MO) in PBS + 1% bovine serum albumin (BSA; Sigma Aldrich, St. Louis, MO). Oocytes were transferred to a permeabilization solution (0.5% Triton X-100 in PBS) for 20 min, blocked with PBS + 0.1% Tween-20 + 0.01% Triton X-100 + 1% BSA for 15 min, and then incubated with an anti-Heat-shock protein 60 antibody (HSP-60; 1:250, Santa Cruz Biotechnologies, sc-1052 [N-20]) overnight at 4°C. Next, oocytes were washed three times in PBS + 0.1% Tween-20 + 0.01% Triton X-100 and then incubated in appropriate secondary antibodies conjugated to Alexa-647 (1:250, Invitrogen) and diamidino-2-phenylindole (DAPI; Thermo Fischer Scientific, 1 ng/ml) for one hour. Oocytes were washed twice in PBS + 0.1% Tween-20 + 0.01% Triton X-100 and mounted in VectaShield (Vector Labs, Burlingame, CA) on 12-well, 5 mm diameter Teflon Printed Slides (Electron Microscope Sciences, Hatfield, PA) .

Mitochondrial DNA copy number quantification

Mitochondrial DNA was extracted from individual GV oocytes after CCCP culture by lysing individual oocytes for 2h at 55 °C in 50 mM Tris-HCl, pH 8.5, 0.1 mM EDTA, 0.5% Tween-20, and 200 µg/ml proteinase K. Enzyme was then inactivated by 10 min incubation at 95 °C. Alternately, mtDNA was extracted from MEFs after CCCP treatment using the Qiagen DNeasy kit (Cat. No. 69504). Mitochondrial DNA copy number for each oocyte was calculated by using SYBR green to perform qPCR of each oocyte sample. Each reaction contained 5 µl SYBR, 0.3 µl ea primer (100 µM stock concentration), 3.4 µl H2O, and 1 µl DNA. Primer sequences were from the MT-ND5 gene on mitochondrial DNA; forward, 5'-AACCTGGCACTGAGTCACCA-3' and reverse, 5'-

GGGTCTGAGTGTATATATCATGAAGAGAAT-3'. Copy number was determined by measuring oocyte mitochondrial DNA against a standard curve. To standardize for cell numbers of MEFs, an additional standard curve containing a region of GAPDH was used. The primers for GAPDH were: Forward, 5'- TGAAATGTGCACGCACCAAG- 3' and Reverse, 5' – GGGAAGCAGCATTCAGGTCT – 3'. To calculate mtDNA abundance in somatic cells, 3 ng of total DNA was loaded in each well. As described in Saben et al., 2016, a version of delta CT was used to quantify mitochondrial abundance: $2^{[Ct(A)\times Ef(A)\}-[Ct(B)\times Ef(B)]}$, where Ct= cycle threshold, Ef= efficiency, A =MT-ND5 and B = GAPDH. The efficiency (out of 100%) was calculated using a standard curve which was generated as described below for both genes. Values were then expressed as fold change from the vehicle treated cell values.

To generate the mitochondrial and genomic DNA standard curves, the MT-ND5 or GAPDH regions were amplified from genomic DNA by using the primers above and the following PCR protocol: 98°C for 5min; 35 cycles of 98 °C for 10 sec, 52.5°C for 30 sec, 72°C for 30 sec; followed by 72°C for 10 min. The MT-ND5 or GAPDH PCR fragment was cloned into the TOPO-TA cloning vector per the manufacturer's protocol. Positive colonies were sequenced, and a plasmid containing one copy of the MT-ND5 or GAPDH region was diluted to 10^8 to 10^2 plasmids per µl by calculating the concentration on a nanodrop and converting to exact copy number by using the following equation (May-Panloup et al., 2005): $\frac{6.3 \; X \; 10^9 \; copies}{ng} =$ $absolute \; number \; of \; plasmids \; in \; a \; reaction.$

In vitro fertilization and collection of blastocysts
MII oocytes were collected from the ampullae of C57B6/J females after superovulation as described above. Preparation of cauda epididymal sperm from male ICR mice, insemination, and embryo culture were performed as described previously (Kim and Moley, 2008). Blastocyst-

stage embryos were collected for western blot, metabolic assays, and staining with MitoTracker CMX Rosamine as described above.

3.4   Results

Previous electron microscopy analysis demonstrated that oocytes from HF/HS-fed mice had damaged mitochondria (Luzzo et al., 2012). To confirm this, we fed wild-type C57Bl6/J mice a high-fat/high-sugar (HF/HS) diet (35.8% hydrogenated coconut oil/17.5% sucrose) for a minimum of six weeks to induce hyperglycemia and obesity (Supplementary Figure 1). We then assessed mitochondrial health by isolating germinal vesical stage (GV) oocytes from HF/HS- and control-fed mice and staining them with the fluorescent dye JC-1, which fluoresces red if the mitochondrial membrane is polarized and green if it is depolarized. We found that oocytes from HF/HS-exposed mice had a lower red/green ratio than those from controls (Figure 1a-b), indicating lower metabolic activity (Reers et al., 1995). To confirm the decrease in activity, we performed microanalytic assays and found that oocytes from the two groups had equivalent levels of total cell ATP (Figure 1c), but those from the HF/HS-fed mice had lower levels of phosopho-creatine (Figure 1d). Phospho-creatine is used as a buffer in skeletal muscle to rapidly phosphorylate ADP to ATP independent of the electron transport chain (Wallimann et al., 2011), and may explain a reduction in oocyte mitochondrial membrane potentital without reduction of ATP levels. These data indicated that six weeks of HF/HS feeding is sufficient to cause mouse oocytes to accumulate damaged mitochondria, as previously described (Igosheva et al., 2010).

To determine whether accumulation of damaged mitochondria occurred because of a lack of mitophagy, we exposed oocytes from control mice to the ionophore CCCP, which completely depolarizes the mitochondrial membrane (Wallimann et al., 2011) and activates mitophagy in other cell types (Chen and Dorn, 2013; Gegg et al., 2010). We first tested different

concentrations of CCCP and found that a two-hour treatment with 10 µm of CCCP was sufficient to depolarize mitochondrial membranes (Supplementary Figure 2a) and induce expression of Pink1 in oocytes (Figure 2), as is observed with two hours of CCCP exposure in mouse embryonic fibroblasts (Figure 2).

In somatic cells, after Pink1 is stabilized and accumulates on damaged, depolarized mitochondria, these mitochondria are trafficked to the autophagosome (Yoshii and Mizushima, 2015). To determine whether this occurred in oocytes, we isolated GV stage cumulus cell – oocyte complexes (COCs) from mice ubiquitously expressing GFP-LC3. To monitor autophagy (which mitophagy is a specific subset of), bafilomyocin A1 (BafA1) can be used to stabilize LC3 by preventing acidification of lysosomes. An increase in LC3 expression after BafA1 treatment indicates autophagic flux occurs normally in that cell type (Klionsky et al., 2016). 5 nM of BafA1 was shown to be sufficient to inhibit acidification lysosomes using the pH sensitive dye LysoTracker (Supplementary Figure 2b). To monitor mitophagy, COCs were treated with 5 nM of BafA1 and 10 µm CCCP simultaneously.

In cumulus cells, treatment with BafA1 results in an increase in the number of LC3 puncta, indicating these cells undergo a basal level of autophagy (Figure 3 a-b). While LC3 puncta are present in oocytes, there was no increase in LC3 expression with BafA1 (Figure 3c), indicating there is no basal autophagy, as described previously (Tsukamoto et al., 2008a; Tsukamoto et al., 2008b). After CCCP treatment or CCCP and BafA1 treatment in combination, cumulus cells increase in the number of LC3 positive puncta (Figure 3a-b). These puncta also colocalize with mitochondria, as where there is an overlap of red (Hsp60; a mitochondria marker) and green (LC3; autophagosomes) fluorescence (Figure 3a). In contrast, GV oocytes did not traffic mitochondria to the autophagosome after CCCP exposure (Figure 3c-d). This can be discerned

because there is no overlap of red and green fluorescence. Additionally, GFP-LC3 positive

puncta were completely eliminated in GV oocytes but not cumulus cells after CCCP exposure

(Figure 3). Surprisingly, this clearance was independent of the lysosome, as treatment BafA1 in

combination with CCCP did not inhibit LC3-II clearance in the oocytes (Figure 3c-d). This

indicates that LC3 puncta are being removed independent of the lysosome and the canonical

autophagy pathway.

To confirm that oocytes did not remove damaged mitochondria in response to CCCP, we

measured mtDNA copy number in individual oocytes. Because each oocyte mitochondrion

harbors, on average, only one copy of mtDNA, mtDNA copy number quantification accurately

assesses total number of mitochondria (Wai et al., 2008). Additionally, mtDNA copy number

decreases in somatic cells after exposure to CCCP ((Klionsky et al., 2016; Okatsu et al., 2010)

Supplementary Figure 3). In both GV and MII oocytes, two-hour 10 µm CCCP treatment did not

affect mtDNA copy number (Figure 4a-b). To ensure that 2h treatment was not too brief to

observe mitophagy, we treated oocytes with 10 µm CCCP for six hours, but this also had on

effect of mtDNA copy number (Figure 4a), though it did greatly impair oocyte survival (Figure

4c).

Finally, we wondered whether the damaged mitochondria that accumulated in the oocytes

of HF/HS-fed mice were transmitted to the offspring. To test this, we isolated oocytes from

either control diet or HF/HS-fed mice and subjected them to *in vitro* fertilization with sperm

from chow-fed males. The number of fertilized oocytes to reach the blastocyst stage was

significantly reduced if the oocytes came from a HF/HS fed donor female (*P=0.03,* Figure 5a).

Additionally, the blastocysts from HF/HS donor oocytes had a significantly lower mitochondrial

membrane potential, as measured by relative fluorescence of MitoTracker (Figure 5b).

Consistent with this finding, the levels of both citrate and phospho-creatine were significantly lower in embryos from HF/HS females than in those from controls, though ATP levels were not affected (Figure 5c-e). As in GV oocytes, this is likely due to phospho-creatine replenished ATP in the embryos (Wallimann et al., 2011). Finally, the level of Pink1 protein expression was significantly higher in embryos from HF/HS-exposed oocytes than in those from controls (Figure 5f), suggesting an increased rate of mitophagy to compensate for inheritance of damaged mitochondria.

3.5   Discussion

In conclusion, we show that oocytes do not activate mitophagy. Therefore, when females consume a HF/HS diet for a sustained period, the damaged mitochondria cannot be cleared from the oocytes. As a result, embryos inherit suboptimal mitochondria which persist at least until the blastocyst stage. There are several potential reasons oocytes do not activate mitophagy. First, only a small pool of mitochondria exhibit high membrane polarity (Fig 1 and (Van Blerkom and Davis, 2006; Van Blerkom et al., 2003; Van Blerkom et al., 2002). Instead, the majority appear to by metabolically quiescent. This can be visualized in the JC-1 stain, in which a sub-population of highly polarized mitochondria are present at the periphery of the GV oocyte. In MII oocytes, this population shifts to surround the spindle (data not shown). Mitochondrial quiescence in the oocyte has been proposed to be in order to reduce oxidative damage to mitochondria and organelles prior to fertilization (Cummins, 2004). Because Pink1 is stabilized on depolarized mitochondrial membranes, normal but inactive mitochondria would be eliminated in oocytes, preventing fertilization.

Second, one of the primary changes that occurs to oocytes during cytoplasmic maturation is a massive increase in the number of mitochondria present (Piko and Taylor, 1987; Wang et al.,

2009). Whereas somatic cells average 200-2,000 mitochondria per cell (depending on the cell type), a fertilization-competent, mature MII oocyte has approximately 100,000 mitochondria (Piko and Taylor, 1987; Reynier et al., 2001). After fertilization, mitochondria inherited from the mother are randomly partitioned to blastomeres as cell divisions occur. Only at the blastocyst stage is mitochondrial biogenesis re-initiated (Piko and Taylor, 1987). Therefore, there is an obvious conflict programmed in the oocyte to have high levels of mitochondria production and a majority of normal mitochondria with low membrane potential paired with a membrane-polarity dependent process for mitochondrial elimination.

Finally, research in both animal and human oocytes have shown that fertilization-competent oocytes must contain mtDNA copy numbers within a specific range. Falling outside of this range results in failed fertilization (Reynier et al., 2001; Wai et al., 2010). In oocytes, mtDNA copy number is representative of the number of mitochondria (Kasashima et al., 2014). Therefore, mitophagy initiation would disrupt this range and result in failed fertilization. The oocyte may be programmed to retain damaged mitochondria in order to successfully fertilize with sub-optimal mitochondria. This is supported by the clearance of LC3B positive puncta but not mitochondria in the oocytes after CCCP treatment.

The autophagosome fuses with the lysosome to break down proteins and organelles, including mitochondria, for recycling or removal (Zhu et al., 2011). However, in oocytes, this does not occur. Although LC3 positive vesicles and/or pre-autophagic structures are present in the oocytes from GFP-LC3 mice (Figure 3), these puncta do not colocalize with mitochondria. Despite elimination of GFP-LC3 after CCCP treatment, mitochondria are still abundant in the oocytes, supporting a lack mitophagy in oocytes. Further, when oocytes were treated with both CCCP and BafA1 to inhibit lysosomal degradation, oocytes still eliminated the LC3 puncta. If

59

oocytes used autophagy to degrade the GFP-LC3, BafA1 would prevent this degradation. This indicates oocytes remove LC3 using a lysosome-independent mechanism. While the mechanism for LC3 elimination is unclear, it is not surprising that the mechanism would be independent of the lysosome and autophagy. Although oocytes deficient for an essential autophagy protein, Autophagy- Related 5 protein (Atg5), are viable and fertilize, the Atg5 null embryos die shortly after implantation (Tsukamoto et al., 2008a; Tsukamoto et al., 2008b). Our data supports these earlier findings and specifically indicates an absence of mitophagy results from this incapacity to activate autophagy.

Possibly, oocytes activate mitophagy independent of macroautophagy in response to mitochondrial damage. There are multiple ways cells can recognize and remove damaged mitochondria (Lemasters, 2014). However, oocytes do not reduce mtDNA copy number in response to CCCP, which makes activation of an autophagy-independent pathway for mitophagy unlikely. Additionally, multiple groups have shown HF/HS oocytes have increased numbers of mitochondria (Igosheva et al., 2010; Luzzo et al., 2012; Schrauwen et al., 2010), suggesting oocytes may recognize the damage and respond by increasing mitochondria numbers as opposed to activating mitophagy. Finally, because oocytes do have an increase in Pink1 protein in response to CCCP exposure after two hours, it is possible once embryos activate autophagy, the mitophagy pathway can also resume. An increase in Pink1 and a decrease in mitochondrial membrane potential at the blastocyst stage in HF/HS embryos supports the hypothesis that the embryos inherit damaged mitochondria because oocytes are incapable of activating mitophagy.

Recent publications show a variety of negative physiological effects in the offspring from obese mothers (Huypens et al., 2016; Sasson et al., 2015). Despite the potential upregulation of mitophagy in the embryo (as evidenced by increased Pink1 expression, Fig 5), the damage may

60

be long lasting. This could be due to the effects of programming. The majority of methylation marks are erased during oocyte maturation and methylation levels remain low during pre-implantation embryo development. Then at the blastocyst stage, embryos rapidly re-establish DNA methylation (Fulka et al., 2008). Additionally, DNA methylation requires ATP to establish methylation sites, closely linking epigenetics with metabolism (Ulrey et al., 2005). Therefore, damaged and less active mitochondria in the blastocyst could alter DNA methylation patterns. While this was suggested in recent publications (Huypens et al., 2016; Sasson et al., 2015), data comparing early stage embryos from lean and obese mothers has yet to be published. This is most likely due to the technical limitations of sequencing technologies, which lack the sensitivity to accurately measure methylation changes in embryos. However, rapid development in the sequencing field should make this data accessible in the near future.

We are the first to address a cellular pathway that explains the retention of mitochondrial damage in oocytes due to prolonged consumption of a HF/HS diet. Additionally, this data suggests that the oocyte itself, independent of the uterine environment, can have effects on embryo quality and offspring health. The inheritance of damaged mitochondria and potential lasting consequences on future generations can explain the persistence of mitochondrial dysfunction and metabolic syndrome in our population. This inheritance has a sustained impact on the offspring's embryonic development and adult life (Huypens et al., 2016; Saben et al., 2016; Sasson et al., 2015). Two questions remain. First, do embryos from HF/HS mothers successfully remove all damaged mitochondria once autophagy and mitophagy are activated after fertilization? Second, what impacts on epigenetics result from inheritance of a large pool of damaged mitochondria? Is this independent of the obese uterine environment? Answers to these

questions will be important in understanding how obesity can influence the health of multiple

generations.

3.6   References

Al Rawi, S., Louvet-Vallee, S., Djeddi, A., Sachse, M., Culetto, E., Hajjar, C., Boyd, L., Legouis, R., Galy, V., 2011. Postfertilization autophagy of sperm organelles prevents paternal mitochondrial DNA transmission. Science (New York, N.Y.) 334, 1144-1147.

Au, H.K., Yeh, T.S., Kao, S.H., Tzeng, C.R., Hsieh, R.H., 2005. Abnormal mitochondrial structure in human unfertilized oocytes and arrested embryos. Annals of the New York Academy of Sciences 1042, 177-185.

Boots, C.E., Boudoures, A., Zhang, W., Drury, A., Moley, K.H., 2016. Obesity-induced oocyte mitochondrial defects are partially prevented and rescued by supplementation with co-enzyme Q10 in a mouse model. Human reproduction (Oxford, England) 31, 2090-2097.

Boudoures, A.L., Chi, M., Thompson, A., Zhang, W., Moley, K.H., 2016. The effects of voluntary exercise on oocyte quality in a diet-induced obese murine model. Reproduction (Cambridge, England) 151, 261-270.

Chen, Y., Dorn, G.W., 2nd, 2013. PINK1-phosphorylated mitofusin 2 is a Parkin receptor for culling damaged mitochondria. Science (New York, N.Y.) 340, 471-475.

Chi, M.M., Hoehn, A., Moley, K.H., 2002. Metabolic changes in the glucose-induced apoptotic blastocyst suggest alterations in mitochondrial physiology. American journal of physiology. Endocrinology and metabolism 283, E226-232.

Chi, M.M., Manchester, J.K., Yang, V.C., Curato, A.D., Strickler, R.C., Lowry, O.H., 1988. Contrast in levels of metabolic enzymes in human and mouse ova. Biology of reproduction 39, 295-307.

Cummins, J.M., 2000. Fertilization and elimination of the paternal mitochondrial genome. Human reproduction (Oxford, England) 15 Suppl 2, 92-101.

Cummins, J.M., 2004. The role of mitochondria in the establishment of oocyte functional competence. European journal of obstetrics, gynecology, and reproductive biology 115 Suppl 1, S23-29.

Fulka, H., St John, J.C., Fulka, J., Hozak, P., 2008. Chromatin in early mammalian embryos: achieving the pluripotent state. Differentiation; research in biological diversity 76, 3-14.

Geisler, S., Holmstrom, K.M., Skujat, D., Fiesel, F.C., Rothfuss, O.C., Kahle, P.J., Springer, W., 2010. PINK1/Parkin-mediated mitophagy is dependent on VDAC1 and p62/SQSTM1. Nature cell biology 12, 119-131.

Georgakopoulos, N.D., Wells, G., Campanella, M., 2017. The pharmacological regulation of cellular mitophagy. Nature chemical biology 13, 136-146.

Huypens, P., Sass, S., Wu, M., Dyckhoff, D., Tschop, M., Theis, F., Marschall, S., Hrabe de Angelis, M., Beckers, J., 2016. Epigenetic germline inheritance of diet-induced obesity and insulin resistance. Nature genetics 48, 497-499.

Igosheva, N., Abramov, A.Y., Poston, L., Eckert, J.J., Fleming, T.P., Duchen, M.R., McConnell, J., 2010. Maternal diet-induced obesity alters mitochondrial activity and redox status in mouse oocytes and zygotes. PloS one 5, e10074.

Jin, S.M., Lazarou, M., Wang, C., Kane, L.A., Narendra, D.P., Youle, R.J., 2010. Mitochondrial membrane potential regulates PINK1 import and proteolytic destabilization by PARL. The Journal of cell biology 191, 933-942.

Kamijo, T., Zindy, F., Roussel, M.F., Quelle, D.E., Downing, J.R., Ashmun, R.A., Grosveld, G., Sherr, C.J., 1997. Tumor Suppression at the Mouse INK4a Locus Mediated by the Alternative Reading Frame Product p19 ARF. Cell 91, 649-659.

Kasashima, K., Nagao, Y., Endo, H., 2014. Dynamic regulation of mitochondrial genome maintenance in germ cells. Reproductive medicine and biology 13, 11-20.

Kim, S.T., Moley, K.H., 2008. Paternal effect on embryo quality in diabetic mice is related to poor sperm quality and associated with decreased glucose transporter expression. Reproduction (Cambridge, England) 136, 313-322.

Klionsky, D.J., Abdelmohsen, K., Abe, A., Abedin, M.J., Abeliovich, H., Acevedo Arozena, A., … Zorzano, A., Zughaier, S.M., 2016. Guidelines for the use and interpretation of assays for monitoring autophagy (3rd edition). Autophagy 12, 1-222.

Lazarou, M., Sliter, D.A., Kane, L.A., Sarraf, S.A., Wang, C., Burman, J.L., Sideris, D.P., Fogel, A.I., Youle, R.J., 2015. The ubiquitin kinase PINK1 recruits autophagy receptors to induce mitophagy. Nature 524, 309-314.

Lee, G.K., Shin, H., Lim, H.J., 2016. Rapamycin Influences the Efficiency of In vitro Fertilization and Development in the Mouse: A Role for Autophagic Activation. Asian-Australasian journal of animal sciences 29, 1102-1110.

Lemasters, J.J., 2014. Variants of mitochondrial autophagy: Types 1 and 2 mitophagy and micromitophagy (Type 3). Redox Biology 2, 749-754.

Luzzo, K.M., Wang, Q., Purcell, S.H., Chi, M., Jimenez, P.T., Grindler, N., Schedl, T., Moley, K.H., 2012. High fat diet induced developmental defects in the mouse: oocyte meiotic aneuploidy and fetal growth retardation/brain defects. PloS one 7, e49217.

Margaret J. R. Heerwagen, M.R.M., Linda A. Barbour and Jacob E. Friedman, 2010. Maternal obesity and fetal metabolic programming: a fertile epigenetic soil. American Journal of Physiology - Regulatory, Integrative and Comparative Physiology 299, R711-R722.

Martin, K.R., Barua, D., Kauffman, A.L., Westrate, L.M., Posner, R.G., Hlavacek, W.S., MacKeigan, J.P., 2013. Computational model for autophagic vesicle dynamics in single cells. Autophagy 9, 74-92.

May-Panloup, P., Vignon, X., Chretien, M.F., Heyman, Y., Tamassia, M., Malthiery, Y., Reynier, P., 2005. Increase of mitochondrial DNA content and transcripts in early bovine embryogenesis associated with upregulation of mtTFA and NRF1 transcription factors. Reproductive biology and endocrinology : RB&E 3, 65.

Mizushima, N., Yamamoto, A., Matsui, M., Yoshimori, T., Ohsumi, Y., 2004. In vivo analysis of autophagy in response to nutrient starvation using transgenic mice expressing a fluorescent autophagosome marker. Molecular biology of the cell 15, 1101-1111.

Motta, P.M., Nottola, S.A., Makabe, S., Heyn, R., 2000. Mitochondrial morphology in human fetal and adult female germ cells. Human reproduction (Oxford, England) 15 Suppl 2, 129-147.

Narendra, D.P., Jin, S.M., Tanaka, A., Suen, D.F., Gautier, C.A., Shen, J., Cookson, M.R., Youle, R.J., 2010. PINK1 is selectively stabilized on impaired mitochondria to activate Parkin. PLoS biology 8, e1000298.

Okatsu, K., Saisho, K., Shimanuki, M., Nakada, K., Shitara, H., Sou, Y.S., Kimura, M., Sato, S., Hattori, N., Komatsu, M., Tanaka, K., Matsuda, N., 2010. p62/SQSTM1 cooperates with Parkin for perinuclear clustering of depolarized mitochondria. Genes to cells : devoted to molecular & cellular mechanisms 15, 887-900.

Parry, W.L., Hemstreet, G.P., 3rd, 1988. Cancer detection by quantitative fluorescence image analysis. The Journal of urology 139, 270-274.

Perelman, A., Wachtel, C., Cohen, M., Haupt, S., Shapiro, H., Tzur, A., 2012. JC-1: alternative excitation wavelengths facilitate mitochondrial membrane potential cytometry. Cell death & disease 3, e430.

Picard, M., Wallace, D.C., Burelle, Y., 2016. The rise of mitochondria in medicine. Mitochondrion 30, 105-116.

Piko, L., Taylor, K.D., 1987. Amounts of mitochondrial DNA and abundance of some mitochondrial gene transcripts in early mouse embryos. Developmental biology 123, 364-374.

Reers, M., Smiley, S.T., Mottola-Hartshorn, C., Chen, A., Lin, M., Chen, L.B., 1995. Mitochondrial membrane potential monitored by JC-1 dye. Methods in enzymology 260, 406-417.

Reynier, P., May-Panloup, P., Chretien, M.F., Morgan, C.J., Jean, M., Savagner, F., Barriere, P., Malthiery, Y., 2001. Mitochondrial DNA content affects the fertilizability of human oocytes. Molecular human reproduction 7, 425-429.

Roberts, R.F., Tang, M.Y., Fon, E.A., Durcan, T.M., 2016. Defending the mitochondria: The pathways of mitophagy and mitochondrial-derived vesicles. Int J Biochem Cell Biol 79, 427-436.

Rojas-Rios, P., Chartier, A., Pierson, S., Severac, D., Dantec, C., Busseau, I, Simonelig, M., 2015. Translational Control of Autophagy by Orb in the Drosophila Germline. Developmental cell 35, 622-631.

Saben, J.L., Boudoures, A.L., Asghar, Z., Thompson, A., Drury, A., Zhang, W., Chi, M., Cusumano, A., Scheaffer, S., Moley, K.H., 2016. Maternal Metabolic Syndrome Programs Mitochondrial Dysfunction via Germline Changes across Three Generations. Cell reports 16, 1-8.

Sasson, I.E., Vitins, A.P., Mainigi, M.A., Moley, K.H., Simmons, R.A., 2015. Pre-gestational vs gestational exposure to maternal obesity differentially programs the offspring in mice. Diabetologia 58, 615-624.

Schrauwen, P., Schrauwen-Hinderling, V., Hoeks, J., Hesselink, M.K., 2010. Mitochondrial dysfunction and lipotoxicity. Biochimica et biophysica acta 1801, 266-271.

Settembre, C., Fraldi, A., Medina, D.L., Ballabio, A., 2013. Signals from the lysosome: a control centre for cellular clearance and energy metabolism. Nature reviews. Molecular cell biology 14, 283-296.

Song, W.H., Yi, Y.J., Sutovsky, M., Meyers, S., Sutovsky, P., 2016. Autophagy and ubiquitin-proteasome system contribute to sperm mitophagy after mammalian fertilization. Proceedings of the National Academy of Sciences of the United States of America.

Sutovsky, P., Moreno, R.D., Ramalho-Santos, J., Dominko, T., Simerly, C., Schatten, G., 1999. Ubiquitin tag for sperm mitochondria. Nature 402, 371-372.

Tsukamoto, S., Kuma, A., Mizushima, N., 2008a. The role of autophagy during the oocyte-to-embryo transition. Autophagy 4, 1076-1078.

Tsukamoto, S., Kuma, A., Murakami, M., Kishi, C., Yamamoto, A., Mizushima, N., 2008b. Autophagy is essential for preimplantation development of mouse embryos. Science (New York, N.Y.) 321, 117-120.

Ulrey, C.L., Liu, L., Andrews, L.G., Tollefsbol, T.O., 2005. The impact of metabolism on DNA methylation. Human molecular genetics 14, R139-R147.

Van Blerkom, J., Davis, P., 2006. High-polarized (Delta Psi m(HIGH)) mitochondria are spatially polarized in human oocytes and early embryos in stable subplasmalemmal domains: developmental significance and the concept of vanguard mitochondria. Reproductive biomedicine online 13, 246-254.

Van Blerkom, J., Davis, P., Alexander, S., 2003. Inner mitochondrial membrane potential (DeltaPsim), cytoplasmic ATP content and free Ca2+ levels in metaphase II mouse oocytes. Human reproduction (Oxford, England) 18, 2429-2440.

Van Blerkom, J., Davis, P., Mathwig, V., Alexander, S., 2002. Domains of high-polarized and low-polarized mitochondria may occur in mouse and human oocytes and early embryos. Human reproduction (Oxford, England) 17, 393-406.

Wai, T., Ao, A., Zhang, X., Cyr, D., Dufort, D., Shoubridge, E.A., 2010. The role of mitochondrial DNA copy number in mammalian fertility. Biology of reproduction 83, 52-62.

Wai, T., Teoli, D., Shoubridge, E.A., 2008. The mitochondrial DNA genetic bottleneck results from replication of a subpopulation of genomes. Nature genetics 40, 1484-1488.

Wallimann, T., Tokarska-Schlattner, M., Schlattner, U., 2011. The creatine kinase system and pleiotropic effects of creatine. Amino acids 40, 1271-1296.

Wang, L.-y., Wang, D.-h., Zou, X.-y., Xu, C.-m., 2009. Mitochondrial functions on oocytes and preimplantation embryos. Journal of Zhejiang University. Science. B 10, 483-492.

Wu, L.L., Dunning, K.R., Yang, X., Russell, D.L., Lane, M., Norman, R.J., Robker, R.L., 2010. High-fat diet causes lipotoxicity responses in cumulus-oocyte complexes and decreased fertilization rates. Endocrinology 151, 5438-5445.

Wu, L.L., Russell, D.L., Wong, S.L., Chen, M., Tsai, T.S., St John, J.C., Norman, R.J., Febbraio, M.A., Carroll, J., Robker, R.L., 2015. Mitochondrial dysfunction in oocytes of obese mothers: transmission to offspring and reversal by pharmacological endoplasmic reticulum stress inhibitors. Development (Cambridge, England) 142, 681-691.

Yoshii, S.R., Mizushima, N., 2015. Autophagy machinery in the context of mammalian mitophagy. Biochimica et biophysica acta.

Zhu, J., Dagda, R.K., Chu, C.T., 2011. Monitoring mitophagy in neuronal cell cultures. Methods in molecular biology (Clifton, N.J.) 793, 325-339.

3.7   Figures Legends

Figure 3-1: Pink1 protein is upregulated in MEFs and Oocytes in response to CCCP treatment.

(A) Representative of GV oocytes stained with MitoTracker CMXRosamine (MTR) showing successful depolarization with 10 µM CCCP or 10 µg/ml AntA. (B) Representative Pink1 western blot of MEFs and GV oocytes incubated for two hours with vehicle (-) or CCCP (+). Gapdh is shown as a marker of total protein, and Tom20 as a marker of total mitochondrial protein. (C) Densitometry of MEF western blots, with Pink1 normalized to Tom20, a mitochondrial loading control (n=3).

Figure 3-2: Cumulus cells activate mitophagy in response to cumulus-oocyte complex mitochondria membrane depolarization. (A, C) Quantification of LC3B puncta in cumulus cells treated with vehicle (Vh), bafilomycin A1 (BafA1), CCCP, AntimycinA (AntA), or CCCP/AntA and BafA1 for two hours. Puncta counts were normalized to nuclei in the same image to control for cell number. (B, D) Representative images cumulus cells in the respective treatment groups; arrows indicate colocalization of mitochondria in autophagosomes. Scale bar = 10 µm. red: Hsp60 (mitochondria), green: GFP-LC3B, white: nuclei; 3 experimental replicates, 2-3 mice per experiment.

Figure 3-3: GV oocytes remove LC3 puncta but do not activate mitophagy in response to mitochondria membrane depolarization. (A, C) Quantification of LC3 puncta in a 10 µm Z-stack section of GV oocytes treated with (A) CCCP or (C) AntA with or without BafA1. (B, D) Representative images of GV oocytes. Scale bar = 25 µm. (d) Quantification of LC3B puncta; n=32-37 oocytes/group. In (B) and (D), red: Hsp60 (mitochondria), green: GFP-LC3B, white: nuclei; 3 experimental replicates, 2-3 mice per experiment.

Figure 3-4: CCCP treatment does not reduce mtDNA in oocytes. mtDNA copy number of GV

oocytes after two hours of (A) 10 µM CCCP treatment (n=27), or (B) 10 µg/ml AntA treatment

(n=45). (C) mtDNA copy number of GV oocytes treated 6 hours with CCCP (n= 6-11) or AntA

(n=5-7). (D) Oocyte survival after treatment with CCCP (dark gray square) or AntA (light gray

triangle) as compared to the respective vehicle (Vh; black circle) treatment.

Figure 3-5: Germinal vesicle stage oocytes from HF/HS diet fed mice have impaired metabolism.

(A) JC-1 staining of GV oocytes. (B) Quantification of JC-1 red/green ratio in GV oocytes from

control (n =86) and HF/HS (90) GV oocytes; Experiment was done in triplicate, 3 mice per diet.

(C) Representative EM images of oocyte mitochondria; 2,500x (scale bar = 2 µm) or 5,000 x

(scale bar = 500 nm). Mitochondrion with ruptured membrane depicted with arrowhead. (D)

Quantitation of oocyte mitochondria electron density (n=339 Con oocyte mitochondria and 393

HF/HS oocyte mitochondria from 11 oocytes per diet) (E) ATP content of GV oocytes

(n=45/diet). (F) Phosphocreatine (pCr) content of GV oocytes (n=15/diet). (G) Blastocyst

formation rate of embryos after *in vitro* fertilization of control or HF/HS oocytes. * $P<0.05$, **

$P<0.01$, **** $P<0.0001$

Figure 3-6: IVF-generated blastocysts from HF/HS fed donor mouse oocytes have impaired

metabolism and increased mitophagy. (A) Representative images and (B) quantitation of

MitoTracker in HF/HS and control blastocysts (n= 5 blastocysts). (C-E) Quantitation of levels of

(C) citrate, (D) phosphocreatine (pCr) and (E) ATP of individual blastocysts (n=15 blastocysts).

(F) Pink1 protein in HF/HS and control blastocysts (n=35 blastocyst/lane).
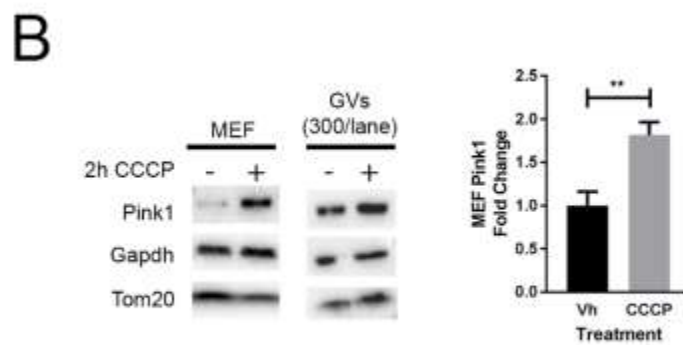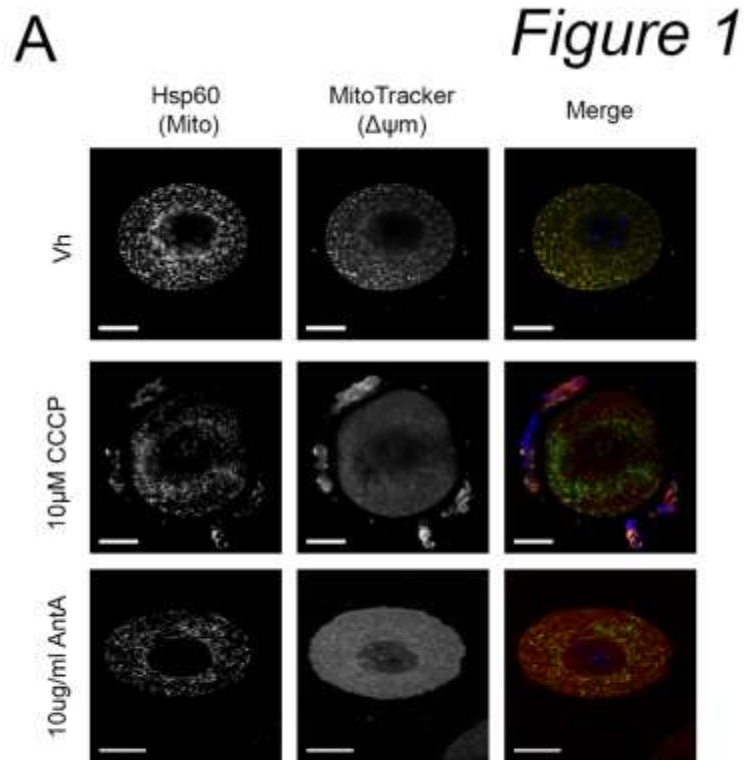
Figure 3- 1: Pink1 protein is upregulated in MEFs and Oocytes in response to CCCP treatment.

Figure 3- 2: Cumulus cells activate mitophagy in response to cumulus-oocyte complex mitochondria membrane depolarization.
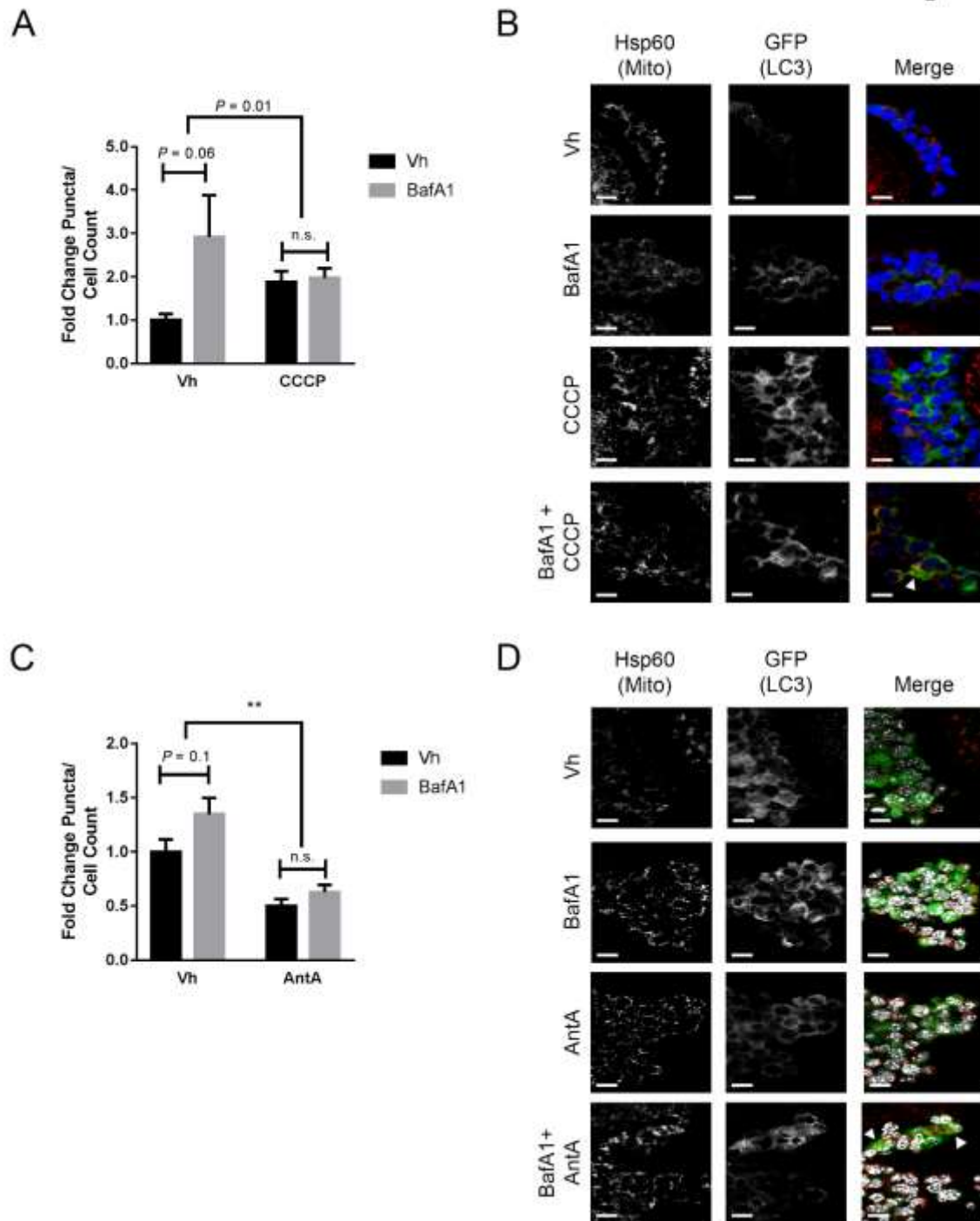
71

Figure 3

Figure 3- 3: GV oocytes remove LC3 puncta but do not activate mitophagy in response to mitochondria membrane depolarization.

Figure 3- 4: CCCP treatment does not reduce mtDNA in oocytes
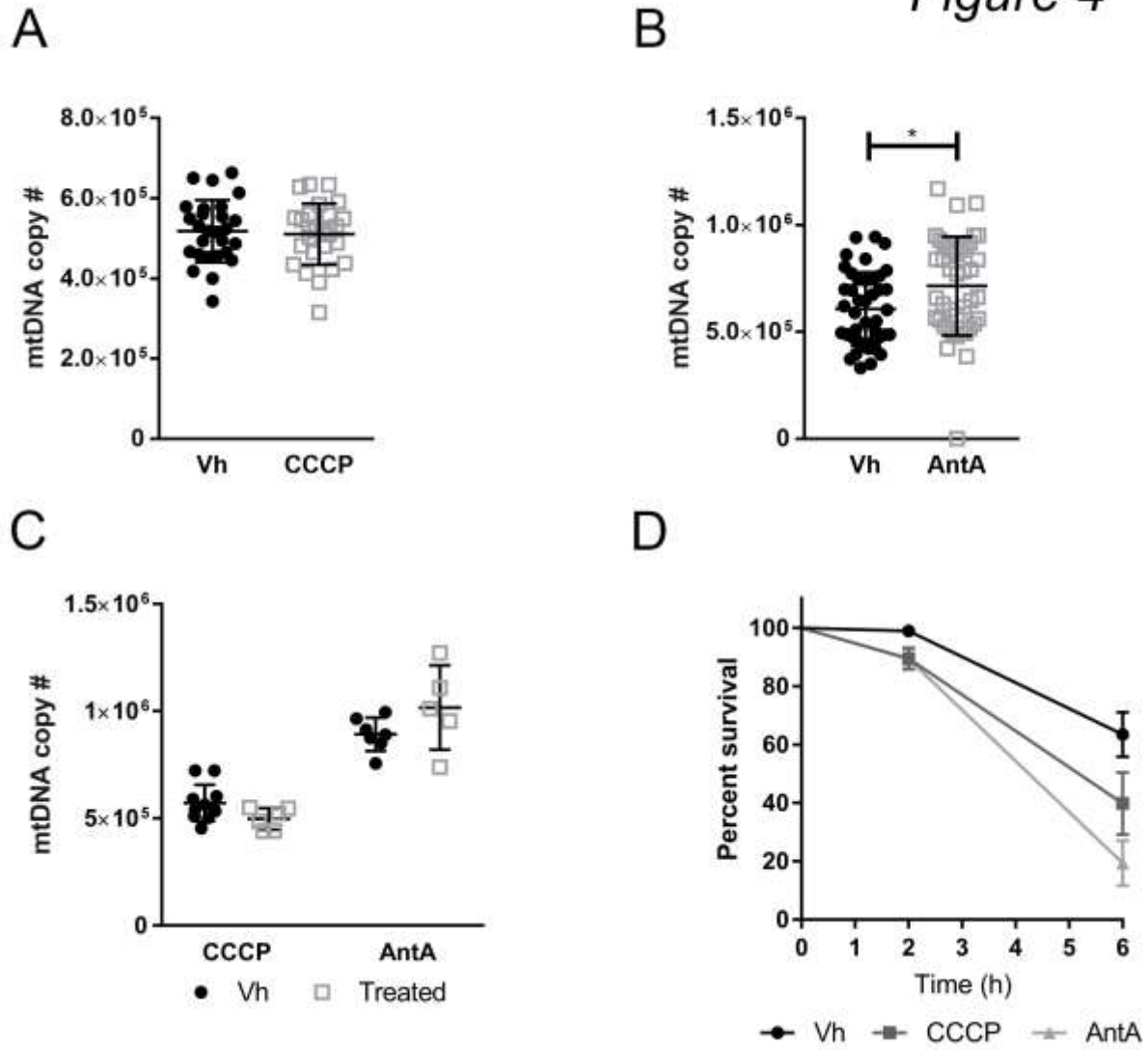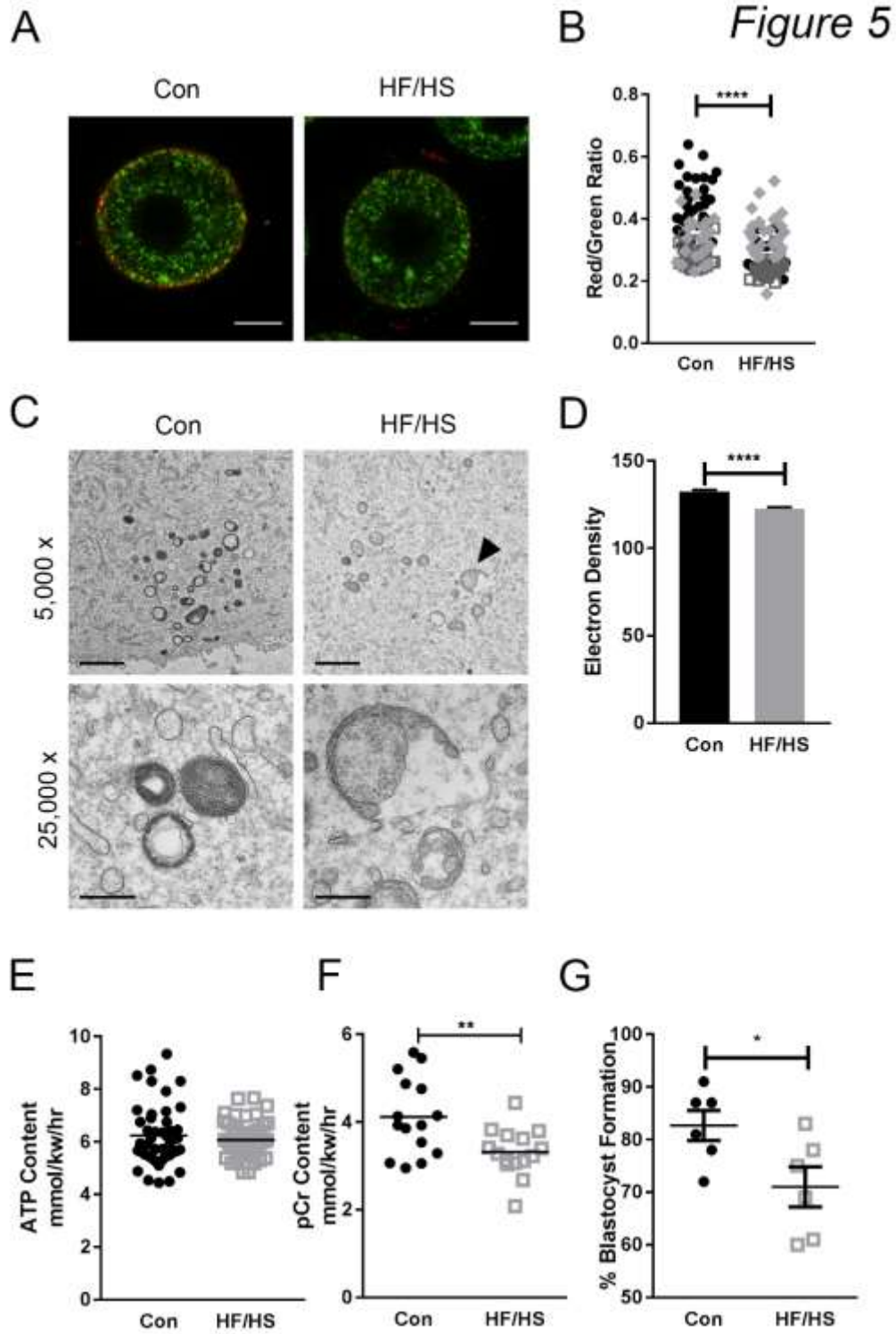
73

Figure 3- 5: Germinal vesicle stage oocytes from HF/HS diet fed mice have impaired metabolism.
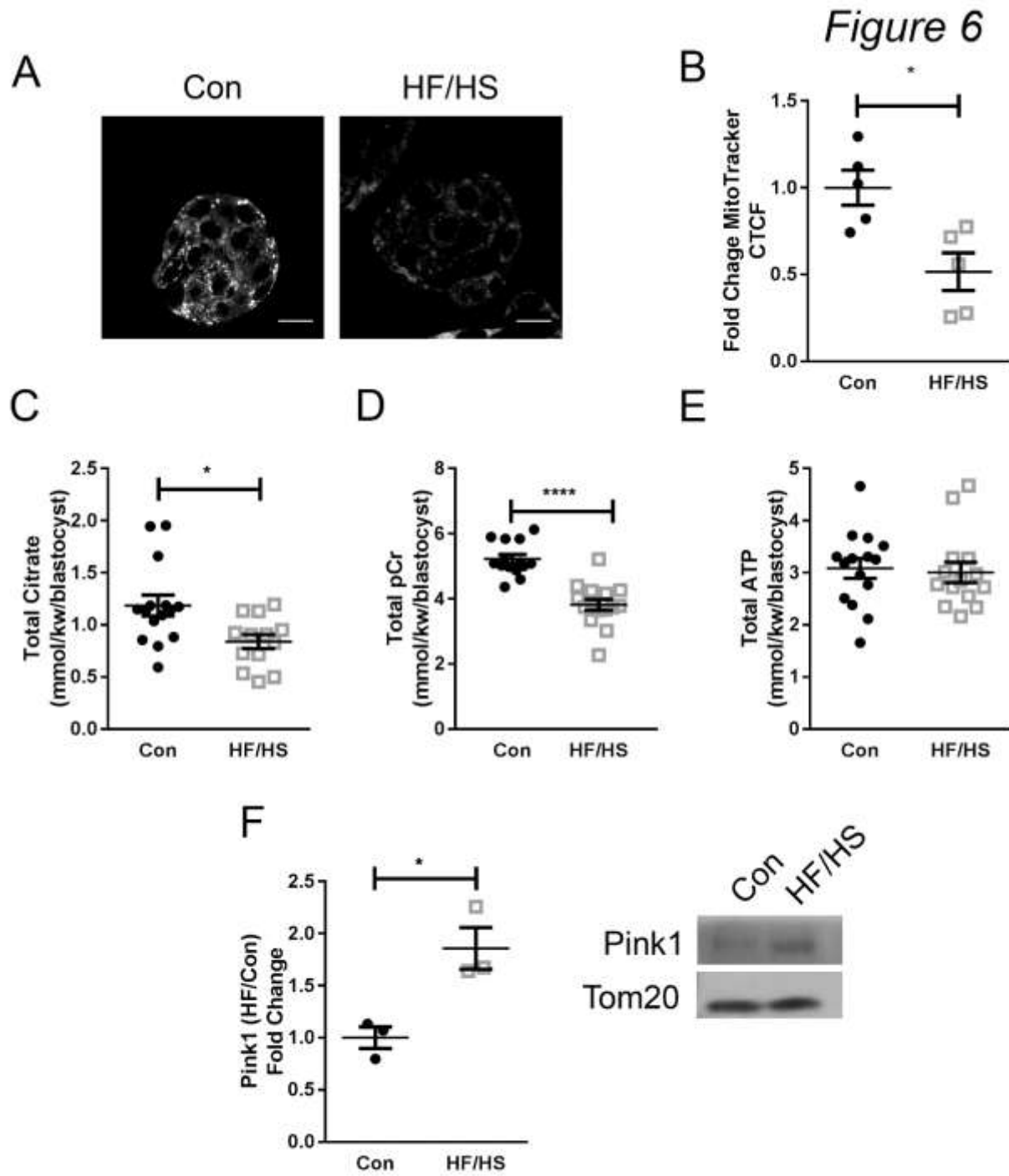
Figure 3- 6: IVF-generated blastocysts from HF/HS fed donor mouse oocytes have impaired metabolism and increased mitophagy.

3.8   Supplementary Figure Legends

Supplementary Figure 3-1: Dose response images of GV oocytes treated with 0 nM (DMSO vehicle) 50 nM BafA1 or 100 nM BafA1 to show 50 nM sufficiently prevents lysosome acidification. LysoTracker DND Red was used to assess lysosome pH, as the dye accumulates in lysosomes based on pH. Mitochondria were labeled with MitoTracker Green FM.

Supplementary Figure 3-2: (a) 20 µM CCCP or greater sufficiently depolarized mitochondria in murine embryonic fibroblasts. MitoTracker CMXRosamine was used to assess polarity. (b) mtDNA copy number is significantly reduced in MEFs after 24 hour treatment with CCCP.

Supplementary Figure 3-3: Phenotype of female HF/HS fed mice. (a) Body weights of mice fed a HF/HS diet for six weeks are significantly greater than mice fed standard mouse chow (Con). (b) Blood glucose is significantly elevated in HF/HS females after a 16 hour fast.
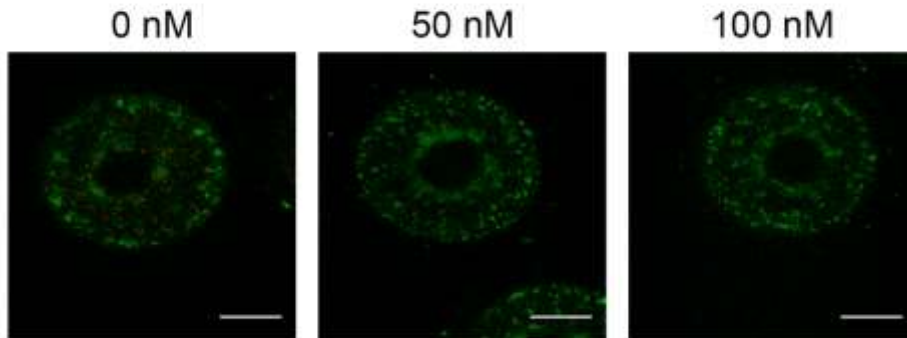
Supplementary Figure 3- 1: Dose response images of GV oocytes
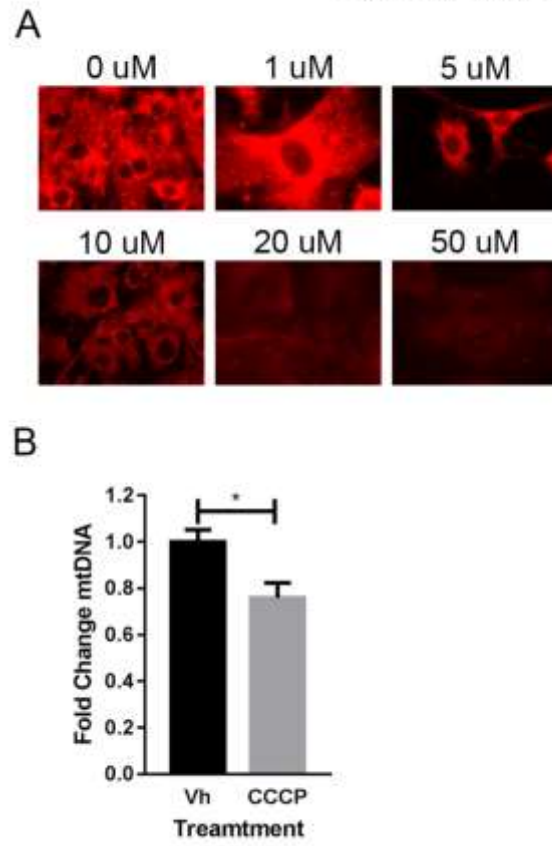
Supplementary Figure 3- 2: MEF positive controls.

A

B
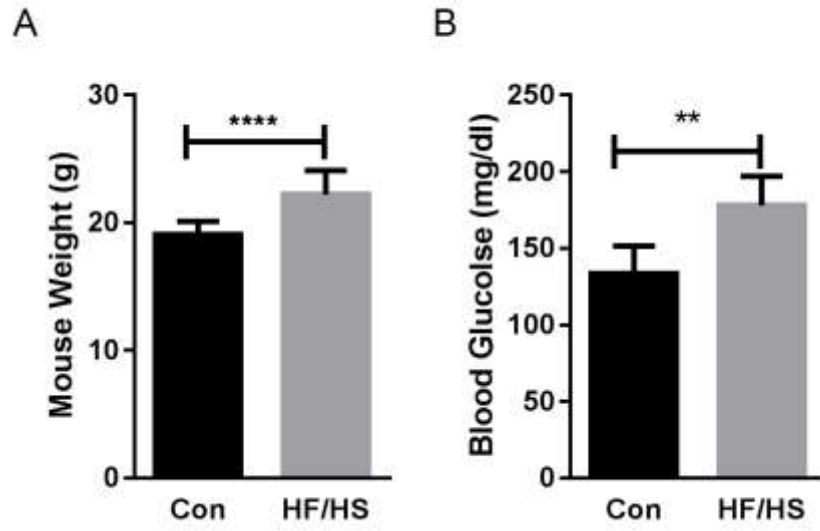
Supplementary Figure 3- 3:Phenotype of female HF/HS fed mice

Chapter 4: Maternal Obesity Disrupts Cardiac Mitochondrial Morphology and Sensitizes Female Offspring to Cardiovascular Disease

Anna Boudoures and Kelle Moley

Center for Reproductive and Health Sciences, Washington University in St. Louis, St. Louis, MO

4.1 Abstract

Cardiomyocytes are mitochondria-dense in order to meet the large energy demands of the continually beating heart. The morphology of the cardiac mitochondria is fine-tuned to support these energy demands – cardiac mitochondria have a very regular structure with numerous cristae to house the electron transport chain and generate ATP. Mitochondrial dynamics proteins dictate mitochondrial structure and therefore how mitochondria produce ATP. Recently, research in mouse models indicates dysregulation to mitochondrial dynamics cause progressively worsening heart failure. Maternal obesity is a risk factor for cardiovascular disease and causes changes to mitochondrial dynamics in other tissues, such as skeletal muscle. However, the effects of maternal obesity on heart mitochondria are not well understood. We hypothesized dysregulated mitochondrial dynamics in the cardiomyocytes from lean offspring of HF/HS fed mothers causes to diminished cardiomyocyte metabolic activity and heart failure. Our data indicate that female offspring born to HF/HS fed mothers develop dilated cardiomyopathy that worsens with age. These offspring also have abnormal cardiac mitochondria that have reduced oxidative phosphorylation capabilities. Additionally, there is reduced expression of the mitochondrial dynamics protein Optic Atrophy-1 (Opa1), indicating the abnormal mitochondria may result from altered mitochondrial dynamics. Our results provide dysregulated mitochondrial dynamics as one mechanism for why maternal obesity results in an increased risk in cardiovascular disease even in the absence of increased adiposity, which was previously thought to be the primary driver of cardiovascular disease.

4.2 Introduction

Dilated cardiomyopathy is one of the most prevalent causes of heart failure; it is the primary indication for heart transplant and accounts for 40 cases per 100,000 individuals globally (Weintraub et al., 2017). Dilated cardiomyopathy occurs when there is an expansion of the left ventricle (LV) without a thickening of the walls, leading to decreased myocardium strength and subsequently reduced capability of the heart to pump blood (Weintraub et al., 2017). Although the mechanisms leading to dilated cardiomyopathy are not fully understood, recent literature shows a link between mitochondrial dynamics and the development of dilated cardiomyopathy.

Maternal obesity has also been shown to be a risk factor for the development of cardiomyopathies and heart failure. Multiple human studies have looked at the predisposition of offspring to cardiovascular disease if their mother is obese. However, these studies are clouded by the fact that in humans, maternal obesity often results in adolescent consumption of an obesogenic diet and obesity (Gaillard et al., 2014; Godfrey et al., 2016). Since obesity is an independent risk factor for cardiovascular disease, it is challenging to outline if maternal obesity predisposes offspring to cardiovascular disease and the underlying mechanism. More controlled studies in mice show that maternal obesity does impart cardiovascular phenotypes in the offspring. For example, male offspring from obese mothers have contractile dysfunction, increased left ventricular diameter, and decreased ejection fraction (Blackmore et al., 2014; Fernandez-Twinn et al., 2012; Turdi et al., 2013). Further, these phenotypes were associated with changes in mitochondrial dynamics proteins.

Disruptions in mitochondrial dynamics can profoundly impact cardiomyocytes. These cells are mitochondria-dense cells and primarily utilize oxidative phosphorylation of fatty acids to obtain the ATP required to meet the high energetic demand of contraction and ion pumps (Ong et al., 2017). The heart relies predominantly on fatty acids under non-stressed conditions,

but can effectively use both fatty acids and glucose as carbon sources for oxidative phosphorylation. The heart switches to consume more glucose in times of increased stress (such as during exercise or in hypertension), as glucose produces more ATP per oxygen molecule, making it a more efficient substrate in terms of oxygen consumption (Stanley et al., 2005). The ability of the heart to switch between substrates in response to environmental and physiological changes, or metabolic flexibility, is critical to prevent heart failure and help the heart protect itself from damage. An inability to appropriately adjust substrate utilization based on energetic or environmental demands will eventually lead to heart failure, and disruptions in mitochondrial oxidative phosphorylation can reduce cardiac metabolic flexibility (Stanley et al., 2005).

Mitochondria are dynamic organelles constantly undergoing fusion and fission in order to maintain functionality. Fusion and fission occur to maintain mitochondrial DNA (mtDNA) integrity, repair mitochondrial damage, and facilitate intracellular communication. The mitofusins - Mitofusin 1 and Mitofusin 2 (Mfn 1 and Mfn2) - dictate outer mitochondrial membrane fusion and Optic Atrophy 1 (Opa1) mediates inner mitochondrial membrane fusion. The GTPase Dynamin Related Protein -1 (Drp1) regulates mitochondrial fission (Hall et al., 2014). The contribution of disrupted mitochondrial dynamics to the development of dilated cardiomyopathy is clearly shown in mice lacking both Mfn1 and Mfn2 in cardiomyocytes, which develop lethal dilated cardiomyopathy at 7-8wks of age (Chen et al., 2011). Furthermore, mice heterozygous for the fusion protein Opa1 develop dilated cardiomyopathy, albeit less severe than the Mfn1/Mfn2 double knockout model (Piquereau et al., 2012).

In addition to directly mediating mitochondrial fission and fusion, the dynamics proteins are also important cell signaling molecules. For example, Opa1 is an important mediator of insulin signaling in the heart. Evidence suggests that insulin may increase transcription of Opa1

via activation of mTOR and NFkB, resulting in structural changes to the mitochondria which allow for metabolic flexibility in the heart in response to metabolic substrate availability (Parra et al., 2014). Additionally, Opa1 mediates changes in cristae structure and mitochondrial electron transport chain supercomplex formation (Cogliati et al., 2013; Patten et al., 2014). Therefore, disruption to mitochondrial dynamics can influence not only the fusion of mitochondria, but also the way a cell utilizes and responds to metabolic substrate availability.

Work from our laboratory demonstrated that female progeny in the first (F1), second (F2), and third (F3) generations born to an obese dam in the parental (F0) generation have severe mitochondrial abnormalities and alterations to mitochondrial dynamics proteins including Opa1 and Mfn2 in their skeletal muscle (Saben et al., 2016). However, whether or not these abnormalities extend to cardiomyocytes is an open question. Therefore, we hypothesized that F0 exposure to a HF/HS diet results in damaged mitochondria in the hearts of female offspring that sensitizes these offspring to development of dilated cardiomyopathy. We further hypothesized the underlying mechanism for the cardiomyopathy results from metabolic inflexibility due to dysregulation of mitochondrial dynamics proteins.

4.3   Materials and Methods

Animals, Diet, and Breeding Paradigm

This study was carried out in strict accordance with the recommendations in the Guide for the Care and Use of Laboratory Animals of the National Institutes of Health. The protocol was approved by the IACUC-accredited Animal Studies Committee of Washington University School of Medicine (Study #20150034). Four-week-old female C57Bl/6J mice (Jackson Laboratories, Bar Harbor, ME) were fed either a high-fat/high-sugar (HF/HS; Test Diet 58R3, 35.8% hydrogenated coconut oil/17.5% sucrose by weight) diet or a diet of standard mouse chow (Lab Diet 5053, 13% Fat/3.25% sucrose by weight) ad libitum to produce the F0 generation. After six weeks of HF/HS feeding, estrous cycle stage was assessed daily and mice were mated to a lean male overnight when they were in proestrus or estrus. The next day, the male was removed from the cage to prevent prolonged exposure to the HF/HS diet and the female was checked for a vaginal plug. Chow fed females were treated identicaly. At three weeks of age, the offspring (F1 generation) were weaned onto a chow diet. When the F1 mice were 8 weeks old, the females were either mated to a lean male or sacrificed for tissue collection. F1 and F2 female mice from each F0 diet were continuously mated to lean males and offspring were weaned at three weeks of age.

Tissue Collection

F1, F2 and F3 female mice were fasted for six hours prior to being sacrificed at 8 weeks of age. Serum was collected via a facial vein puncture into serum separator tubes and spun at 15,000 rcf for 5 min at room temperature. After serum collection, mice were sacrificed by cervical dislocation. The heart was excised and the right ventricle and atria were dissected away.

The left ventricle was was weighed on a microbalance. The apical tip was utilized for electron microscopy, as described below. The remaining heart tissue was snap frozen in liquid nitrogen for protein and RNA isolation.

Echocardiography

Echocardiography was performed as described previously by the Washington University Mouse Cardiovascular Phenotyping Core Facility (DeBosch et al., 2014).

Transmission Electron Microscopy

The apical portion of the left ventricle of the heart was was fixed in 2% paraformaldehyde and 2.5% glutaraldehyde in cacodylate buffer for one hour prior to embedding in 2% agarose. Agarose blocks were fixed in 1% OsO_4 (Electron Microscopy Sciences, Hartfield, PA), stained in 1% uranyl acetate, and dehydrated in a series of ethanol washes. Next, agarose-embedded tissues were washed twice in propylene oxide (Electron Microscopy Science) and then infiltrated with resin by using the Eponate 12 Kit (Ted Pella, Redding, CA). After infiltration, blocks were embedded, cured, and then sectioned with a Leica Ultracut UCT ultramicrotome (Leica Microsystems Inc., Bannockburn, IL). Sections (90 nm) were stained with uranyl acetate and Reynolds' lead citrate before viewing at 3,000x - 20,000x magnification with a JEOL 1200 EX transmission electron microscope (JEOL USA Inc., Peabody, MA) equipped with an AMT 8-megapixel digital camera (Advanced Microscopy Techniques, Woburn, MA).

Mitochondria Morphology Analysis

Transmission electron micrographs were utilized to measure mitochondrial electron density, mitochondrial area, and mitochondrial roundness. All measurements were made in FIJI

(Schindelin et al., 2012). Briefly, the polygon tool was used to fit an approximate outline of individual mitochondria in a 5,000x image. The polygon was converted to a spline, and the border was adjusted to more closely fit the perimeter of the mitochondrion to measure the mean grey value, area (in nanometers), and roundness. Measurements for all mitochondria were compiled and appropriate statistical tests were applied as described in *Statistical Analysis*. Mitochondria were measured from at least seven images per mouse from at least three mice per experimental group.

Western Blot

The ventricles of the heart were lysed in RIPA buffer using the Bullet Blender bead homogenizer (Next Advance, Averill, NY) by adding approximately 10 0.9 – 2.0 mm stainless steel RNase free beads (Next Advance) to the tube and homogenizing five times for five minutes at setting 10. Protein was diluted in 4x NuPage LDS sample buffer (Invitrogen, Carlsbad, CA) and heated to 95°C for 5 min, except in the case of the OXPHOS cocktail, in which case protein was heated to 37°C for five min. After heating, 50μg of protein was loaded in each lane. All protein samples were subjected to SDS-PAGE on 10% acrylamide gels (BioRad), and transferred to nitrocellulose by using the iBlot® 2 Dry Blotting System (Thermo Fischer Scientific, Waltham, MA) at 20 V for 7 min. Blots were processed according to standard Western blot procedures and probed with primary antibodies listed in Table 4-1. Anti-rabbit or anti-mouse secondary antibodies (1:10,000, Cell Signaling Technologies) were used as appropriate, and signal was detected with SuperSignal™ West Pico Chemiluminescent Substrate (Thermo Fischer Scientific) and developed using the ChemiDoc (BioRad). All experiments were performed in triplicate. Relative protein levels were quantified in using the BioRad software and normalized to either Tom20 or total protein loaded in each lane detected with a Ponceau stain.

High Resolution Respirometry

After excision, the heart was immersed in cold BIOPS (10 mM EGTA, 50 mM MES, 0.5 mM DTT, 6.56 mM MgCL2, 5.77 mM ATP, 20 mM Imidazole, 15 mM phosphocreatine, pH 7.1) until fiber preparation. After all samples were collected, a piece of the inner wall of the left ventricle was isolated and fibers were separated on ice by using two sharp-tipped forceps under a dissection microscope. Separated fibers were permeabilized with BIOPS solution containing 50 μg/mL saponin for 30 minutes at 4 °C. Next, fibers were washed for 10 minutes in ice-cold mitochondrial respiration solution (MIR05, 0.5 mM EGTA, 3 mM MgCl2, 60 mM K-lactobionate, 20 mM taurin, 10 mM KH2PO4, 20 mM HEPES, 110 mM sucrose, 1 g/L BSA, pH 7.1). Fibers were weighed, blotted dry (3-5 mg total tissue weight) and placed in an Oxygraph 2K (OROBOROS Instruments, Innsbruck, Austria) chamber containing 2 mL of 37 °C MirO5. To measure O2 flux, the following substrates were added sequentially: either 5 mM malate, 10 mM glutamate and 10 mM succinate, or palmitoyl carnitine, 2.5 mM ADP, 2 μg/mL Oligomycin, followed by 3 pulses of 0.5 μM FCCP. A period of stabilization followed the addition of each substrate, and DatLab Software (OROBOROS Instruments, Innsbruck, Austria) was used to record oxygen flux per mass.

In Vitro Fertilization and Embryo Transfers

MII oocytes were collected from the ampullae of C57B6/J females 13 hours after superovulation with 5 IU human chorionic gonadotropin (Sigma Aldrich) which had been administered 46–48 hours after mice received 5 IU pregnant mare serum gonadotropin (Sigma Aldrich). Preparation of cauda epididymal sperm from a single male C57Bl6/J mouse, insemination, and embryo culture were performed as described previously (Kim and Moley,

89

2008). 24 hours after fertilization, two-cell embryos were surgically transferred to the ampullae of a lean ICR recipient (Envigo, Huntingdon, Cambridgeshire, United Kingdom).

RNA isolation and Quantitative Reverse Transcription PCR

Left ventricle tissue was homogenized in Trizol Reagent (Invitrogen, Carlsbad, CA) using the Bullet Blender bead homogenizer (Next Advance, Averill, NY) by adding approximately 10 0.9 – 2.0 mm stainless steel RNase free beads (Next Advance) to the tube and homogenizing five times for five minutes at setting 10. RNA was extracted per manufacturer's protocol. RNA quantity and quality was measured on a Nanodrop. 1 μg of RNA was reverse transcribed using the QuantiTect Reverse Transcription kit (Quiagen) according to the manufacturer's protocol. Transcript level was measured using the TaqMan Gene Expression 2X Master Mix (Catalog No: 4370074, Thermo Fisher Scientific) and the TaqMan Gene Expression 20X Assays listed in Table 4-2. Expression of genes for each diet was normalized to beta actin using the $\Delta\Delta C_T$ method and reaction kinetics were monitored using an inter-run control sample.

Statistical Analyses

All data was analyzed using Graphpad Prism 8. Each generation was analyzed independently using a Student's T-test to compare effect of F0 diet exposure. At least three mice per F0 diet exposure were used per experiment. All data is reported as mean $\pm$ standard error.

4.4   Results

Our laboratory has developed a transgenerational colony of mice in which the parental generation (F0) females were fed an obesogenic high fat/high sugar diet (HF/HS, 35.8% hydrogenated coconut oil/17.5% sucrose by weight) prior to and during pregnancy as well as during lactation (Saben et al., 2016). Subsequent generations (F1-F3) are all fed a control diet in order to understand the consequences of obesity during pregnancy on multiple generation of offspring, even if those offspring are lean.

We first asked if female mice in the F1 generation from HF/HS dams exhibit dysfunctional cardiac phenotypes, such as dilated cardiomyopathy, independent of consumption of a HF/HS diet themselves. To do so, we subjected offspring of HF/HS or chow fed dams to echocardiography under light general anesthetic. At 8 weeks of age, female mice from HF/HS mothers displayed a trend towards dilated cardiomyopathy as evidenced by an increase in left ventricular (LV) end diameter in systole and diastole (Figure 1 A-B). Additionally, they had a significant reduction in fractional shortening (Figure 1C) and a subtle reduction in the ratio of intraventricular contraction time to the ejection time of the left ventricle (Figure 1 D); geometrical and velocity-based parameters of the ability of the left ventricle to efficiently supply blood to the body (Stypmann et al., 2009). These phenotypes were present in the absence of an increase in body weight (Figure 1 E), heart size indexed to body weight (Figure 1 F), and diastolic heart failure as measured by the E/E' ratio (Figure 1 G).

At 42 weeks of age, F1 female mice from HF/HS dams exhibited more noticeable signs of systolic heart failure and dilated cardiomyopathy. The HF/HS offspring had a significant increase in the LV end diameter (Figure 2 A-B), a significant decrease in the fractional shortening (Figure 2 C) and a significant decrease in the ratio of intraventricular contraction time to the ejection time of the left ventricle (Figure 2D) in the absence to a change in body weight

and heart size (Figure 2E-F). There was also evidence of diastolic heart failure, evidenced by a significant decrease in the ratio of E/E' (Figure 2G), the clinically accepted measure of atrial pressure (Park and Marwick, 2011). This data suggests that the mice from a HF/HS dam are developing dilated cardiomyopathy.

Previous research in heart failure indicates that disruption to mitochondrial dynamics can lead to dilated cardiomyopathy, heart failure, and sensitivity to ischemia/reperfusion damage (Hall et al., 2014). Because these mice exhibit severe mitochondrial damage in their skeletal muscle which was linked to altered insulin signaling and mitochondrial dynamics, (Saben et al., 2016) we hypothesized the same may be the case in the hearts of these mice, due to the high density of mitochondria in cardiomyocytes and the important role mitochondrial dynamics play in maintaining a healthy mitochondrial population (Hall et al., 2014).

To begin, we assessed the mitochondrial morphology by electron microscopy and ETC proteins were measured by western blot. HF/HS F1 had significant changes to their mitochondria; specifically, larger mitochondria with reduced electron density and abnormal cristae (Figure 3A-C). Additionally, these changes persisted for three generation of female progeny, as EM from F2 and F3 progeny looked similar to images from the F1 generation (Figure 3D-I). In the F1 generation, mice had a significant reduction in complexes I and II (CI and CII, respectively) and a trend towards a reduction in complex V (Figure 4A-B). However, in the F2 and F3 generations, ETC protein expression remained unchanged (Figure 4C).

The changes to mitochondrial structure and dysregulation of ETC proteins led us to ask if there were subsequent function changes in oxidative phosphorylation (OXPHOS), which occurs in the cristae of the mitochondrial matrix (Friedman and Nunnari, 2014). To do so, we used high-resolution respirometry of permeabilized LV fibers and utilized succinate, malate, and pyruvate

to specifically enhance carbohydrate-stimulated OXPHOS (Lark et al., 2016). In concordance with previous data in skeletal muscle, HF/HS F1 had significant reduction in state 3 respiration through complexes I and II independent of a change in leak respiration (Figure 4D-F). These data indicate the reduction in CI and CII protein expression, and/or disrupted cristae integrity, results in decreased ETC functionality and carbohydrate metabolism via OXPHOS.

EM images showing damaged mitochondria with disarrayed cristae in multiple generations of progeny from a HF/HS F0 generation led me to hypothesize the abnormal mitochondria could be an inherited, epigenetic consequence of obesity since all mitochondria are inherited maternally (Piko and Taylor, 1987). To test this hypothesis, female mice fed a HF/HS diet were superovulated and the oocytes were utilized for *in vitro* fertilization. Oocytes that successfully fertilized and developed to the two-cell stage were transferred into lean recipient dams (Figure 5A). Female offspring were sacrificed at 8 weeks and heart tissue was collected for EM. Images revealed that exposure to a HF/HS diet prior to conception was sufficient to induce abnormal cristae formation, a significant reduction in electron density of mitochondria, and a trend towards increased mitochondrial area (Figure 5B-D).

Our data from EM images, ETC function, and ETC protein expression led us to next hypothesized Opa1 may also be downregulated in the myocardium of these progeny. We based this on two pieces of evidence; the known role of Opa1 in mitochondrial fusion, maintenance of mtDNA, and cristae structure and our previously published data that Opa1 is downregulated in HF/HS progeny skeletal muscle (Cogliati et al., 2013; Friedman and Nunnari, 2014; Saben et al., 2016). In line with this hypothesis, HF/HS F1 females have approximately a 50% reduction of Opa1 protein expression as compared to control F1 mice (Figure 6A-B). However, Mfn2 protein expression is unchanged in female offspring hearts (Figure 6C). This supports our hypothesis and

suggests that decreased Opa1 expression in the heart may explain the disorganized cristae structure and decreased ETC expression observed.

Alterations to cristae structure and mitochondrial dynamics were not the only observed phenotype in the HF/HS lineage. EM revealed an increase in the presence of cardiac lipid droplets which persisted across three generations of control-fed offspring from F0 dams fed a HF/HS diet (Figure 7A-B). This accumulation of lipid was associated with a subtle but significant increase in the 4-HNE modified proteins, which occurs during lipotoxicity (Figure 7C-D). To begin to assess the mechanism of the lipid accumulation, we took a three pronged approach and collected preliminary data to assess fatty acid oxidation (FAO) activity, increased lipid uptake, and decreased lipid catabolism.

To measure changes in FAO, we utilized high resolution respirometry in the F1 generation or protein expression in the F2 and F3 generations. High resolution respirometry experiments with palmitoylcarnitine as a substrate to preferentially drive permeabilized fibers to utilize FAO (Lanza et al., 2009). However, there was no difference in the respiration of permeabilized fibers from F1 HF/HS females as compared to controls (Figure 7E-G). In the F2 and F3 generations, protein expression of hydroxylacyl-CoA dehydrogenase, a key FAO enzyme, was unchanged (Figure 7H-I). Taken together, these data suggest FAO impairment may not cause the observed lipid accumulation.

Alternately, increased lipid uptake may cause increased lipid accumulation. To this end, we measured transcript levels of CD36, one of the primary fat transporters into the cell. However, CD36 was downregulated at the transcript level in F2 and unchanged in F3 hearts from HF/HS F0 dams (Figure 7J-K), suggesting the lipid accumulation was not a result of increased import of fat into the heart.

94

Finally, previous research has shown mice lacking adipose triglyceride lipase (ATGL) have increased cardiac lipid accumulation and die significantly earlier than control littermates (Haemmerle et al., 2006; Haemmerle et al., 2011). Supportive of this hypothesis, ATGL was downregulation at the transcript level in F2 and F3 progeny from the HF/HS lineage (Figure 7L-M).

4.5   Discussion

Our preliminary data suggest pre- and post-conception changes to mitochondria predispose offspring to cardiovascular disease. We show here that female F1 offspring begin to develop moderate dilated cardiomyopathy. This may be due to decreased Opa1 protein, which results in abnormal cristae structure that reduces OXPHOS respiration. Decreased respiration may cause the observed accumulation of lipid which then induces lipotoxicity, reinforcing the inherited mitochondrial damage.

Transgenerational Effects of a HF/HS Diet on Cardiac Function

In our initial studies, we chose to focus solely on females because effects of HFD on cardiovascular health in the offspring has previously only been shown in males (Blackmore et al., 2014; Turdi et al., 2013). Similar to males, female mice from HF/HS dams display an age-dependent progressive worsening dilated cardiomyopathy. Additionally, stressing male mice from HFD fed mothers results in development of a more severe phenotype (Turdi et al., 2013). We anticipate such will be the case with females as well, and are planning to expose F1 females to a HF/HS diet in order to test this hypothesis.

Similar to skeletal muscle, cardiomyocytes appear to be susceptible to the transgenerational consequences of maternal HF/HS diet exposure (Figure 3). Future studies will continue to investigate the molecular signature of not only cardiac tissue from F1 mice, but also

F2 and F3 generations. These studies will also be extended to encompass the effects of HF/HS maternal exposure prior to conception by utilizing embryo transfer studies, since mitochondrial morphology changes appear to be programmed prior to conception (Figure 5). Future studies will be aimed at comparing the molecular signature of cardiomyocytes from embryo transfer offspring to naturally mated offspring to determine if this results from similar changes in Opa1 protein expression or via an alternate mechanism. Previous embryo transfer studies indicate mitochondrial dysfunction may be programmed at the level of the oocyte, prior to conception, since offspring fertilized from obese donor oocytes have increased body weights and impaired glucose tolerance (Huypens et al., 2016).

Dysregulation of Mitochondrial Dynamics in Cardiomyocytes

Much of our data points to dysregulation of mitochondrial dynamics proteins, which drive the development of dilated cardiomyopathy potentially via dysregulation of electron transport chain (ETC) supercomplex formation. Opa1 heterozygotes display similar mitochondrial morphology in cardiomyocytes as our HF/HS offspring (Piquereau et al., 2012). This includes an increase in mitochondrial area and disarrayed cristae structure. Opa1 has an important roles in maintaining appropriate levels of mtDNA, likely via promoting mitochondrial fusion (Cogliati et al., 2013; Patten et al., 2014). Because mtDNA carries genes for key ETC complex proteins, maintaining appropriate levels insure subsequent levels of ETC proteins are maintained (Shadel and Clayton, 1997). Because we see a decrease in ETC proteins and Opa1, there may be a link between the decreased expression of both. We plan to address if the observed decrease of ETC proteins is due to a reduction of mtDNA copy number in the future. Additionally, it will be important to attempt to rescue the expression of ETC proteins by

pharmacologically or genetically enhancing Opa1 expression to determine the mechanism driving the reduction in ETC expression.

Opa1 also interacts with mitochondrial solute carriers required for OXPHOS. Opa1 complexes with proteins that transport malate and succinate into the mitochondria, which are required for completion of OXPHOS. However, metabolism of fatty acid oxidation substrates, such as palmitoylcarnitine, does not change in response to variation in Opa1 levels or activity (Patten et al., 2014). Given that in the F1 HF/HS hearts we observe a deficiency in malate and succinate driven respiration (Figure 4), but not palmitoylcarnitine respiration (Figure 7), in addition to disarrayed cristae and downregulation of Opa1, suggest that impaired ETC supercomplex formation is driving our observed phenotypes.

Appropriate formation of ETC proteins into different supercomplexes mediates metabolic flexibility within the cell (Lapuente-Brun et al., 2013). To determine if our observed downregulation of Opa1 is causing disruption of supercomplex proteins, which may mediate the observed disruption of State 3 respiration with carbohydrate substrates, we will employ blue native gel electrophoresis of mitochondrial preparations isolated from cardiomyocytes to measure levels and composition of supercomplexes within cardiomyocytes from each generation.

The observed downregulation of Opa1 in our HF/HS progeny is potentially mediated by alterations to insulin signaling in the hearts of the HF/HS exposed offspring. Female progeny have previously been shown to have altered insulin signaling in skeletal muscle (Saben et al., 2016). Additionally, insulin signaling mediates Opa1 expression (Parra et al., 2014). While we have yet to measure insulin signaling proteins and mTOR in our samples, this will be important in determining if there is a similar link between glucose metabolism and our observed decreased Opa1 expression.

Inappropriate Lipid Droplet Catabolism in Cardiomyocytes

Another striking phenotype observed in EM images was a significant accumulation of lipid droplets. Lipid is stored in droplets as a mechanism to prevent lipotoxic damage to cells that can be induced by free fatty acids (Brindley et al., 2010). Previously, knockout of adipose triglyceride lipase (ATGL), which is responsible for lipid droplet catabolism in the heart, results in cardiac lipid accumulation (Haemmerle et al., 2006). Additionally, mice with a cardiomyocyte specific knockout of ATGL showed decreased fatty acid transporter gene expression, increased mitochondrial size, decreased CI and CII ETC protein expression, and decreased State 3 respiration, all phenotypes we observed in our HF/HS progeny (Haemmerle et al., 2011). Future studies should be directed towards assessing whether ATGL is dysregulated in HF/HS progeny cardiomyocytes.

Conclusions

In conclusion, maternal exposure to a HF/HS diet predisposes female progeny to cardiac mitochondrial damage which is associated with progressively worsening dilated cardiomyopathy. We have shown this may be programmed prior to conception. However, the data presented here is preliminary and warrants extensive experimentation to definitively link mitochondrial dynamics and cardiac dysfunction in offspring. However, understanding this mechanistic link will aid in our understanding of how and why cardiovascular disease develops.

4.6   References

Blackmore, H.L., Niu, Y., Fernandez-Twinn, D.S., Tarry-Adkins, J.L., Giussani, D.A., Ozanne, S.E., 2014. Maternal diet-induced obesity programs cardiovascular dysfunction in adult male mouse offspring independent of current body weight. Endocrinology 155, 3970-3980.

Brindley, D.N., Kok, B.P., Kienesberger, P.C., Lehner, R., Dyck, J.R., 2010. Shedding light on the enigma of myocardial lipotoxicity: the involvement of known and putative regulators of fatty acid storage and mobilization. American journal of physiology. Endocrinology and metabolism 298, E897-908.

Chen, Y., Liu, Y., Dorn, G.W., 2nd, 2011. Mitochondrial fusion is essential for organelle function and cardiac homeostasis. Circulation research 109, 1327-1331.

Cogliati, S., Frezza, C., Soriano, M.E., Varanita, T., Quintana-Cabrera, R., Corrado, M., Cipolat, S., Costa, V., Casarin, A., Gomes, L.C., Perales-Clemente, E., Salviati, L., Fernandez-Silva, P., Enriquez, J.A., Scorrano, L., 2013. Mitochondrial cristae shape determines respiratory chain supercomplexes assembly and respiratory efficiency. Cell 155, 160-171.

DeBosch, B.J., Kluth, O., Fujiwara, H., Schurmann, A., Moley, K., 2014. Early-onset metabolic syndrome in mice lacking the intestinal uric acid transporter SLC2A9. Nature communications 5, 4642.

Fernandez-Twinn, D.S., Blackmore, H.L., Siggens, L., Giussani, D.A., Cross, C.M., Foo, R., Ozanne, S.E., 2012. The programming of cardiac hypertrophy in the offspring by maternal obesity is associated with hyperinsulinemia, AKT, ERK, and mTOR activation. Endocrinology 153, 5961-5971.

Friedman, J.R., Nunnari, J., 2014. Mitochondrial form and function. Nature 505, 335-343.

Gaillard, R., Steegers, E.A., Duijts, L., Felix, J.F., Hofman, A., Franco, O.H., Jaddoe, V.W., 2014. Childhood cardiometabolic outcomes of maternal obesity during pregnancy: the Generation R Study. Hypertension (Dallas, Tex. : 1979) 63, 683-691.

Godfrey, K.M., Reynolds, R.M., Prescott, S.L., Nyirenda, M., Jaddoe, V.W., Eriksson, J.G., Broekman, B.F., 2016. Influence of maternal obesity on the long-term health of offspring. The lancet. Diabetes & endocrinology.

Haemmerle, G., Lass, A., Zimmermann, R., Gorkiewicz, G., Meyer, C., Rozman, J., Heldmaier, G., Maier, R., Theussl, C., Eder, S., Kratky, D., Wagner, E.F., Klingenspor, M., Hoefler, G., Zechner, R., 2006. Defective lipolysis and altered energy metabolism in mice lacking adipose triglyceride lipase. Science (New York, N.Y.) 312, 734-737.

Haemmerle, G., Moustafa, T., Woelkart, G., Buttner, S., Schmidt, A., van de Weijer, T., Hesselink, M., Jaeger, D., Kienesberger, P.C., Zierler, K., Schreiber, R., Eichmann, T., Kolb, D.,

Kotzbeck, P., Schweiger, M., Kumari, M., Eder, S., Schoiswohl, G., Wongsiriroj, N., Pollak, N.M., Radner, F.P., Preiss-Landl, K., Kolbe, T., Rulicke, T., Pieske, B., Trauner, M., Lass, A., Zimmermann, R., Hoefler, G., Cinti, S., Kershaw, E.E., Schrauwen, P., Madeo, F., Mayer, B., Zechner, R., 2011. ATGL-mediated fat catabolism regulates cardiac mitochondrial function via PPAR-alpha and PGC-1. Nature medicine 17, 1076-1085.

Hall, A.R., Burke, N., Dongworth, R.K., Hausenloy, D.J., 2014. Mitochondrial fusion and fission proteins: novel therapeutic targets for combating cardiovascular disease. British journal of pharmacology 171, 1890-1906.

Huypens, P., Sass, S., Wu, M., Dyckhoff, D., Tschop, M., Theis, F., Marschall, S., Hrabe de Angelis, M., Beckers, J., 2016. Epigenetic germline inheritance of diet-induced obesity and insulin resistance. Nature genetics 48, 497-499.

Lapuente-Brun, E., Moreno-Loshuertos, R., Acin-Perez, R., Latorre-Pellicer, A., Colas, C., Balsa, E., Perales-Clemente, E., Quiros, P.M., Calvo, E., Rodriguez-Hernandez, M.A., Navas, P., Cruz, R., Carracedo, A., Lopez-Otin, C., Perez-Martos, A., Fernandez-Silva, P., Fernandez-Vizarra, E., Enriquez, J.A., 2013. Supercomplex assembly determines electron flux in the mitochondrial electron transport chain. Science (New York, N.Y.) 340, 1567-1570.

Lark, D.S., Torres, M.J., Lin, C.T., Ryan, T.E., Anderson, E.J., Neufer, P.D., 2016. Direct real-time quantification of mitochondrial oxidative phosphorylation efficiency in permeabilized skeletal muscle myofibers. American journal of physiology. Cell physiology 311, C239-245.

Ong, S.B., Kalkhoran, S.B., Hernandez-Resendiz, S., Samangouei, P., Ong, S.G., Hausenloy, D.J., 2017. Mitochondrial-Shaping Proteins in Cardiac Health and Disease - the Long and the Short of It! Cardiovascular drugs and therapy.

Park, J.H., Marwick, T.H., 2011. Use and Limitations of E/e' to Assess Left Ventricular Filling Pressure by Echocardiography. Journal of cardiovascular ultrasound 19, 169-173.

Parra, V., Verdejo, H.E., Iglewski, M., Del Campo, A., Troncoso, R., Jones, D., Zhu, Y., Kuzmicic, J., Pennanen, C., Lopez-Crisosto, C., Jana, F., Ferreira, J., Noguera, E., Chiong, M., Bernlohr, D.A., Klip, A., Hill, J.A., Rothermel, B.A., Abel, E.D., Zorzano, A., Lavandero, S., 2014. Insulin stimulates mitochondrial fusion and function in cardiomyocytes via the Akt-mTOR-NFkappaB-Opa-1 signaling pathway. Diabetes 63, 75-88.

Patten, D.A., Wong, J., Khacho, M., Soubannier, V., Mailloux, R.J., Pilon-Larose, K., MacLaurin, J.G., Park, D.S., McBride, H.M., Trinkle-Mulcahy, L., Harper, M.E., Germain, M., Slack, R.S., 2014. OPA1-dependent cristae modulation is essential for cellular adaptation to metabolic demand. The EMBO journal 33, 2676-2691.

Piko, L., Taylor, K.D., 1987. Amounts of mitochondrial DNA and abundance of some mitochondrial gene transcripts in early mouse embryos. Developmental biology 123, 364-374.

Piquereau, J., Caffin, F., Novotova, M., Prola, A., Garnier, A., Mateo, P., Fortin, D., Huynh, L.H., Nicolas, V., Alavi, M.V., Brenner, C., Ventura-Clapier, R., Veksler, V., Joubert, F., 2012. Down-regulation of OPA1 alters mouse mitochondrial morphology, PTP function, and cardiac adaptation to pressure overload. Cardiovascular research 94, 408-417.

Saben, J.L., Boudoures, A.L., Asghar, Z., Thompson, A., Drury, A., Zhang, W., Chi, M., Cusumano, A., Scheaffer, S., Moley, K.H., 2016. Maternal Metabolic Syndrome Programs Mitochondrial Dysfunction via Germline Changes across Three Generations. Cell reports 16, 1-8.

Schindelin, J., Arganda-Carreras, I., Frise, E., Kaynig, V., Longair, M., Pietzsch, T., Preibisch, S., Rueden, C., Saalfeld, S., Schmid, B., Tinevez, J.Y., White, D.J., Hartenstein, V., Eliceiri, K., Tomancak, P., Cardona, A., 2012. Fiji: an open-source platform for biological-image analysis. Nature methods 9, 676-682.

Shadel, G.S., Clayton, D.A., 1997. Mitochondrial DNA maintenance in vertebrates. Annual review of biochemistry 66, 409-435.

Stanley, W.C., Recchia, F.A., Lopaschuk, G.D., 2005. Myocardial substrate metabolism in the normal and failing heart. Physiological reviews 85, 1093-1129.

Stypmann, J., Engelen, M.A., Troatz, C., Rothenburger, M., Eckardt, L., Tiemann, K., 2009. Echocardiographic assessment of global left ventricular function in mice. Laboratory animals 43, 127-137.

Turdi, S., Ge, W., Hu, N., Bradley, K.M., Wang, X., Ren, J., 2013. Interaction between maternal and postnatal high fat diet leads to a greater risk of myocardial dysfunction in offspring via enhanced lipotoxicity, IRS-1 serine phosphorylation and mitochondrial defects. J Mol Cell Cardiol 55, 117-129.

Weintraub, R.G., Semsarian, C., Macdonald, P., 2017. Dilated cardiomyopathy. Lancet.

4.7   Figure Legends

Figure 4-1: 8 week old female offspring of HF/HS exposed dams show a trend toward dilated cardiomyopathy. Left Ventricular (LV) inner diameter in (A) systole and (B) diastole. (C) Fractional shortening of the long axis of the heart. (D) Isovolumetric contration time (ICVT) normalized to the ejection time (ET) of the left ventricle. (E) Body weight of mice utilized (g). (F) LV mass normalized to body weight. (G) Heart rate. (H) Peak mitral flow velocity, E, normalized to the peak velocity of early mitral annular velocity, E'. N=4 mice/group; * indicates $P < 0.05$, student's T-test.

Figure 4-2: 42 week old female offspring of HF/HS exposed dams are developing dilated cardiomyopathy. Left Ventricular (LV) inner diameter in (A) systole and (B) diastole. (C) Fractional shortening of the long axis of the heart. (D) Isovolumetric contration time (ICVT) normalized to the ejection time (ET) of the left ventricle. (E) Body weight of mice utilized (g). (F) LV mass normalized to body weight. (G) Heart rate. (H) Peak mitral flow velocity, E, normalized to the peak velocity of early mitral annular velocity, E'. N=4 mice/group; * $P < 0.05$, ** $P < 0.01$, *** $P < 0.001$; Student's T-test.

Figure 4-3: Cardiomyocyte mitochondria from HF/HS F1 generation progeny have changes to mitochondrial ultrastructure. F1 offspring cardiomyocyte mitochondria (A) electron density, (B) mitochondrial area (um^2), and (C) representative electron micrographs showing changes to cristae structure. * $P < 0.05$, ** $P < 0.01$, *** $P < 0.001$; Student's T-test; scale bar 2 um.

Figure 4-4: Cardiomyocyte mitochondria from HF/HS F2 generation progeny have changes to mitochondrial ultrastructure. (A) electron density, (B) mitochondrial area (nm2) and (C) representative EM. * $P < 0.05$, ** $P < 0.01$, *** $P < 0.001$; Student's T-test; scale bar 2 um.

Figure 4-3: Cardiomyocyte mitochondria from HF/HS F3 generation progeny have changes to mitochondrial ultrastructure. (A) electron density (B) mitochondria area, and (C) representative EM. * $P <0.05$, ** $P < 0.01$, *** $P < 0.001$; Student's T-test; scale bar 2 um.

Figure 4-6: F1 offspring from HF/HS mothers have significant changes to their electron transport chain protein and respiration capabilities. (A) representative western blot showing electron transport chain protein expression and (B) quantitation of the western blot. (C) Oxidative phosphorylation (OXPHOS) respiration levels, (D) Leak respiration levels, and (E) a ratio of OXPHOS/lead levels measured by high resolution respirometery. N=4 mice/group.

Figure 4-7: Embryo transfer offspring display similar mitochondrial phenotypes to naturally mated F1 offspring. (A) Schematic representation of experimental design. (B) Electron density and (C) mitochondrial area of individual mitochondria measured from EM. (D) Representative EM of cardiomyocyte from control (Con) and HF/HS exposed donor mothers. *** $P < 0.001$; Student's T-test.

Figure 4-8: Mitochondrial dynamics protein expression is altered in naturally mated F1 offspring from HF/HS exposed dams. (A) Representative western blot for Opa1 and Mfn2. (B) Densitometery of Opa1 long (L) and short (S) isoforms. (C) Densiotmetery of Mfn2 protein expression. ** $P < 0.01$,; Student's T-test.

Figure 4-9: Progeny from a HF/HS exposed F0 generation show signs of lipotoxicity in the absence of impaired fatty acid oxidation. (A) average number of lipid droplets counted per EM of cardiomyocytes. Generation is inidicated on the X-axis; data is represented as mean +/- SEM. (B) Representative western blot for 4-HNE in F2 and F3 progeny with (C) densitometery of the 55 kD band and 22 kD band.

Figure 4-10: Fatty acid oxidation capacity of heart mitochondria is unchanged in F1 offspring from HF/HS dams. (A-C) High resolution respirometry utilizing the fatty acid substrate palmitolycarnitine shows no change in (A) OXPHOS, (B) Leak, or (C) the ratio of OXPHOS to leak respiration in F1 LV fiber mitochondria. (D) Western blot of hydroxyacyl-CoA dehydrogenase (HADH) protein from F2 and F3 generation heart muscle. (E) Densiotometery of HADH western blot normalized to GAPDH.

Figure 4-11: Changes to the transcript levels of a fat transporter and lipolysis enzyme in cardiac tissue from HF/HS progeny. Transcript levels of the fat transporter CD36 in the LV of (A) F2 and (B) F3 progeny. Transcript levels of adipose triglyceride lipase (ATGL) in heart tissue from (C) F2 and (D) F3 progeny. * $P < 0.05$, ** $P < 0.01$, *** $P < 0.001$; Student's T-test.
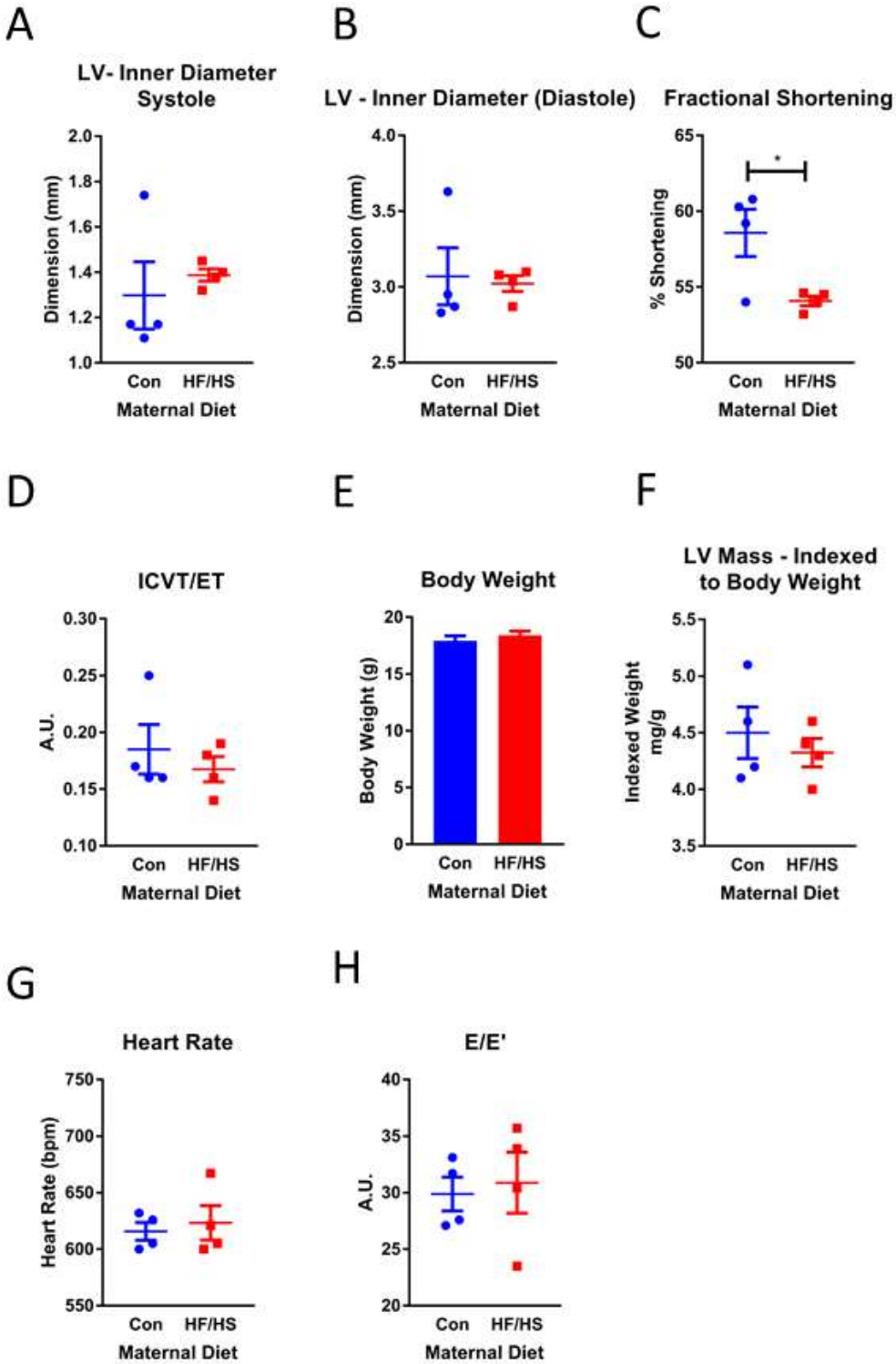
Figure 4- 1: 8 week old female offspring of HF/HS exposed dams show a trend toward dilated cardiomyopathy
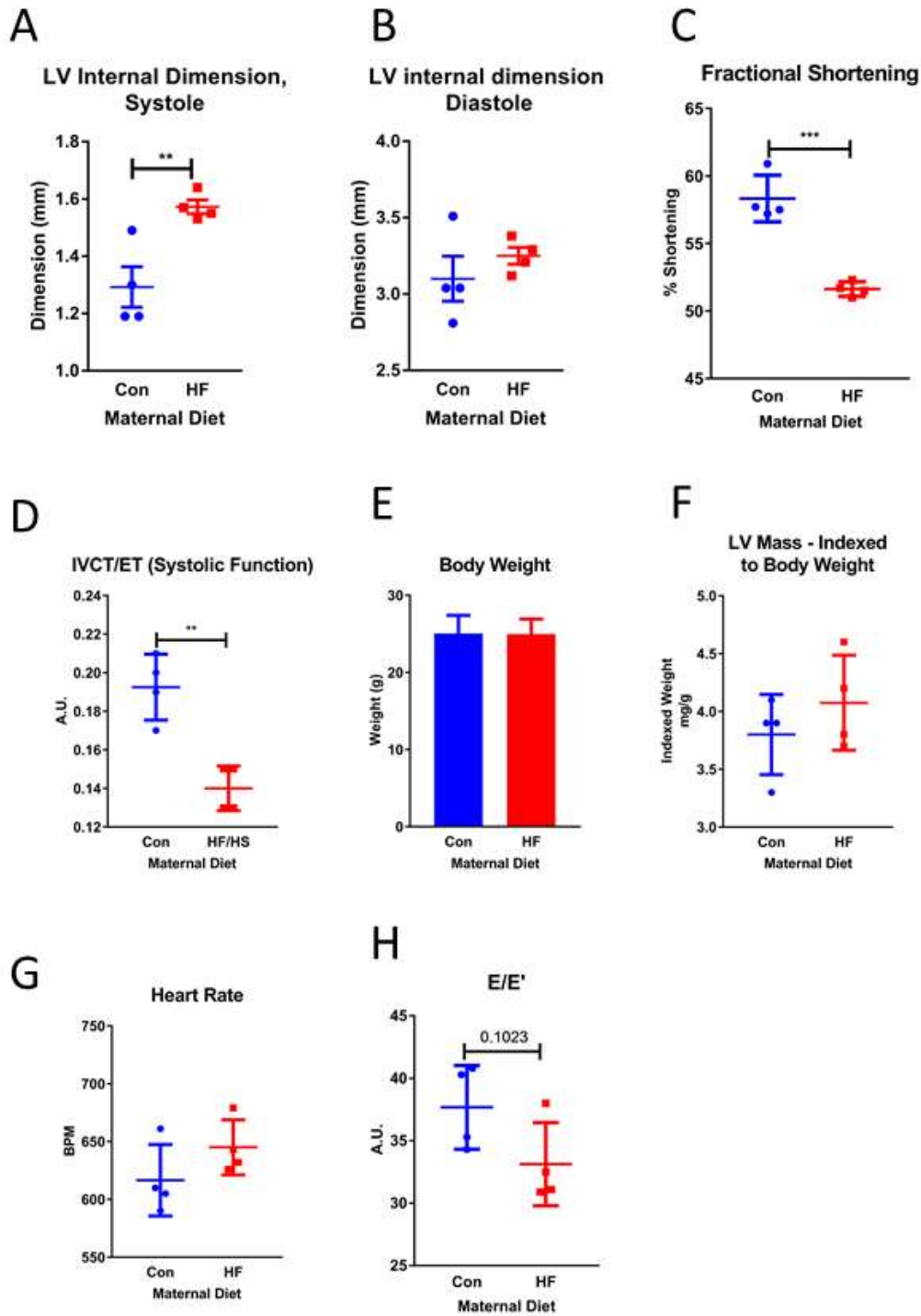
Figure 4- 2: 42 week old female offspring of HF/HS exposed dams are developing dilated cardiomyopathy
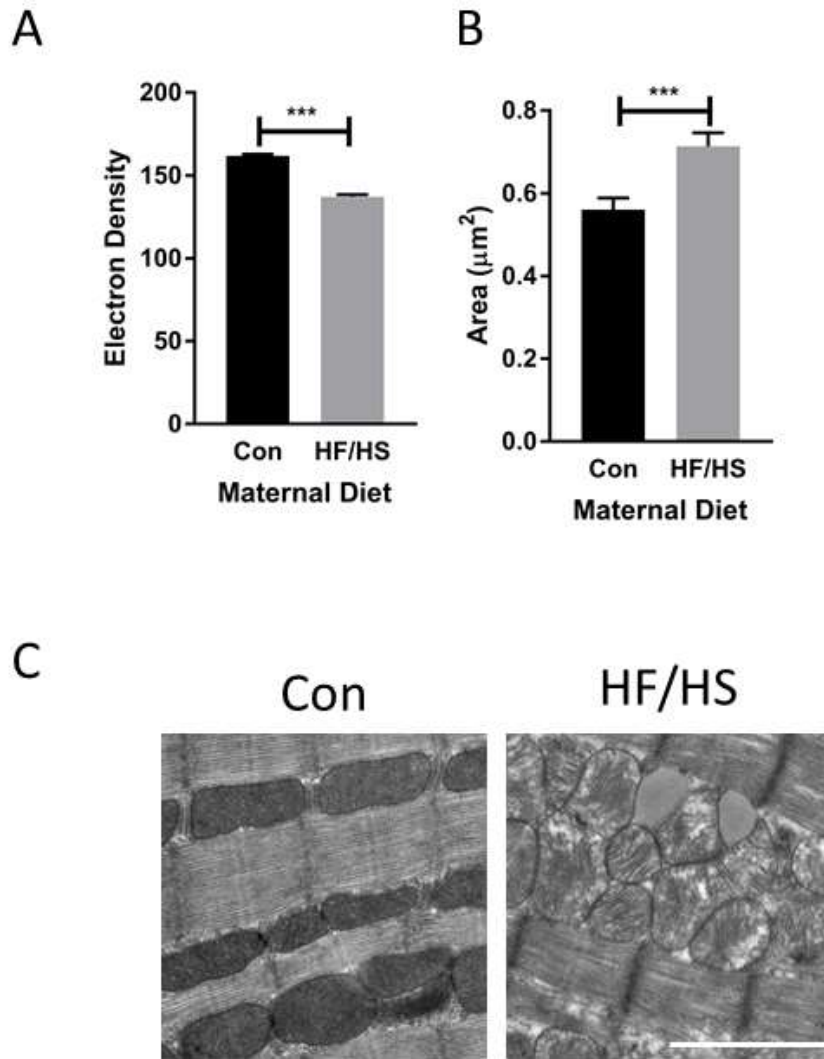
Figure 4- 3: Cardiomyocyte mitochondria from HF/HS F1 generation progeny have changes to mitochondrial ultrastructure
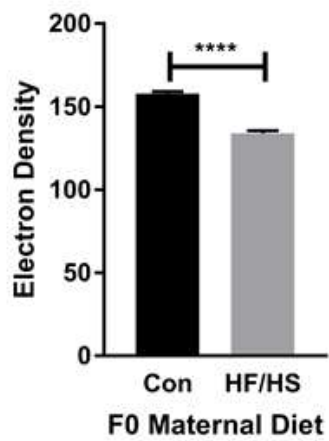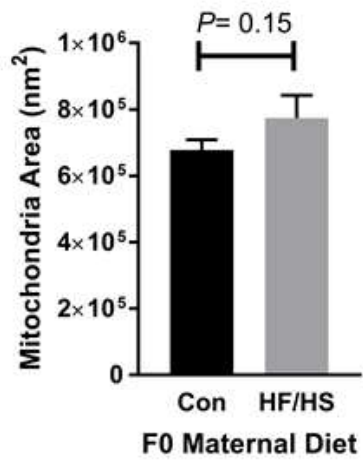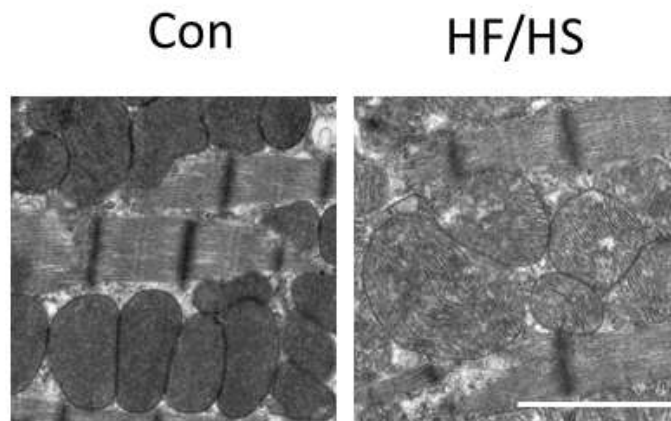
Figure 4- 4: Cardiomyocyte mitochondria from HF/HS F2 generation progeny have changes to mitochondrial ultrastructure
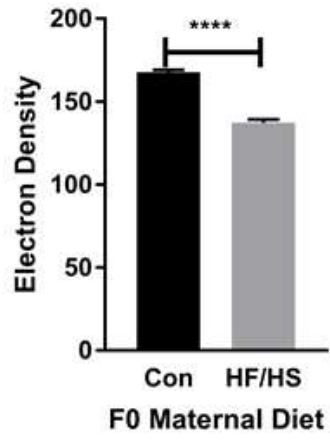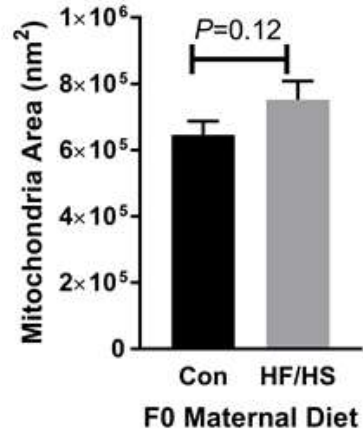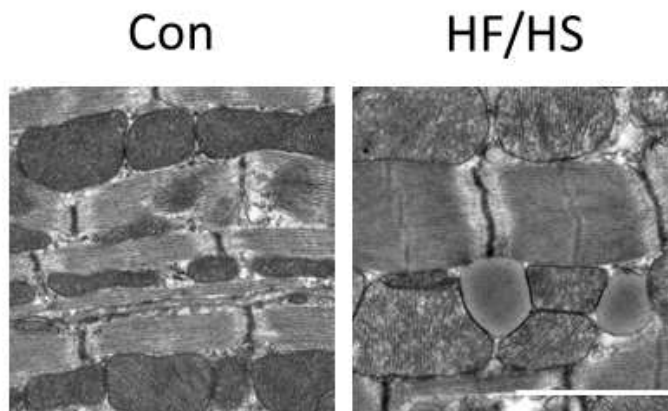
Figure 4- 5: Cardiomyocyte mitochondria from HF/HS F3 generation progeny have changes to mitochondrial ultrastructure
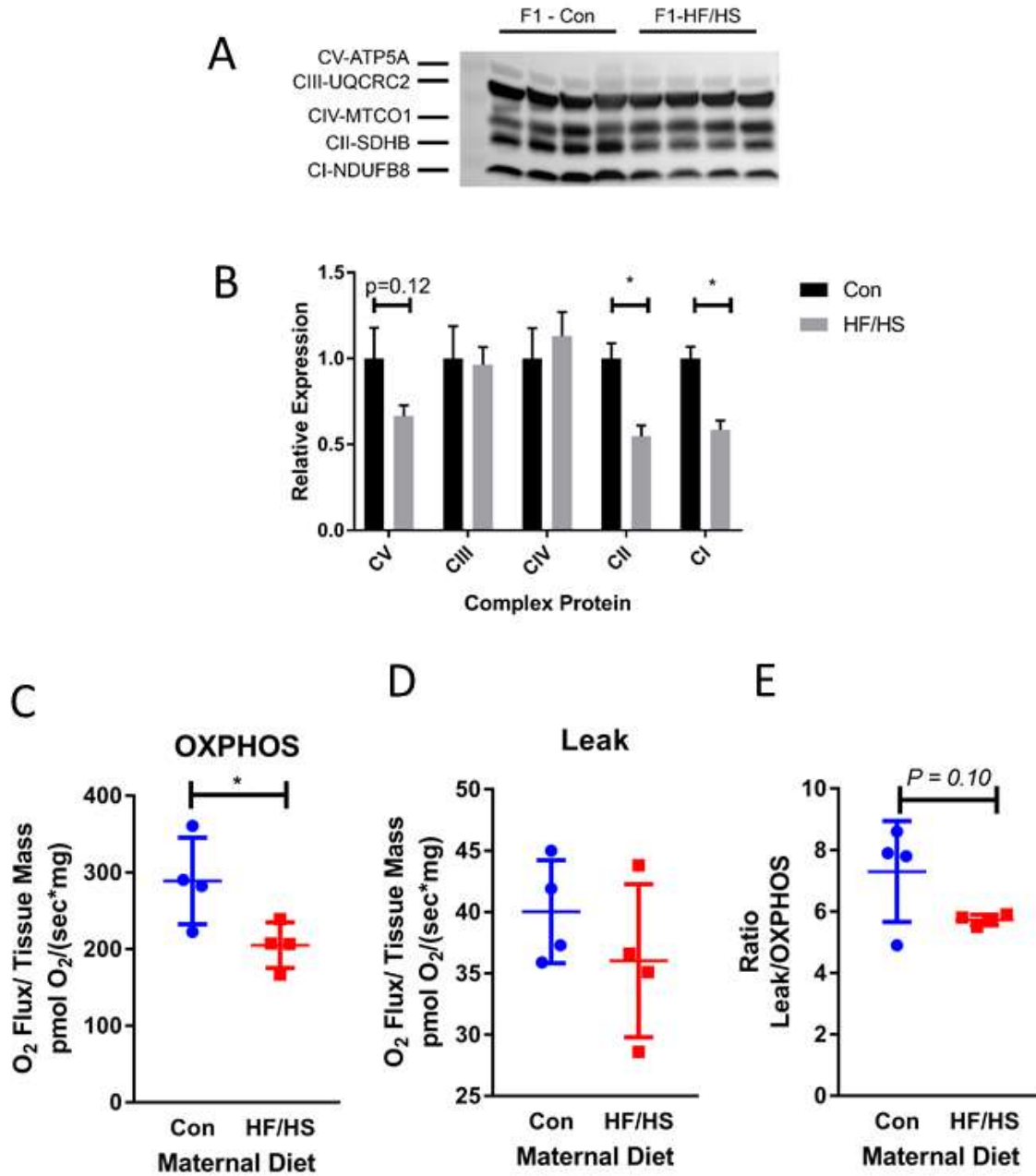
Figure 4- 6:F1 offspring from HF/HS mothers have significant changes to their electron transport chain protein and respiration capabilities.
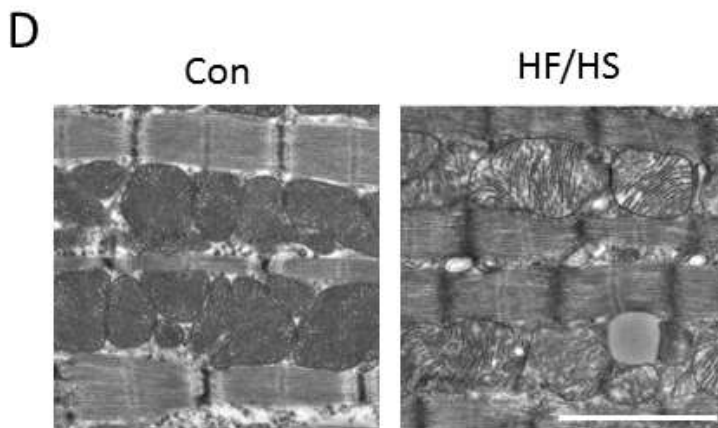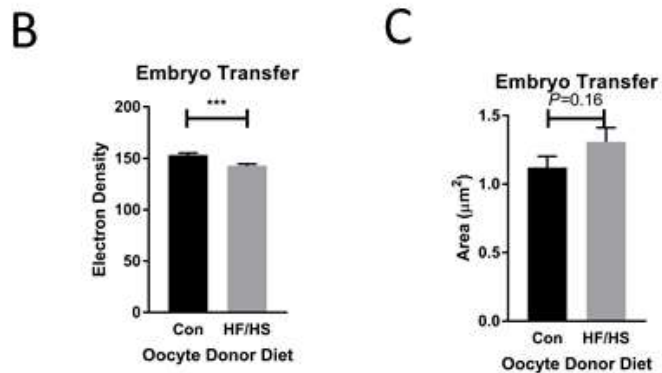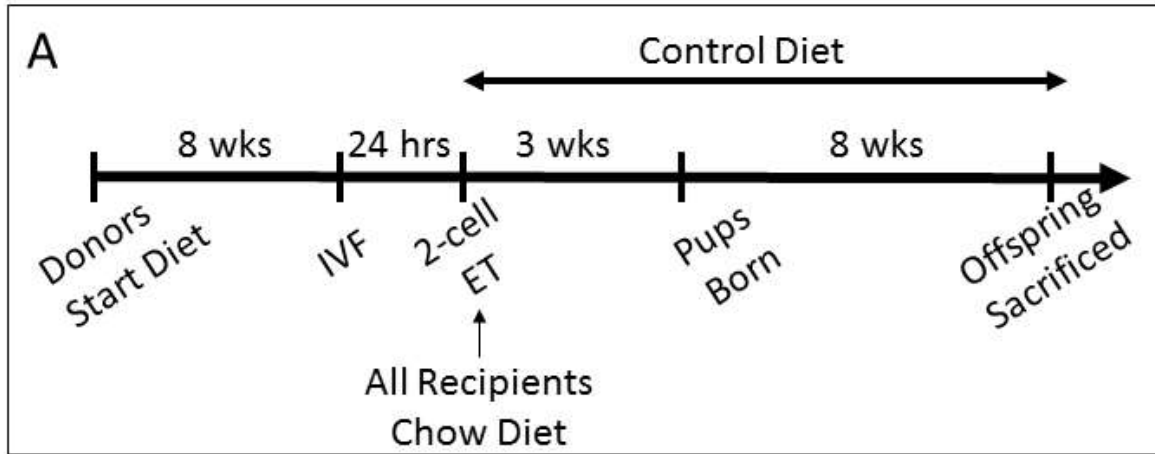
Figure 4- 7:Embryo transfer offspring display similar mitochondrial phenotypes to naturally mated F1 offspring.
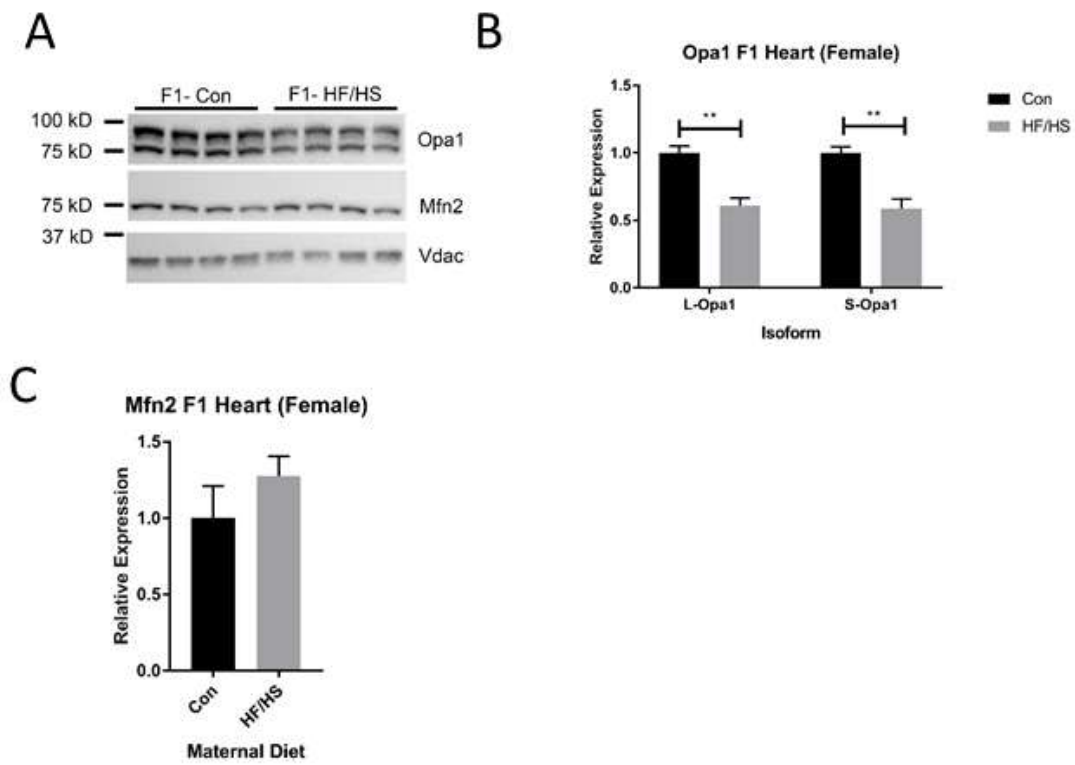
Figure 4- 8:: Mitochondrial dynamics protein expression is altered in naturally mated F1 offspring from HF/HS exposed dams.
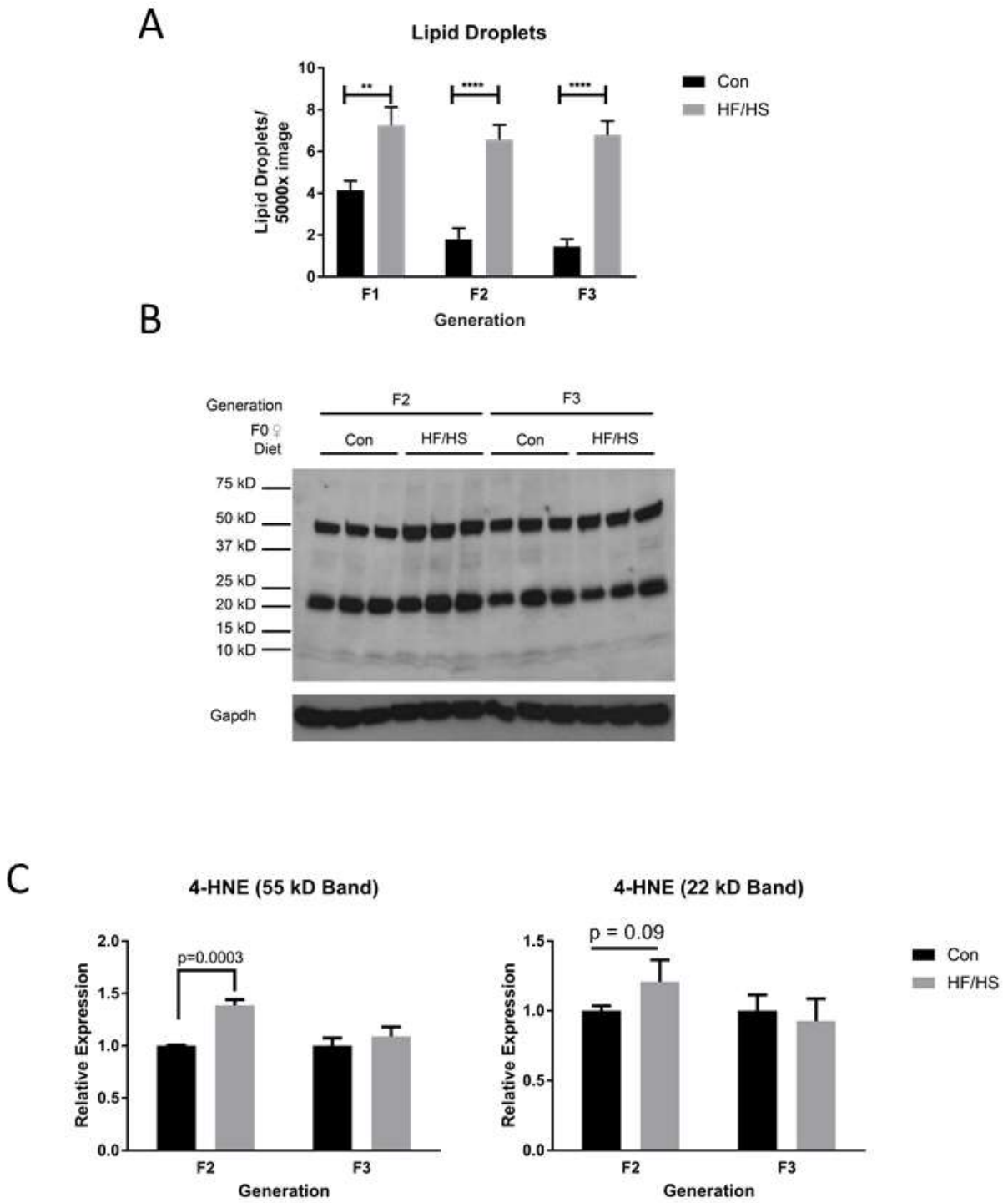
Figure 4- 9:Progeny from a HF/HS exposed F0 generation show signs of lipotoxicity in the absence of impaired fatty acid oxidation.
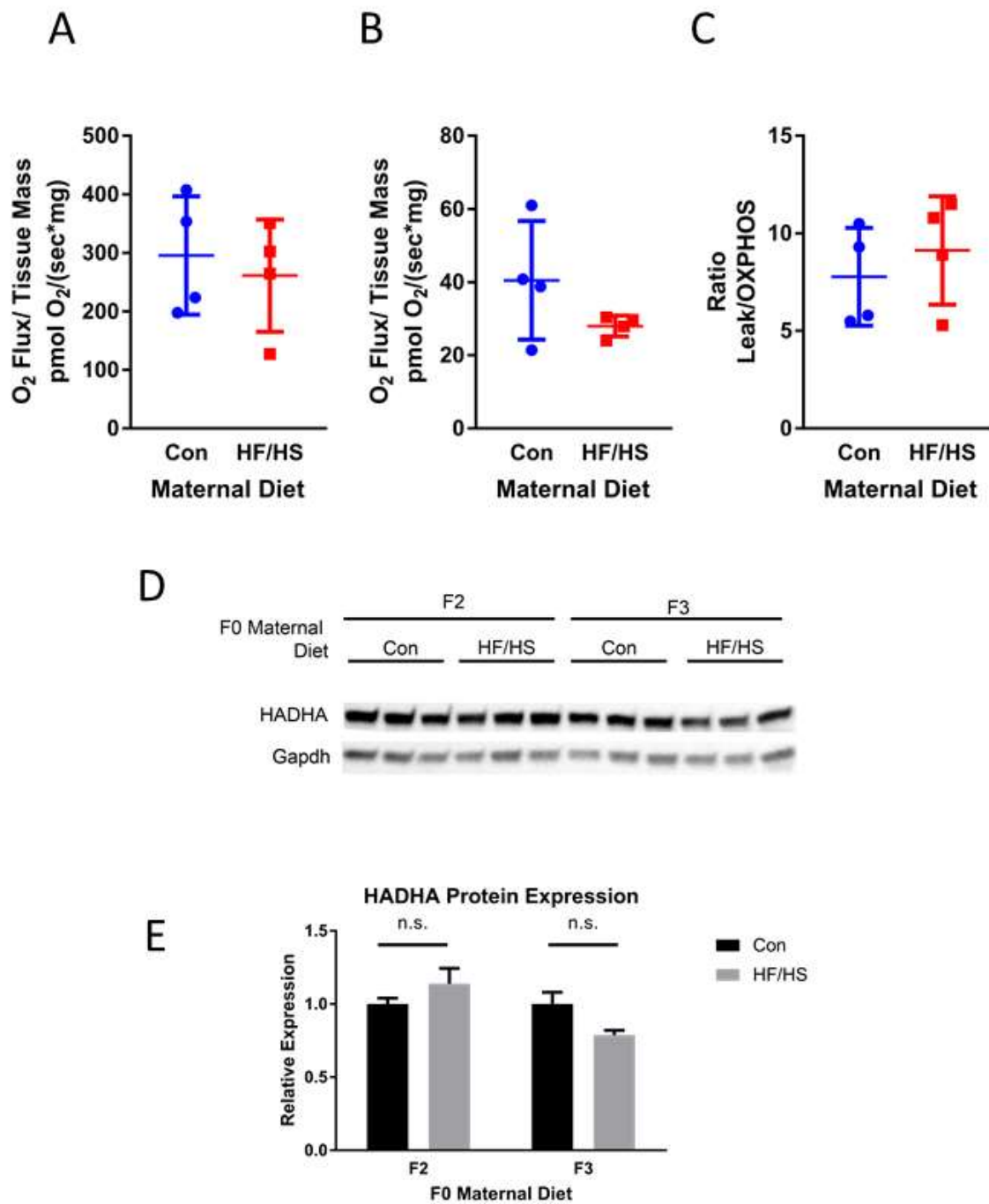
Figure 4- 10:: Fatty acid oxidation capacity of heart mitochondria is unchanged in F1 offspring from HF/HS dams.
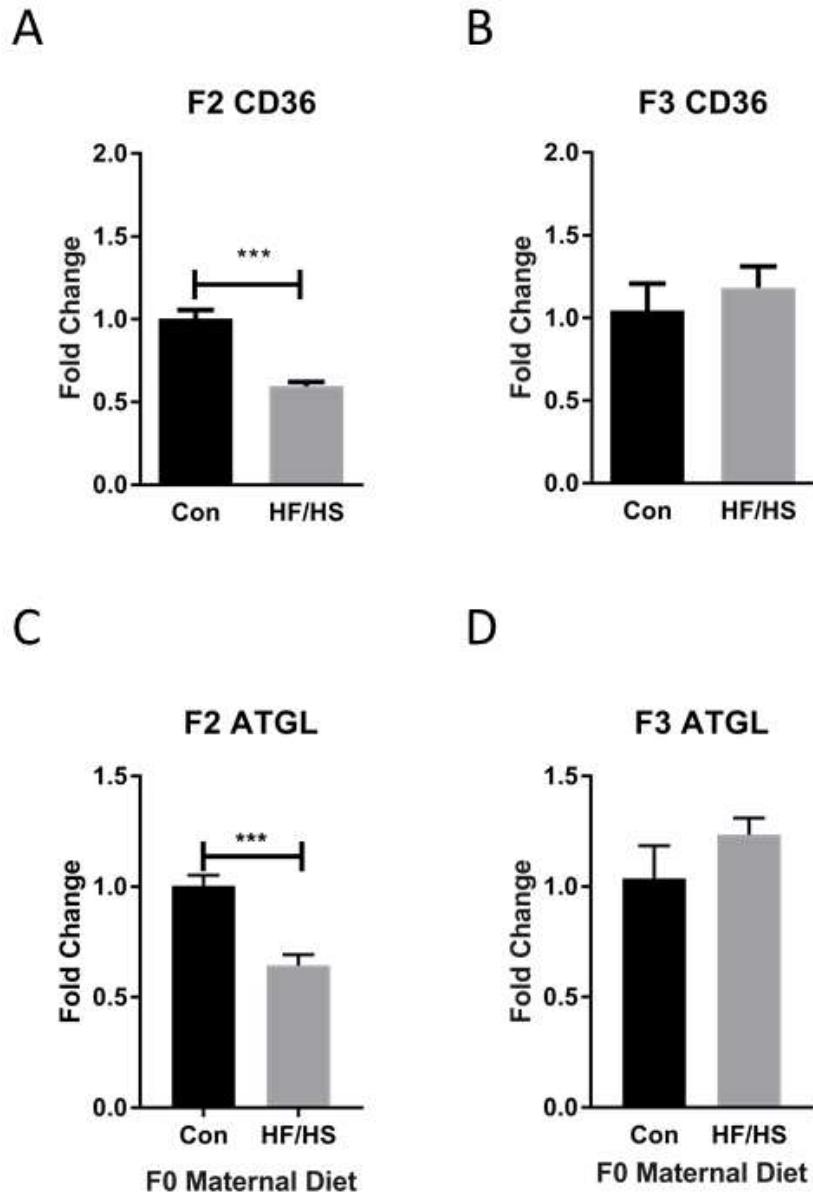
Figure 4- 11: Changes to the transcript levels of a fat transporter and lipolysis enzyme in cardiac tissue from HF/HS progeny

4.8 Tables

Table 4- 1: Antibodies used for western blotting

Antibody	Dilution	Vendor	Catalog Number
Opa-1	1:1000	BD Biosciences	612606
Mfn2 (D2D10)	1:1000	Cell Signaling	9482S
Tom20 (FL-145)	1:1000	Santa Cruz	sc-11415
Total OXPHOS Rodent WB Antibody Cocktail	1:1000	Abcam	ab110413

Table 4- 2: TaqMan Primer Assays Used for qPCR

Gene Symbol	Gene Name	Catalog Number
CD36	CD36 Antigen	Mm1135198_m1
Mfn1	Mitofusin 1	Mm00612599_m1
Mfn2	Mitofusin 2	Mm00500120_m1
Opa1	Optic Atrophy 1	Mm01349707_g1
PnplA2	Adipose Triglyceride ipase(ATGL)	Mm00495359_m1
Actb	Beta Actin	Mm00607939_s1

Chapter 5: Conclusions and Future Directions

5.1   Conclusions

Oocytes provide all of the mitochondria to an embryo for the first seven days of life. Understanding how detrimental environmental conditions, such as obesity, affect oocyte mitochondria and subsequent offspring health are critical in ensuring the health of our global population. Previous studies from our lab showed that obesity damages oocyte mitochondria and that this damage is not reversible by weight loss alone. Additionally, maternal obesity affects blastocyst development (Jungheim et al., 2010), cardiovascular function (Blackmore et al., 2014; Fernandez-Twinn et al., 2012; Turdi et al., 2013), and offspring mitochondria morphology (Saben et al., 2016). This work was dedicated to showing:

A. If exercise, a beneficial environmental activity, improved oocyte quality

B. If oocytes activated mitophagy in response to increased mitochondrial damage induced by a HF/HS diet

C. If the mitochondrial damage caused by preconception and in utero exposure to a maternal HF/HS diet resulted in atypical mitochondria morphology and dynamics in the myocardium, which predisposes offspring to cardiovascular disease and heart failure.

Through this research, we have shown that exercise can reverse lipid accumulation and some aspects of mitochondrial morphology, which resulted in partial improvement to oocyte metabolism (Chapter 2). However, obese mice, irrespective of their exposure to exercise, still ovulated oocytes with significantly more spindle abnormalities. This indicates that the beneficial effects of maternal exercise on offspring health seen in other studies may be due to changes that occur in utero during development and are not a result of the oocyte (Carter et al., 2013; Schulkey et al., 2015). Additionally, incomplete reversal of obesity-induced phenotypes suggests

oocytes may lack mechanisms to respond to negative stimuli and invoke cellular repair in the same manner as somatic cells.

In order to test if oocytes are able to repair HF/HS diet induced mitochondrial damage, we attempted to activate the mitophagy pathway in oocytes. However, supraphysiological levels of mitochondrial uncoupling, which is effective in rapidly inducing mitophagy in somatic cells, did not elicit a response in oocytes. We concluded that mitophagy is not active in oocytes. We further show this is because autophagy is not active in oocytes, in agreement with previously published data. This results in inheritance of damaged mitochondria and impaired embryo metabolism. Future work, detailed below, will be aimed at determining how this may program offspring phenotypes.

Because oocyte cannot repair damage to mitochondria, we investigated the effects inheritance of damaged mitochondria have on adult offspring. We show that cardiac tissue from maternal obesity exposed offspring displays disrupted mitochondrial membrane potential, metabolism, and mitochondrial dynamics in cardiac tissue. Previous research indicates disruption to mitochondrial dynamics and normal mitochondrial function in the heart results in the development of heart failure (Chen and Dorn, 2013; Piquereau et al., 2012). The first generation of mice from obese mothers also develops worsening dilated cardiomyopathy with age (Chapter 4), suggesting that disrupted mitochondrial dynamics cause heart failure in these mice.

5.2   Future Directions

5.2.1 *Cause of oocyte damage – lipotoxicity and ER stress*
This work strengthens the evidence that preconception exposure to a HF/HS diet damages mitochondria and expands this knowledge to demonstrate it is non-reversible due to an inability

to activate mitophagy. However, the initial cause of damage is still unknown. Future work understanding the mechanisms that cause the initial damage will be important in treating and preventing it. Previous evidence suggests that lipotoxicity contributes to obesity induced oocyte damage. Oocytes accumulate lipid in response to obesity. Lipid droplet formation occurs in response to increased cytoplasmic triglycerides (Aon et al., 2014). L-carnitine is an intermediate required for fatty acid oxidation, and administration increases that pathway (Dunning and Robker, 2012). In oocytes, promoting lipid utilization by supplementing culture medium with L-carnitine improves oocyte quality, oocyte maturation, fertilization rates, and blastocyst development rates (Dunning et al., 2011; Dunning et al., 2010). L-carnitine may positively affect oocytes by reducing hydrogen peroxide induced damage in the embryos (Abdelrazik et al., 2009). This data would suggest that enhancing lipid utilization in oocytes may prove beneficial in preventing some of the obesity induced damage and suggests a potential therapeutic mechanism that can be tested in the clinic.

Mitochondria are particularly susceptible to lipotoxic damage. Lipotoxicity creates truncated triglycerides and reactive aldehydes that damage membranes (Hauck and Bernlohr, 2016). Cardiolipin is resident in the inner mitochondrial membrane and is susceptible to lipid peroxidation (Paradies et al., 2014). There are very few published studies about cardiolipin in oocytes. In *C. elegans* cardiolipin is only necessary for germ cell mitochondrial activity but not somatic cell mitochondrial activity. Inhibiting cardiolipin synthesis severely impedes germ cell development and causes animals to be sterile without causing somatic cell complications (Sakamoto et al., 2012). This indicates that cardiolipin is important for germ cell function. It would be interesting to determine if there are changes to the amounts of cardiolipin in oocytes from HF/HS exposed animals and if those cardiolipin pools are being modified by the free

radicals produced by lipotoxicity. Unfortunately, studies to measure levels of lipid species, including cardiolipin, are currently not possible due to the limited cell number relative to the amount of material needed to produce reliable results from mass spectrometry analysis. While strides are being made, the ability to measure lipid species and lipotoxicity intermediates remains limited in oocytes (Onjiko et al., 2015). Early evidence of lipotoxicity in oocytes could be determined by using a western blot analysis for increased 4-hydroxynonenal adducts in oocytes from HF/HS fed dams using the antibody described in Chapter 4 (Figure 4-9). This is a lipid modification that is a signature of lipotoxicity (Hauck and Bernlohr, 2016).

Lipotoxicity can activate all three arms of the unfolded protein response and activate an endoplasmic reticulum (ER) stress response (Hauck and Bernlohr, 2016). ER stress is increased in oocytes and cumulus-oocyte complexes (COCs) collected from HF/HS exposed females (Igosheva et al., 2010; Wu et al., 2011; Wu et al., 2012; Wu et al., 2015). Salubrinal, an ER stress inhibitor, can reverse the obesity induced ER stress observed in COCs (Wu et al., 2015). This subsequently improves fertilization and blastocyst development rate. However, the effects of salubrinal were shown only in cumulus-oocyte complexes, not oocytes alone. When we repeated these experiments in isolated oocytes, the same upregulation in ER stress gene expression was not observed (Figure 5-1). This suggests that ER stress and the effects of salubrinal are restricted to the cumulus cells. Future work should focus on differentiating the cumulus cell and oocyte ER stress response in order to provide a more specific mechanism for how obesity affects the female germ cells.

5.2.2 *Metabolic regulation of tubulin acetylation to stabilize the meiotic spindle during metaphase II arrest*

*This work was modified from my F31 fellowship application submitted in august of 2015

In addition to mitochondrial damage, oocyte from obese females also have significantly more spindle abnormalities. No causative mechanism for the increase in spindle abnormalities has been defined. However, mitochondrial damage and metabolic inactivity may reduce tubulin stability, leading to abnormal spindle formation. During oocyte maturation and embryonic development, α-tubulin, the building block of the meiotic spindle, is acetylated at lysine 40 (K40). This modification is thought to stabilize the microtubules (L'Hernault and Rosenbaum, 1985). The donor group for virtually all acetylation modifications is acetyl-CoA (Choudhary et al., 2009; Choudhary et al., 2014). One enzyme that produces acetyl-CoA is pyruvate dehydrogenase (PDH), which is localized in the mitochondrial matrix (Rardin et al., 2009). PDH activity is necessary for oocyte meiotic maturation – most oocytes arrest during meiosis if PDH is not expressed. Additionally, embryos without PDH cannot develop past embryonic day post-coitum 8.5 (Johnson et al., 2007; Johnson et al., 2001). This is likely because PDH deficiency both decreases oocyte oxidative metabolism and changes microtubule acetylation patterns ((Hou et al., 2015; Johnson et al., 2007), Figure 5-2). Because oocytes that do not express PDH have a similar, albeit more extreme, phenotype to oocytes from obese mice, testing how PDH activity affects spindle formation will be an important future direction.

PDH can be phosphorylated and inactivated on up to three serine residues, S232, S293, and S300 (Rardin et al., 2009). Therefore, the phospho-PDH/total-PDH ratio can be used as an approximation for PDH activity. GV oocytes collected from HF/HS fed mice, had a higher phosphorylated PDH/total PDH ratio than oocytes from control mice (Figure 5-3A, B). This was

further confirmed with immunofluorescent staining of GV oocytes for both S293-pPDH and S300-pPDH (Figure 5-3C,D). Intense staining of PDH was also observed in the nucleus of GV oocytes and on spindles during meiosis (Figure 5-3E). PDH has previously been reported to localize to the nucleus in order to generate acetyl-CoA for histone acetylation (Choudhary et al., 2014). These preliminary data suggest that decreased PDH activity in HF/HS females may be contributing to meiotic maturation and microtubule acetylation by localizing to the nucleus and acetylating microtubules during meiosis (Figure 5-2). It will be important to directly assess if PDH is responsible for producing the acetyl-CoA used to acetylate K40 of α-tubulin. This can be done by utilizing oocytes that are deficient in PDH to measure tubulin acetylation levels throughout meiosis via immunofluorescent staining and measuring the relative intensity.

Endogenously, PDH is inactivated by the pyruvate dehydrogenase kinases (PDKs) 1-4, which phosphorylate PDHE1α at serines 293, 232 and 300 (S293-pPDH, S232-pPDH, and S300-pPDH, respectively) (Hou et al., 2015). Inactivation at S293-pPDH causes decreased ATP production and also a significant increase in spindle deformation and chromosome misalignment (Hou et al., 2015), but the contribution to microtubule acetylation was not addressed. On possible approach to determine a direct contribution of PDH to acetylation of microtubules during meiosis is by utilizing site directed mutagenesis of PDHE1α to mimic constitutive phosphorylation and inactivate at either S293, S232, or S300. These mutations can be made individually or in combination by conversion of these serines to aspartate. Conversely, to constitutively activate PDH, site directed mutagenesis will be used again to create PDH mutants in which S293, S232 or S300 will be converted to alanine (Hou et al., 2015; Vagnoni et al., 2011). Individual mRNAs for the activated or inactivated PDH can be injected into PDH-deficient GV stage oocytes that were described initially in (Johnson et al., 2007). Subsequent

meiotic progression and spindle formation can be monitored during IVM and utilizing immunofluorescence.

It is also important to test if microtubule acetylation is required for in spindle stability and completion of oocyte meiosis. Site directed can also be used to create α-tubulin mutants that mimic either constitutively acetylated K40 by converting the lysine to a glutamine (K40Q substitution), or constitutively de-acetylated α-tubulin by converting the lysine to arginine (K40R substitution) (Gal et al., 2013; Gao et al., 2010). Finally, to show insufficient tubulin acetylation via PDH inactivation is the mechanism underlying the observed spindle defects in the oocytes from HF/HS exposed females, injection of the PDH and tubulin mRNAs described above into HF/HS oocytes should rescue the effects of the diet. These studies would give mechanistic insight into the cause of spindle abnormalities in oocytes from obese females.

5.2.3 The role of mitofusin 2 in oocyte maturation and embryo development
The presence of abnormal mitochondria is one of the most well-defined phenotypes in oocytes from obese females. Mitochondria are the most abundant organelles in the oocyte (Motta et al., 2000; Sathananthan and Trounson, 2000). Additionally, mitochondria are dynamic, constantly undergoing fission and fusion to alter their shape to meet the metabolic demands of a particular cell type (Friedman and Nunnari, 2014). In oocytes, mitochondrial dynamics are important for meiosis and fertilization. Inhibiting the fusion protein Mitofusin 2 (Mfn2) causes abnormalities in spindle structure (Liu et al., 2016a). Alternately, overexpression of Mfn2 increases interaction of mitochondria with the ER, which depletes $Ca2+$ supply in the oocyte and impairs fertilization (Wakai et al., 2014). Both of these studies indicate a critical role for Mfn2 in oocyte maturation and fertilization. We have preliminary data that shows oocytes from HF/HS females have significantly decreased levels of Mfn2 at the GV and MII stage (Figure 5-4). It will

be important to determine if the obesity induced reduction in Mfn2 causes increased spindle abnormalities and changes to mitochondrial morphology in these oocytes. This can be tested by rescuing Mfn2 expression in HF/HS oocytes either via a genetic hypermorph or microinjection. One challenge in this approach will be tittering Mfn2 expression, since both too much and to little inhibit oocyte function.

Mfn2 also has an important role in embryo development. Embryo mitochondria undergo morphological changes that correlate with the pattern of embryo metabolism. Prior to the 8-cell stage, mitochondria retain the morphology of the mature oocyte – small and round with a few, dense cristae that wrap the periphery of the oocyte (Motta et al., 2000; Sathananthan and Trounson, 2000). However, at the 8-cell stage, mitochondria begin to elongate and cristae extend into the matrix (Motta et al., 2000). By the blastocyst stage, there are distinct mitochondrial morphologies, with inner cell mass (ICM) mitochondria retaining the structural characteristics of oocyte and early embryos, while the trophectoderm (TE) mitochondria have elongated and have ladder-like cristae (Sathananthan and Trounson, 2000). These changes accompany a distinct metabolic signature for each cell type, with the TE relying primarily on oxidative phosphorylation (OXPHOS) and the ICM utilizing glycolysis (Kaneko, 2016). No research to date has addressed the role of Mfn2 in directing these morphological changes. We observe the HF/HS blastocysts from in vitro fertilization have decreased Mfn2 protein abundance and decreased metabolic intermediates (Figure 3-6 and Figure 5-4). Potentially, a reduction in Mfn2 alters the metabolism of these embryos. Future research should investigate the role of Mfn2 in embryonic mitochondrial morphology and metabolism and how a HF/HS diet imparts changes to the embryo during preimplantation via Mfn2 expression.

Evidence from the literature supports the hypothesis that Mfn2 reduction caused by obesity is directly affecting blastocyst metabolism. Mfn2 knockdown by siRNA in embryos leads to delayed preimplantation development, decreased mitochondrial membrane potential, increased apoptosis, and changes in calcium homeostasis, which may promote embryo death (Zhao et al., 2015). We observed decreased mitochondrial membrane potential in the blastocysts from HF/HS oocytes (Chapter 3). A decreased litter size is reported in the literature as a consequence of maternal obesity (Skaznik-Wikiel et al., 2016). Investigation into the expression of mitochondrial dynamics proteins during each stage of preimplantation development and the potential changes in expression that occur during obesity may underlie the increase in failed fertilization and implantation.

In addition to the role that Mfn2 may have in driving the restructuring of mitochondria in the preimplantation embryo, research also suggests this protein is critical in placental development and may be dysregulated in the placenta as a result of obesity. In support of this hypothesis, the labyrinth zone of placentas from male offspring of an overfed rat model had a significant decrease of Mfn2 expression, in an RNA sequencing experiment. These changes in gene expression were accompanied by placental inefficiency (Borengasser et al., 2014). Mitochondrial dynamics proteins are necessary for embryo invasion and establishment of the placenta. Mfn2 knockout embryos die at e9.5-e11.5 due to errors in trophoblast giant cell (GC) development. These embryos had fewer GCs and these GCs also had lower mtDNA copy numbers (Chen et al., 2003). Future studies should determine if obesity-induced placental insufficiency and maternal obesity are cause by reduced Mfn2 gene expression and changes to mitochondrial dynamics. It will also be important to link a decrease in Mfn2 protein expression to functional differences, such as changes in mitochondrial morphology. Rescue experiments

using cell lines and mice that overexpress Mfn2 in tandem with diet exposure will also confirm a role for Mfn2 in GC cell development.

The literature also suggests Mfn2 is important in a second placental cell type, syncytiotrophoblasts. These are the hormone-producing cells within the labyrinth zone of the placenta (Wang and Zhao, 2010). Within the syncitiotrophoblasts, the mitochondria are the site of hormone production. This has been correlated with the unique mitochondrial morphology observed in these cells (Poidatz et al., 2015). Ablation of Mfn2 in a syncytiotrophoblast cell line inhibited pregnenolone production, which is necessary to maintain a viable pregnancy (Wasilewski et al., 2012). Further, placental samples from women with unexplained miscarriage also had a decrease in Mfn2 expression (Pang et al., 2013). One potential cause of the miscarriages is that reduced Mfn2 expression alters mitochondrial dyanmics and impairs hormone production and pregnancy maintenance. Given that obesity increases miscarriage rate, it will be important to conduct more detailed studies using cell-type specific knockout of Mfn2 in different placental cell types to determine how this protein affects placental development and subsequently, embryo development.

5.2.4 *The mechanism causing obesity induced epigenetic changes to the oocyte and embryo*

The epigenetic landscape is sensitive to metabolic changes because the two are tightly intertwined. For example, acetyl-CoA, an intermediate of both FAO and carbohydrate metabolism, is also the sole acetyl group donor for histone modifications (Choudhary et al., 2014; Kinnaird et al., 2016). DNA and histone methylation receive methyl groups from the methionine cycle, which requires α-ketoglutarate and ATP to complete the cycle (Teperino et al., 2010). Additionally, inactivation of two TCA cycle enzymes, succinate dehydrogenase and

fumarate hydratase cause significant changes to demethylation of both DNA and histone proteins, further linking mitochondrial metabolism to epigenetic modifications (Hoekstra et al., 2015). Therefore, changes to the metabolism, such as that caused by damage to mitochondria, directly changes how genes are expressed.

Given the close relationship between mitochondria and epigenetics, obesity induced damage to oocyte mitochondria may cause stably inherited epigenetic changes to the offspring. During preimplantation development, the embryo is much more reliant on maternal genes than paternal genes due to unequal inheritance of cytosine methylation and histone modifications between sperm and egg. While paternal DNA cytosine methylation (5mC DNA) is erased during the pronuclear stage, the maternal DNA remains methylated (Amouroux et al., 2016). The trophectoderm maintains differential methylation as these cells further differentiate into the placenta, while the inner cell mass of the embryo reestablishes biallelic DNA modifications after implantation (Branco et al., 2016; Li et al., 2016; Sanchez-Delgado et al., 2016).

Biased inheritance of the maternal epigenome and maternal gene expression are important to consider in light of HF/HS diet induced changes that can occur to DNA methylation. Preliminary studies show that exposing mice to a HF/HS diet results in a reduction in 5mc DNA in their GV oocytes (Hou et al., 2016). Research from cattle indicates that blastocysts inherit these oocyte-induced changes in 5mC DNA. Culturing bovine oocytes in high concentrations of nonesterified fatty acids to mimic an obese uterine environment prior to and after *in vitro* fertilization results in significant changes to DNA methylation patterns in the embryos (Desmet et al., 2016). However, this study did not address if these epigenetic marks were maintained because the embryos were cultured in similar levels of NEFAs as the oocyte or if the changes to the epigenome are maintained in the absence of NEFA exposure in the embryo.

While these two studies suggest exposure to obesity causes inherited changes to the embryo, it will be important to study how preconception exposure exclusively programs 5mC DNA modifications.

Histone modifications control gene expression by dictating chromatin compaction (Harr et al., 2016). Maternal and paternal alleles retain histone modifications after fertilization and during preimplantation development (Fraser and Lin, 2016; Kim and Ogura, 2009). For example, Histone H3 lysine 4 methylation (H3K4me) and H3 lysine 27 trimethylation (H3K27me3) are only present on maternal chromatin. Embryos maintain maternal distribution patterns of H3K4me until the two cell stage, while maternal distribution of H3K27me3 is retained until implantation (Zhang et al., 2016; Zheng et al., 2016). Both modifications are marks of active gene expression and corroborate data that a significant proportion of genes expressed during preimplantation development are transcribed only from maternal alleles (Sanchez-Delgado et al., 2016; Zhang et al., 2016; Zheng et al., 2016). Consumption of a HF/HS diet is known to change histone modification patterns (Williams et al., 2014) and maternal dietary changes have been linked to changes in gene expression in the offspring (Barres and Zierath, 2016). However, little research to date has shown the mechanisms for how these exposures affect gene expression in the offspring are poorly understood and warrant further investigation.

Recently, histone modifications have been shown to be important in establishing inheritance of traits in the offspring. In *C. elegans*, a phenomenon termed hormesis occurs when an animal is exposed to low levels of an environmental toxicant during development. The animal exhibits minor reductions in growth but a significant increase in lifespan (Kishimoto et al., 2017). Additionally, this benefit is transmitted across three generations of un-stressed offspring via histone H3K3 methylation in the germline (Kishimoto et al., 2017). This study demonstrates

that there are mechanisms by which epigenetic marks are altered by the environment and promote inheritance of traits for multiple generations. Although this particular study demonstrated the inheritance of advantageous epigenetic modifications, detrimental modifications may also be passed on. It will be important to understand whether beneficial or detrimental inheritance of histone modification occurs in mammalian offspring in response to maternal obesity.

Given the important role of the metabolism in the establishment of histone post-translational modifications and the inherited mitochondrial damage from HF/HS diet, it would be interesting to measure and compare changes in the histone modifications of embryos in response to maternal exposure to a HF/HS. During preimplantation development, histone marks are reprogrammed during the maternal to zygotic transition during preimplantation development (Liu et al., 2016b). Linking changed levels of post-translational histone modifications with changes in gene and protein expression would demonstrate a mechanism for how damaged mitochondria can program maladaptive gene expression. This could best be done by conducting nuclear transfer experiments. In this instance, the maternal pronuclei from zygotes fertilized from control and HF/HS mothers are swapped (McGrath and Solter, 1983). Appropriate control to control and HF/HS to HF/HS pronuclear transfers are critical to analysis. As the embryos develop, patterns of histone modifications and 5mC DNA can be monitored and compared. Analyzing differences and similarities of histone and 5mC between all four groups can indicate how mitochondria influence epigenetic regulation in embryos (Hyslop et al., 2016; Morrow and Ingleby, 2017). Demonstrating roles of genes controlled by these epigenetic changes during development and in adults would further link the harm that preconception obesity and inheriting damaged mitochondria have on all levels of cell function in the offspring.

131

Multiple studies have shown that maternal obesity causes changes offspring global methylation patterns in a variety of tissue types including liver (Dudley et al., 2011), cardiomyocytes (Wing-Lun (Wing-Lun et al., 2016), and adipose (Borengasser et al., 2013). We have shown that there are damaged mitochondria in the oocytes that are inherited by the blastocyst, which causes a reduction in mitochondrial membrane potential, indicating less active mitochondria (Chapter 3). Additionally, we show that there are mitochondrial abnormalities in the adult female offspring from HF/HS mice in three different muscle types, fast twitch myocytes, slow twitch myocytes, and cardiomyocytes ((Saben et al., 2016) and Chapter 4). These appear to be inherited as a result of preconception maternal exposure to the HF/HS diet, since similar abnormal mitochondria are found in cardiomyocytes and muscle from embryo transfer offspring (Chapter 4 and Figure 5-5). It will be important to delineate if these changes are occurring as a result of changes to maternal DNA methylation, DNA methylation kinetics during preimplantation development, or as a result of development in a sub-optimal uterine environment such as that of a HF/HS female. Utilizing our established system of embryo transfer will be important in dissecting the differences and how these play out both during development and in adulthood.

5.3   References

Abdelrazik, H., Sharma, R., Mahfouz, R., Agarwal, A., 2009. L-carnitine decreases DNA damage and improves the in vitro blastocyst development rate in mouse embryos. Fertil Steril 91, 589-596.

Amouroux, R., Nashun, B., Shirane, K., Nakagawa, S., Hill, P.W., D'Souza, Z., Nakayama, M., Matsuda, M., Turp, A., Ndjetehe, E., Encheva, V., Kudo, N.R., Koseki, H., Sasaki, H., Hajkova, P., 2016. De novo DNA methylation drives 5hmC accumulation in mouse zygotes. Nature cell biology 18, 225-233.

Aon, M.A., Bhatt, N., Cortassa, S.C., 2014. Mitochondrial and cellular mechanisms for managing lipid excess. Frontiers in physiology 5, 282.

Barres, R., Zierath, J.R., 2016. The role of diet and exercise in the transgenerational epigenetic landscape of T2DM. Nature reviews. Endocrinology 12, 441-451.

Blackmore, H.L., Niu, Y., Fernandez-Twinn, D.S., Tarry-Adkins, J.L., Giussani, D.A., Ozanne, S.E., 2014. Maternal diet-induced obesity programs cardiovascular dysfunction in adult male mouse offspring independent of current body weight. Endocrinology 155, 3970-3980.

Borengasser, S.J., Faske, J., Kang, P., Blackburn, M.L., Badger, T.M., Shankar, K., 2014. In utero exposure to prepregnancy maternal obesity and postweaning high-fat diet impair regulators of mitochondrial dynamics in rat placenta and offspring. Physiological genomics 46, 841-850.

Borengasser, S.J., Zhong, Y., Kang, P., Lindsey, F., Ronis, M.J., Badger, T.M., Gomez-Acevedo, H., Shankar, K., 2013. Maternal obesity enhances white adipose tissue differentiation and alters genome-scale DNA methylation in male rat offspring. Endocrinology 154, 4113-4125.

Branco, M.R., King, M., Perez-Garcia, V., Bogutz, A.B., Caley, M., Fineberg, E., Lefebvre, L., Cook, S.J., Dean, W., Hemberger, M., Reik, W., 2016. Maternal DNA Methylation Regulates Early Trophoblast Development. Developmental cell 36, 152-163.

Carter, L.G., Qi, N.R., De Cabo, R., Pearson, K.J., 2013. Maternal exercise improves insulin sensitivity in mature rat offspring. Medicine and science in sports and exercise 45, 832-840.

Chen, H., Detmer, S.A., Ewald, A.J., Griffin, E.E., Fraser, S.E., Chan, D.C., 2003. Mitofusins Mfn1 and Mfn2 coordinately regulate mitochondrial fusion and are essential for embryonic development. The Journal of cell biology 160, 189-200.

Chen, Y., Dorn, G.W., 2nd, 2013. PINK1-phosphorylated mitofusin 2 is a Parkin receptor for culling damaged mitochondria. Science (New York, N.Y.) 340, 471-475.

Choudhary, C., Kumar, C., Gnad, F., Nielsen, M.L., Rehman, M., Walther, T.C., Olsen, J.V., Mann, M., 2009. Lysine acetylation targets protein complexes and co-regulates major cellular functions. Science (New York, N.Y.) 325, 834-840.

Choudhary, C., Weinert, B.T., Nishida, Y., Verdin, E., Mann, M., 2014. The growing landscape of lysine acetylation links metabolism and cell signalling. Nature reviews. Molecular cell biology 15, 536-550.

Desmet, K.L., Van Hoeck, V., Gagne, D., Fournier, E., Thakur, A., O'Doherty, A.M., Walsh, C.P., Sirard, M.A., Bols, P.E., Leroy, J.L., 2016. Exposure of bovine oocytes and embryos to elevated non-esterified fatty acid concentrations: integration of epigenetic and transcriptomic signatures in resultant blastocysts. BMC genomics 17, 1004.

Dudley, K.J., Sloboda, D.M., Connor, K.L., Beltrand, J., Vickers, M.H., 2011. Offspring of mothers fed a high fat diet display hepatic cell cycle inhibition and associated changes in gene expression and DNA methylation. PloS one 6, e21662.

Dunning, K.R., Akison, L.K., Russell, D.L., Norman, R.J., Robker, R.L., 2011. Increased beta-oxidation and improved oocyte developmental competence in response to l-carnitine during ovarian in vitro follicle development in mice. Biology of reproduction 85, 548-555.

Dunning, K.R., Cashman, K., Russell, D.L., Thompson, J.G., Norman, R.J., Robker, R.L., 2010. Beta-oxidation is essential for mouse oocyte developmental competence and early embryo development. Biology of reproduction 83, 909-918.

Dunning, K.R., Robker, R.L., 2012. Promoting lipid utilization with l-carnitine to improve oocyte quality. Animal reproduction science 134, 69-75.

Fernandez-Twinn, D.S., Blackmore, H.L., Siggens, L., Giussani, D.A., Cross, C.M., Foo, R., Ozanne, S.E., 2012. The programming of cardiac hypertrophy in the offspring by maternal obesity is associated with hyperinsulinemia, AKT, ERK, and mTOR activation. Endocrinology 153, 5961-5971.

Fraser, R., Lin, C.J., 2016. Epigenetic reprogramming of the zygote in mice and men: on your marks, get set, go! Reproduction (Cambridge, England) 152, R211-r222.

Friedman, J.R., Nunnari, J., 2014. Mitochondrial form and function. Nature 505, 335-343.

Gal, J., Chen, J., Barnett, K.R., Yang, L., Brumley, E., Zhu, H., 2013. HDAC6 regulates mutant SOD1 aggregation through two SMIR motifs and tubulin acetylation. The Journal of biological chemistry 288, 15035-15045.

Gao, Y.S., Hubbert, C.C., Yao, T.P., 2010. The microtubule-associated histone deacetylase 6 (HDAC6) regulates epidermal growth factor receptor (EGFR) endocytic trafficking and degradation. The Journal of biological chemistry 285, 11219-11226.

Harr, J.C., Gonzalez-Sandoval, A., Gasser, S.M., 2016. Histones and histone modifications in perinuclear chromatin anchoring: from yeast to man. EMBO reports 17, 139-155.

Hauck, A.K., Bernlohr, D.A., 2016. Oxidative stress and lipotoxicity. Journal of lipid research 57, 1976-1986.

Hoekstra, A.S., de Graaff, M.A., Briaire-de Bruijn, I.H., Ras, C., Seifar, R.M., van Minderhout, I., Cornelisse, C.J., Hogendoorn, P.C., Breuning, M.H., Suijker, J., Korpershoek, E., Kunst, H.P., Frizzell, N., Devilee, P., Bayley, J.P., Bovee, J.V., 2015. Inactivation of SDH and FH cause loss of 5hmC and increased H3K9me3 in paraganglioma/pheochromocytoma and smooth muscle tumors. Oncotarget 6, 38777-38788.

Hou, X., Zhang, L., Han, L., Ge, J., Ma, R., Zhang, X., Moley, K., Schedl, T., Wang, Q., 2015. Differential function of pyruvate dehydrogenase kinases during mouse oocyte maturation. Journal of cell science.

Hou, Y.J., Zhu, C.C., Duan, X., Liu, H.L., Wang, Q., Sun, S.C., 2016. Both diet and gene mutation induced obesity affect oocyte quality in mice. Scientific reports 6, 18858.

Hyslop, L.A., Blakeley, P., Craven, L., Richardson, J., Fogarty, N.M., Fragouli, E., Lamb, M., Wamaitha, S.E., Prathalingam, N., Zhang, Q., O'Keefe, H., Takeda, Y., Arizzi, L., Alfarawati, S., Tuppen, H.A., Irving, L., Kalleas, D., Choudhary, M., Wells, D., Murdoch, A.P., Turnbull, D.M., Niakan, K.K., Herbert, M., 2016. Towards clinical application of pronuclear transfer to prevent mitochondrial DNA disease. Nature 534, 383-386.

Igosheva, N., Abramov, A.Y., Poston, L., Eckert, J.J., Fleming, T.P., Duchen, M.R., McConnell, J., 2010. Maternal diet-induced obesity alters mitochondrial activity and redox status in mouse oocytes and zygotes. PloS one 5, e10074.

Johnson, M.T., Freeman, E.A., Gardner, D.K., Hunt, P.A., 2007. Oxidative metabolism of pyruvate is required for meiotic maturation of murine oocytes in vivo. Biology of reproduction 77, 2-8.

Johnson, M.T., Mahmood, S., Hyatt, S.L., Yang, H.S., Soloway, P.D., Hanson, R.W., Patel, M.S., 2001. Inactivation of the murine pyruvate dehydrogenase (Pdha1) gene and its effect on early embryonic development. Molecular genetics and metabolism 74, 293-302.

Jungheim, E.S., Schoeller, E.L., Marquard, K.L., Louden, E.D., Schaffer, J.E., Moley, K.H., 2010. Diet-induced obesity model: abnormal oocytes and persistent growth abnormalities in the offspring. Endocrinology 151, 4039-4046.

Kaneko, K.J., 2016. Metabolism of Preimplantation Embryo Development: A Bystander or an Active Participant? Current topics in developmental biology 120, 259-310.

Kim, J.M., Ogura, A., 2009. Changes in allele-specific association of histone modifications at the imprinting control regions during mouse preimplantation development. Genesis (New York, N.Y. : 2000) 47, 611-616.

Kinnaird, A., Zhao, S., Wellen, K.E., Michelakis, E.D., 2016. Metabolic control of epigenetics in cancer. Nature reviews. Cancer 16, 694-707.

Kishimoto, S., Uno, M., Okabe, E., Nono, M., Nishida, E., 2017. Environmental stresses induce transgenerationally inheritable survival advantages via germline-to-soma communication in Caenorhabditis elegans. Nature communications 8, 14031.

L'Hernault, S.W., Rosenbaum, J.L., 1985. Chlamydomonas alpha-tubulin is posttranslationally modified by acetylation on the epsilon-amino group of a lysine. Biochemistry 24, 473-478.

Li, Y., Seah, M.K., O'Neill, C., 2016. Mapping global changes in nuclear cytosine base modifications in the early mouse embryo. Reproduction (Cambridge, England) 151, 83-95.

Liu, Q., Kang, L., Wang, L., Zhang, L., Xiang, W., 2016a. Mitofusin 2 regulates the oocytes development and quality by modulating meiosis and mitochondrial function. Scientific reports 6, 30561.

Liu, X., Wang, C., Liu, W., Li, J., Li, C., Kou, X., Chen, J., Zhao, Y., Gao, H., Wang, H., Zhang, Y., Gao, Y., Gao, S., 2016b. Distinct features of H3K4me3 and H3K27me3 chromatin domains in pre-implantation embryos. Nature 537, 558-562.

McGrath, J., Solter, D., 1983. Nuclear transplantation in the mouse embryo by microsurgery and cell fusion. Science (New York, N.Y.) 220, 1300-1302.

Morrow, E.H., Ingleby, F.C., 2017. Detecting differential gene expression in blastocysts following pronuclear transfer. BMC research notes 10, 97.

Motta, P.M., Nottola, S.A., Makabe, S., Heyn, R., 2000. Mitochondrial morphology in human fetal and adult female germ cells. Human reproduction (Oxford, England) 15 Suppl 2, 129-147.

Onjiko, R.M., Moody, S.A., Nemes, P., 2015. Single-cell mass spectrometry reveals small molecules that affect cell fates in the 16-cell embryo. Proceedings of the National Academy of Sciences of the United States of America 112, 6545-6550.

Pang, W., Zhang, Y., Zhao, N., Darwiche, S.S., Fu, X., Xiang, W., 2013. Low expression of Mfn2 is associated with mitochondrial damage and apoptosis in the placental villi of early unexplained miscarriage. Placenta 34, 613-618.

Paradies, G., Paradies, V., De Benedictis, V., Ruggiero, F.M., Petrosillo, G., 2014. Functional role of cardiolipin in mitochondrial bioenergetics. Biochimica et biophysica acta 1837, 408-417.

Piquereau, J., Caffin, F., Novotova, M., Prola, A., Garnier, A., Mateo, P., Fortin, D., Huynh, L.H., Nicolas, V., Alavi, M.V., Brenner, C., Ventura-Clapier, R., Veksler, V., Joubert, F., 2012. Down-regulation of OPA1 alters mouse mitochondrial morphology, PTP function, and cardiac adaptation to pressure overload. Cardiovascular research 94, 408-417.

Poidatz, D., Dos Santos, E., Gronier, H., Vialard, F., Maury, B., De Mazancourt, P., Dieudonne, M.N., 2015. Trophoblast syncytialisation necessitates mitochondrial function through estrogen-related receptor-gamma activation. Molecular human reproduction 21, 206-216.

Rardin, M.J., Wiley, S.E., Naviaux, R.K., Murphy, A.N., Dixon, J.E., 2009. Monitoring phosphorylation of the pyruvate dehydrogenase complex. Analytical biochemistry 389, 157-164.

Saben, J.L., Boudoures, A.L., Asghar, Z., Thompson, A., Drury, A., Zhang, W., Chi, M., Cusumano, A., Scheaffer, S., Moley, K.H., 2016. Maternal Metabolic Syndrome Programs Mitochondrial Dysfunction via Germline Changes across Three Generations. Cell reports 16, 1-8.

Sakamoto, T., Inoue, T., Otomo, Y., Yokomori, N., Ohno, M., Arai, H., Nakagawa, Y., 2012. Deficiency of cardiolipin synthase causes abnormal mitochondrial function and morphology in germ cells of Caenorhabditis elegans. The Journal of biological chemistry 287, 4590-4601.

Sanchez-Delgado, M., Court, F., Vidal, E., Medrano, J., Monteagudo-Sanchez, A., Martin-Trujillo, A., Tayama, C., Iglesias-Platas, I., Kondova, I., Bontrop, R., Poo-Llanillo, M.E., Marques-Bonet, T., Nakabayashi, K., Simon, C., Monk, D., 2016. Human Oocyte-Derived Methylation Differences Persist in the Placenta Revealing Widespread Transient Imprinting. PLoS genetics 12, e1006427.

Sathananthan, A.H., Trounson, A.O., 2000. Mitochondrial morphology during preimplantational human embryogenesis. Human reproduction (Oxford, England) 15 Suppl 2, 148-159.

Schulkey, C.E., Regmi, S.D., Magnan, R.A., Danzo, M.T., Luther, H., Hutchinson, A.K., Panzer, A.A., Grady, M.M., Wilson, D.B., Jay, P.Y., 2015. The maternal-age-associated risk of congenital heart disease is modifiable. Nature 520, 230-233.

Skaznik-Wikiel, M.E., Swindle, D.C., Allshouse, A.A., Polotsky, A.J., McManaman, J.L., 2016. High-Fat Diet Causes Subfertility and Compromised Ovarian Function Independent of Obesity in Mice. Biology of reproduction 94, 108.

Teperino, R., Schoonjans, K., Auwerx, J., 2010. Histone methyl transferases and demethylases; can they link metabolism and transcription? Cell metabolism 12, 321-327.

Turdi, S., Ge, W., Hu, N., Bradley, K.M., Wang, X., Ren, J., 2013. Interaction between maternal and postnatal high fat diet leads to a greater risk of myocardial dysfunction in offspring via enhanced lipotoxicity, IRS-1 serine phosphorylation and mitochondrial defects. J Mol Cell Cardiol 55, 117-129.

Vagnoni, A., Rodriguez, L., Manser, C., De Vos, K.J., Miller, C.C., 2011. Phosphorylation of kinesin light chain 1 at serine 460 modulates binding and trafficking of calsyntenin-1. Journal of cell science 124, 1032-1042.

Wakai, T., Harada, Y., Miyado, K., Kono, T., 2014. Mitochondrial dynamics controlled by mitofusins define organelle positioning and movement during mouse oocyte maturation. Molecular human reproduction.

Wang, Y., Zhao, S., 2010. Vascular Biology of the Placenta. Morgan & Claypool Life Sciences, San Rafael (CA).

Wasilewski, M., Semenzato, M., Rafelski, S.M., Robbins, J., Bakardjiev, A.I., Scorrano, L., 2012. Optic atrophy 1-dependent mitochondrial remodeling controls steroidogenesis in trophoblasts. Current biology : CB 22, 1228-1234.

Williams, L., Seki, Y., Vuguin, P.M., Charron, M.J., 2014. Animal models of in utero exposure to a high fat diet: a review. Biochimica et biophysica acta 1842, 507-519.

Wing-Lun, E., Eaton, S.A., Hur, S.S., Aiken, A., Young, P.E., Buckland, M.E., Li, C.C., Cropley, J.E., Suter, C.M., 2016. Nutrition has a pervasive impact on cardiac microRNA expression in isogenic mice. Epigenetics 11, 475-481.

Wu, L.L., Norman, R.J., Robker, R.L., 2011. The impact of obesity on oocytes: evidence for lipotoxicity mechanisms. Reproduction, fertility, and development 24, 29-34.

Wu, L.L., Russell, D.L., Norman, R.J., Robker, R.L., 2012. Endoplasmic reticulum (ER) stress in cumulus-oocyte complexes impairs pentraxin-3 secretion, mitochondrial membrane potential (DeltaPsi m), and embryo development. Molecular endocrinology (Baltimore, Md.) 26, 562-573.

Wu, L.L., Russell, D.L., Wong, S.L., Chen, M., Tsai, T.S., St John, J.C., Norman, R.J., Febbraio, M.A., Carroll, J., Robker, R.L., 2015. Mitochondrial dysfunction in oocytes of obese mothers: transmission to offspring and reversal by pharmacological endoplasmic reticulum stress inhibitors. Development (Cambridge, England) 142, 681-691.

Zhang, B., Zheng, H., Huang, B., Li, W., Xiang, Y., Peng, X., Ming, J., Wu, X., Zhang, Y., Xu, Q., Liu, W., Kou, X., Zhao, Y., He, W., Li, C., Chen, B., Li, Y., Wang, Q., Ma, J., Yin, Q., Kee, K., Meng, A., Gao, S., Xu, F., Na, J., Xie, W., 2016. Allelic reprogramming of the histone modification H3K4me3 in early mammalian development. Nature 537, 553-557.

Zhao, N., Zhang, Y., Liu, Q., Xiang, W., 2015. Mfn2 Affects Embryo Development via Mitochondrial Dysfunction and Apoptosis. PloS one 10, e0125680.

Zheng, H., Huang, B., Zhang, B., Xiang, Y., Du, Z., Xu, Q., Li, Y., Wang, Q., Ma, J., Peng, X., Xu, F., Xie, W., 2016. Resetting Epigenetic Memory by Reprogramming of Histone Modifications in Mammals. Molecular cell 63, 1066-1079.

5.4   Figure Legends

Figure 5-1: Endoplasmic stress response genes are unchanged in MII oocytes by exposure to a HF/HS diet and salubrinal. Transcript levels of three MII oocytes from three different mice per treatment group were analyzed for expression of (A) *Pdia4* (B) *Xbp1* (C) *Atf4* (D) *Ddit3* (E) *Dnajc3* (F) *Herpud1* and (G) *Edem1*. Black bars indicate control diet fed mice, and grey bars indicate HF/HS diet fed mice. Two-way ANOVA with Tukey-Kramer correction for multiple analyses was done to assess statistical significance; none was found.

Figure 5-2: Spindle acetylation is significantly decreased in MII oocytes from HF/HS females. a) MII oocytes from control diet or HF/HS females were stained using antibodies specific for lysine-40 acetylated α-tubulin (acK40 α-Tubulin; left panels) and Dapi to visualize chromosomes. Yellow arrowhead indicates spindle, red arrow indicates polar body; scale bar = 25µm. b) Intensity of tubulin acetylation was measured as a surrogate for total spindle acetylation. Only bipolar spindles with well aligned chromosomes were measured by drawing a polygon around the spindle in the acK40 α-Tubulin channel as shown in c).

Figure 5-3: Pyruvate dehydrogenase (PDH) is phosphorylated and inactivated in HF/HS oocytes at multiple serine residues. a) Representative western blot of GV oocytes probed for total PDH and phosphorylated PDH (pPDH) at serine 293 (S293). b) Densitometry of western blots to compare ratio of pPDH to total PDH in GV oocytes. Values were normalized to GAPDH, averaged and compared with a Student's t-test, *** $P<0.001$. c) Representative images of GV oocytes stained for pPDH at S293 (top panels) or S300 (bottom panels). Staining was done at the same time and all images were taken at the same gain to appropriately quantify values. d) Quantification of S300 or S293 pPDH fluorescence in GV oocytes. n=at least 50 oocytes per group; staining

repeated 3 independent times for each antibody; values compared using a Student's t-test, *p<0.05.

e) S300 pPDH also localizes to the meiotic spindle. In all images, scale bar = 25 µm.

Figure 5-4: Maternal HF/HS diet exposure downregulates Mfn2 in oocytes and blastocysts. (A) Representative western blot of 100 GV oocytes probed for Mfn2 and GAPDH. (B) Densitometry of three GV oocyte western blots. Total Mfn2 was normalized to GAPDH. (C) Representative confocal images of MII oocytes stained using an Mfn2 antibody; scale bar = 25 µm. (D) Corrected total cell fluorescence (CTCF) of MII oocytes stained with MII. (E) Representative western blot of in vitro fertilized blastocysts probed for Mfn2. (F) Densitometry of three embryo western blots. All values compared using a Student's t-test, *p<0.05.
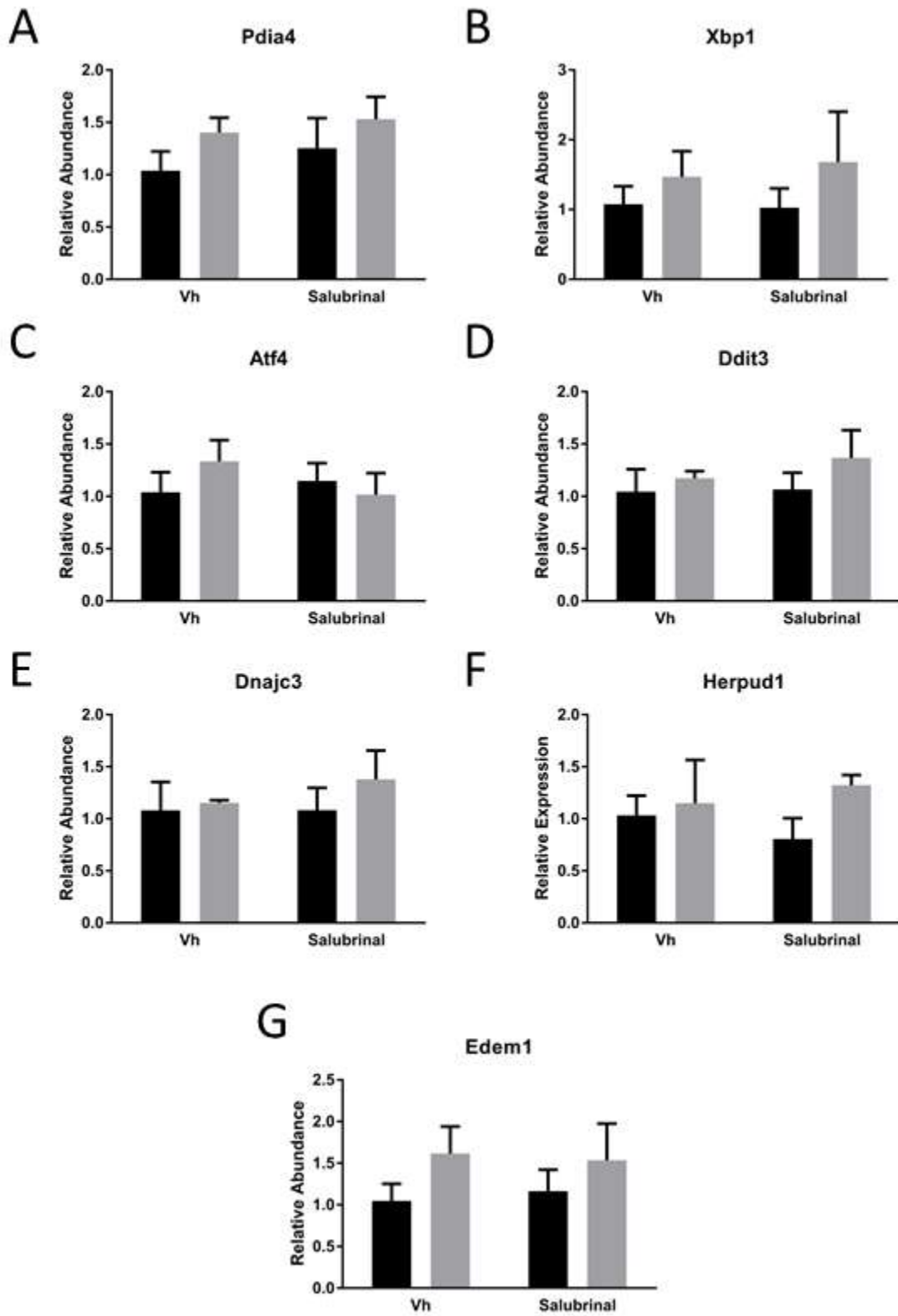
Figure 5- 1: Endoplasmic stress response genes are unchanged in MII oocytes by exposure to a HF/HS diet and salubrinal
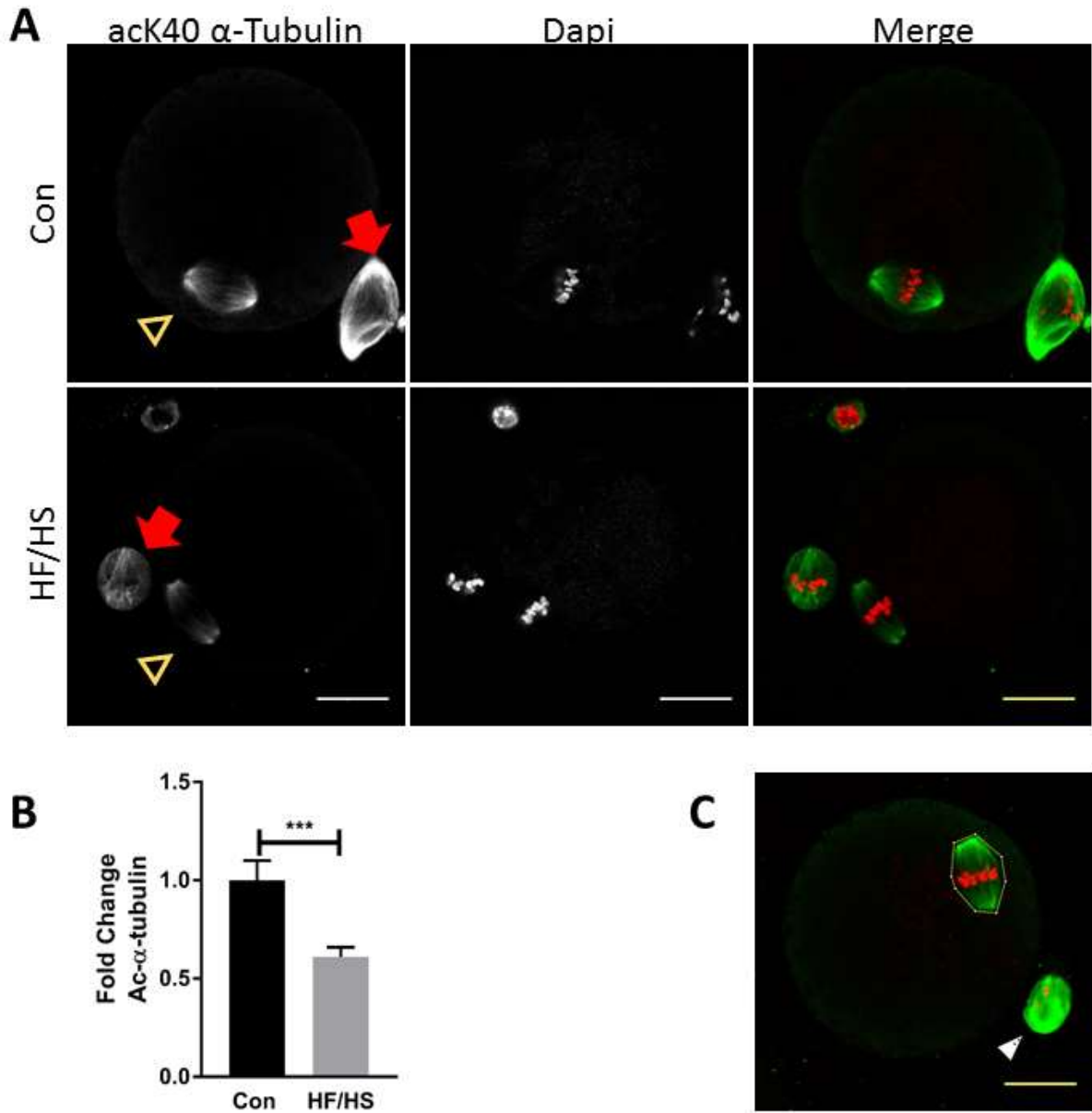
Figure 5- 2: Spindle acetylation is significantly decreased in MII oocytes from HF/HS females.
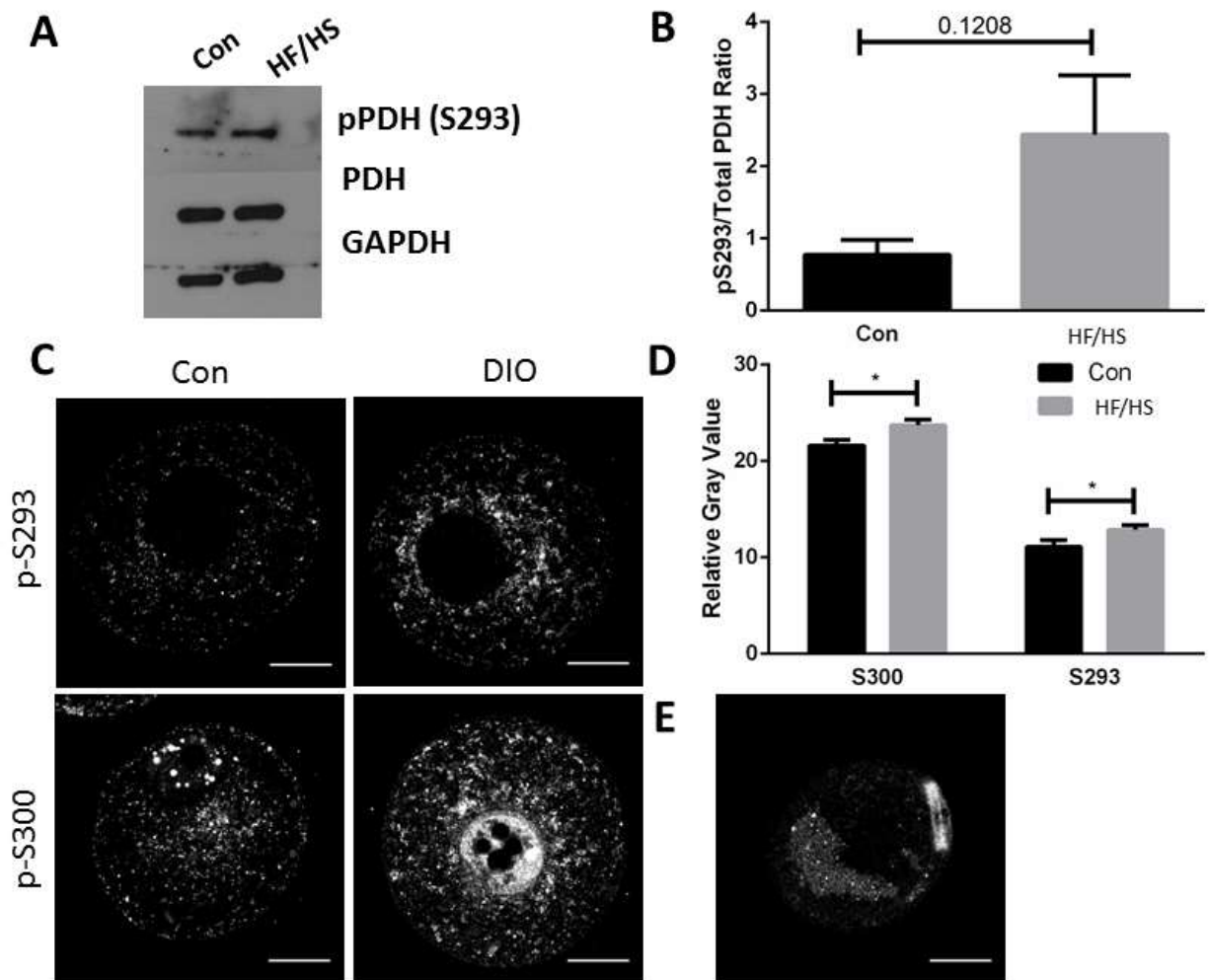
Figure 5- 3: Pyruvate dehydrogenase (PDH) is phosphorylated and inactivated in HF/HS oocytes at multiple serine residues.
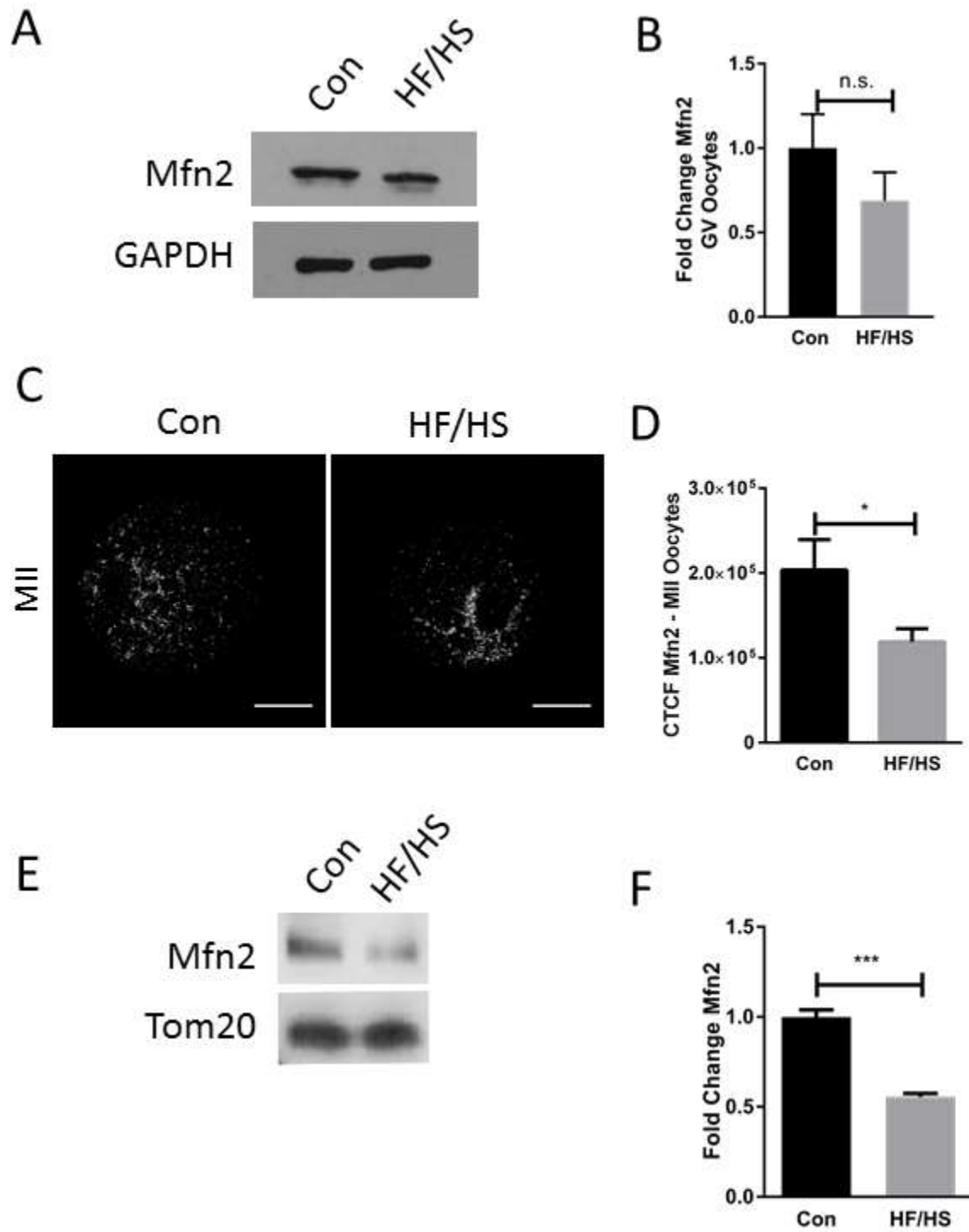
Figure 5- 4: Maternal HF/HS diet exposure downregulates Mfn2 in oocytes and blastocysts.

5.5 Table

Table 5- 1: List of primers used in Figure 5-1

Gene Symbol	Gene Name	Catalog Number
Pdia4	Protein Disulfide-Isomerase A4	Mm00437958_m1
Xbp1	X-Box Binding Protein 1	Mm00457357_m1
Atf4	Activating Transcription Factor 4	Mm00515325_g1
Ddit3	DNA Damage Inducible Transcript 3	Mm01135937_g1
Dnajc3	DnaJ Homolog Subfamily C Member 3	Mm00515299_m1
Edem1	ER Degradation Enhancer, Mannosidase Alpha-Like 1	Mm00551797_m1
Actb	Beta Actin	Mm00607939_s1

Appendix: Insights into mechanisms causing the maternal age-induced decrease in oocyte quality

Anna L Boudoures and Kelle H Moley

Department of Obstetrics and Gynecology, Center for Reproductive Health Sciences,

Washington University in St. Louis School of Medicine, St. Louis, MO 63110 USA

A1. Abstract

Female fertility declines with age, but the underlying mechanisms remain unclear. Clinical and laboratory studies point to the oocyte as the source of the decline. Here, we review the recent literature on the role of reactive oxygen species (ROS) within oocytes, as well as highlighting the role of cohesin proteins in preventing aneuploidy and some promising treatments to reduce the age-induced decrease in fertility. ROS increase with age, damaging mitochondria and proteins important in oocyte maturation and meiosis. The damages to mitochondria impair ATP production. ATP levels in oocytes have been linked to successful completion of meiosis prior to ovulation and mediating the appropriate response to sperm binding. ROS also damage proteins important in DNA repair. Meiosis-specific homologs of DNA repair proteins have a critical role in recombination and preventing aneuploidy. Therefore, ROS-induced mitochondrial damage has wide-spread impacts on multiple aspects of oocyte quality. Some treatments are discussed which have shown to be effective in decreasing ROS-induced damage and lowering aneuploidy, providing hope to older women hoping to conceive. However, gaps in knowledge remain and require further investigation before more targeted treatments can be developed.

A2. Abbreviations:

ALA - alpha lipoic acid, ATP – Adenosine Triphosphate, Ca^{2+} - Calcium, COI – Cyctochrome c Oxidase Subunit I, CuZnSOD – Copper-Zinc Superoxid Dismutase, DNA – Deoxyribonucleic Acid, ER - endoplasmic reticulum, ETC – Electron Transport Chain, $FADH_2$ – Flavin Adenine Dinucleotide, FCCP – Carbonylcyanide p-trifluoro-methyoxyphenylhydrazone, GV – Germinal Vesicle, GVBD – Germinal Vesicle Breakdown, H_2O_2 – Hydrogen Peroxide, iKT – interkinetochore, IVF – In Vitro Fertilization, MI – Meiosis I, MII – Meiosis II, MnSOD – Manganese Superoxide Dismutase, mtDNA – Mitochondrial DNA, NAC - N-acetyl-L-cysteine, NADH – Nicotinamide Adenin Dinucleotide, NADPH – Nicotinamide Adenine Dinucleotide Phosphate, O^{2-} – Superoxide, PMCA - plasma membrane Ca^{2+} -ATPase, REC8 – Meiotic Recombination Protein 8, REDOX – Reduction and Oxidation, ROS – Reactive Oxygen Species, SC - Synaptonemal Complex, SERCA - sarco/endoplasmic reticulum Ca^{2+}-ATPase, SGO2 -

Shugosin-2, SIRT1 – Sirtuin-1, SMC - Structural Maintenance of Chromosome, SMC1β –
Structural Maintenance of Chromosome 1B, SMC3 – Structural Maintenance of Choromsome 3,
STAG3 – Stromal Antigen 3

A3.   Overview and Introduction

Female fertility sharply declines with increasing age. One prominent cause of this decline in
fertility is that females are born with a fixed number of primordial oocytes that are gradually lost.
Although recent evidence suggests that a small pool of oogonial stem cells produces mature
oocytes, the contribution of this slowly renewing stem cell pool to the ovarian reserve is not
sufficient to prevent menopause (1, 2). The fate of most oocytes is atresia, which occurs in two
phases. First, oocyte number decreases linearly from birth until approximately 35 years of age in
humans(3) (equivalent to about 12 months in mice (4)). This loss of primordial follicles can also
be observed in mice between the time of birth and sexual maturity (5). In the second phase,
follicle loss increases with each menstrual cycle until menopause at around age 50 in humans
(reviewed in (3)).

Evidence from *in vitro* fertilization (IVF) indicates that another contributor to declining
fertility is loss of oocyte quality. Women over the age of 50 who used their own oocytes for IVF
had significantly lower pregnancy rates than women who used oocytes donated by younger
women. In fact, older women receiving young donor oocytes experienced pregnancy rates
similar to those of young women undergoing IVF (6). This suggests that oocyte quality and not
endometrial receptivity is the main cause for the age-related decline in fertility.

Here, we will review the recent literature indicating that oocyte quality declines with
maternal age because of an accumulation of reactive oxygen species (ROS), which can cause
mitochondrial, spindle, and DNA damage. We will also summarize potential avenues of
treatment to improve oocyte quality for older women.

A4.   Process of oocyte maturation

The development of a mature oocyte capable of fertilization takes place in a series of steps occurring over many years in humans. At birth, all oocytes are arrested at diplotene of prophase I and remain at this developmental stage until puberty (Figure 1a). When oocytes are selected to resume maturation, they contain a prominent nucleus, or germinal vesicle. These immature oocytes are referred to as GV oocytes due to the prominent nucleus (Figure 1b). Oocyte maturation is induced by changes in hormone levels in response to the estrous cycle in most mammals and the menstrual cycle in humans (Figure 1). During this process, the ovarian follicles surrounding and supporting each oocyte, and the oocytes themselves, grow in size. The resumption of meiosis is triggered by a surge of luteinizing hormone immediately prior to ovulation, which signals breakdown of the nuclear envelope in a step known as germinal vesicle breakdown (GVBD) (7). During GVBD, chromatin condenses, the chromosomes align along the metaphase I plate, and a transient but well-defined spindle forms (Figure 1c)(8).

The oocyte cytoplasm divides unevenly at the end of meiosis I, resulting in formation of a small polar body with half of the chromosomes. The spindle reforms, the chromosomes re-align on the metaphase II plate and the oocyte arrests again until fertilization (9-11) (Figure 1d). At fertilization, meiosis II (MII) resumes leading to the extrusion of a second polar body and a haploid pronucleus in the oocyte (12) (Figure 1e).

The process of oocyte maturation is energy intensive, requiring high levels of nutrient consumption and ATP production to fuel transcription as well as the increases in follicle and oocyte size (13, 14). The main source of this energy is glucose, which is utilized only by the cumulus cells surrounding each oocyte (15). The cumulus cells supply the oocyte with pyruvate, which the oocyte uses to generate ATP via oxidative phosphorylation and the electron transport chain (ETC) (15, 16). Underscoring the importance of sufficient ATP production in oocyte

maturation, the ATP content of human oocytes at MII arrest is positively correlated with successful fertilization and IVF outcome (17). ATP production occurs at three distinct times during oocyte maturation: at GVBD, during spindle migration in MI, and during polar body extrusion at the MI to MII transition (Figure 1b-d) (18). At each of these times, mitochondria cluster around the nucleus. These observations suggest that ATP produced by mitochondria plays an important role in faithful meiosis and gene expression during nuclear maturation in the oocyte.

A4.1   Oocyte Reactive Oxygen Species Production

The generation of ATP also results in the production of reactive oxygen species (ROS) as a by-product of the mitochondrial electron transport chain (ETC). In order to generate the necessary proton gradient for ATP production, electrons are passed across the mitochondrial membrane. Inefficiencies in transport generate free radicals, especially at complexes I and III of the ETC, where the free electrons generate superoxide (O_2^-) and hydrogen peroxide (H_2O_2) from water instead of being transferred to their normal intermediates of succinate or $FADH_2$. While this is not the only cellular process that generates ROS, it is a major source of ROS in aerobic cells, including the oocyte. ROS damage DNA and inappropriately modify proteins and unsaturated fatty acids in cell and organelle membranes (19).

ROS cause mitochondrial DNA damage (mtDNA), which encodes the ETC proteins. These proteins are necessary for cellular metabolism. ROS-induced mutations in mtDNA create inefficient ETC proteins that increase production of ROS, creating a vicious cycle (reviewed in (20)). Therefore, a major cause of spindle abnormalities and aneuploidy in oocytes may be due to the adverse effects of oxidative stress on mtDNA and ETC proteins.

To study the role of mitochondria and the ETC in oocytes, the mitochondrial membrane potential can be disrupted with FCCP (Carbonylcyanide p-trifluoro-methyoxyphenylhydrazone) (21). FCCP exposure during *in vitro* oocyte meiotic maturation delays the completion of meiosis I and meiosis II. FCCP exposure in culture also causes an increased proportion of abnormal spindles and abnormal chromosome alignment in oocytes (22). Therefore, ETC inhibition causes an increase in spindle abnormalities in oocytes.

Another mechanism to induce oxidative damage specifically to oocyte mitochondria is to use the mitochondrial dye CMXRos combined with photo-sensitization. Oxidative damage using this technique caused a significant decrease in meiotic progression and fertilization. Therefore, mitochondria are critical for successful oocyte maturation and fertilization. In the same study, when investigators transplanted the GV nucleus from a damaged oocyte to an undamaged, enucleated oocyte, investigators observed a significant increase in successful meiosis, fertilization and development to blastocyst (23). This indicates that oxidative damage specifically to mitochondria leads to decreased fertility.

However, not all effects of ROS on cells, including oocytes, are negative. In oocytes, the initiation of nuclear maturation has been linked to ROS concentration. Depleting ROS and H_2O_2 inhibited ovulation indicating that ROS are needed to induce oocyte maturation in response to hormone signals (Figure 1). Similarly, it has also been shown that ROS are likely required to activate gene transcription during ovulation (24). Thus levels of ROS that are either too high or two low may have detrimental effects on oocyte development.

A4.2 Compensation Mechanisms

Because the oocyte relies on ROS to activate gene transcription and oocyte maturation and because oxidative stress is unavoidable, the oocyte has endogenous mechanisms in place to

minimize oxidative damage. Oocytes are able to utilize pyruvate for more than just ATP

production (25). Pyruvate is also critical for maintaining the appropriate REDOX potential in the

oocyte. Metabolism of pyruvate in the cytoplasm by lactate dehydrogenase and by pyruvate

dehydrogenase in the mitochondria ensures that the appropriate levels of the antioxidants

NADPH and NADH are produced to compensate for ROS production during the production of

ATP by the electron transport chain (26).

Oocytes also transcribe endogenous antioxidant enzymes. Evidence from hamster oocytes

demonstrates a rise in glutathione, an endogenous antioxidant, occurs concomitantly with

chromosome condensation and spindle formation as the oocytes mature. There is also a

glutathione increase in cumulus cells of maturing oocytes (27). Therefore, the oocyte has

mechanisms in place to combat oxidative damage that is continuously occurring during the

growth and maturation processes.

In addition to endogenous antioxidants, the oocyte also has mechanisms to remove

damaged mtDNA molecules. Recently, an elegant study in *Drosophila* oocytes demonstrated that

mitochondrial function also plays a critical role in mtDNA replication and removal of damaged

mtDNA. Investigators showed that ETC protein mutations, such as a mutation to COI

(cyctochrome *c* oxidase subunit I), impaired mtDNA replication. While quantitation was not

possible, observations suggested the oocyte has mechanisms to reduce heteroplasmy by

preferentially transcribing copies of mtDNA molecules that did not carry a mutation to the

necessary COI. Over time, this resulted in the elimination of mutated mtDNA. Furthermore, the

elimination of mutated mtDNA continued to occur not only in females' reproductive lifespans,

but also in her offsprings' lifespan (28). Therefore, the oocyte has mechanisms in place to reduce

heteroplasmy and selectively remove damaged copies of mtDNA. Moreover, mitochondrial function is intimately linked to and dependent on healthy mtDNA.

A5. Effects of Age on Oocytes

Increased oxidative stress occurs in all tissues with age and is a direct result of ROS produced by the mitochondria. To determine the source of ROS, reserachers genetically engineered a mouse model with increased expression of the endogenous antioxidant enzyme catalase targeted exclusively in mitochondria. Catalase expressio significantly lengthens their lifespan by direct reduction of oxidative damage. Importantly, parallel mouse models that targeted catalase expression to either the peroxisome or the nucleus did not have the same effect (29). Because only catalase expression in mitochondria increased lifespan, mitochondrial ROS production are a main source of oxidative damage that increases with age. While this experiment was in all somatic tissues, it is relevant to oocytes because there is an age-related increase in oxidative stress in the oocytes (4, 30-32) that is likely due to increased production of ROS by inefficient mitochondria.

ROS accumulation has been studied in a variety of ways in fixed oocytes. However a non-invasive technique to study live oocytes remained elusive until recently. Now, Raman spectra imaging can be applied to oocytes (33). Raman spectra imaging uses lasers to create vibrational energy within chemical bonds in a single live cell. This vibration energy causes photons to scatter in predictable, unique patterns for different biological molecules. This spectrum can be analyzed by principal component analysis to reveal the unique molecular profiles for individual cells, including oocytes (34). When CD-1 mouse oocytes were analyzed using Raman spectroscopy, oocytes exposed to oxidizing agents showed a significant change in

their lipid profile. Importantly, analysis of live oocytes collected from aged females and young females showed significant differences in the between the Raman spectra for multiple molecules. These differences were similar, though not as extreme, as the changes induced by ROS in vitro (33). This indicates that increased ROS are one mechanism impacting oocyte quality in females of advanced maternal age.

Mammalian oocyte mitochondria are unique in structure and function. Structurally, they are round and may have large, clear vacuoles within the matrix. Cristae either traverse the matrix or are arch shaped and outline its periphery (11). Functionally, the role of the mitochondria is also unique, as oocyte microinjection with stem cell mitochondria failed to rescue damaged oocytes. However, microinjection of healthy oocyte mitochondria into oocytes from females of advanced reproductive age did improve metabolic parameters (35). While this technique is not suitable for the clinic, it highlights the unique properties of oocyte mitochondria and the importance of healthy mitochondria in fertilization and development.

The increase in oocyte ROS production with age has been linked to notable, significant changes to mitochondira. Both human and mouse oocytes from females of advanced maternal age have increased mitochondrial aggregates and ROS (4, 36). Previously, it was shown that aggregated mitochondria are correlated with poor quality oocytes and decreased fertilization (37). This would suggest that ROS increase with age and cause a decrease in mitochondrial quality. Supporting ROS-induced mitochondrial damage, the mitochondria in oocytes of aged females also appear abnormal with large vacuoles present (38). Additionally, ATP content and mtDNA copy number are decreased in both mouse and hamster oocytes from females of advanced maternal age (38). The decrease in mtDNA copy number indicates decreased mitochondrial numbers, which is supported by lower levels of ATP production.

155

mtDNA copy number can be used to estimate the total number of mitochondria present in a cell (39). Oocytes from women of advanced maternal age have decreased mtDNA copy numbers and thus decreased numbers of mitochondria. This decrease in oocyte mtDNA correlated with an increase in the proportion of unfertilized oocytes after IVF. Additionally, fertilized oocytes that developed to cleavage stage embryos also had significantly more mtDNA copies than unfertilized oocytes or zygotes that did not progress. These data indicate that sufficient copies of mtDNA are necessary for fertilization and embryo development (40) and suggest that an age-related reduction in oocyte mitochondria adversely affects fertility and development.

If DNA repair enzyme genes transcribed from nuclear DNA are mutated by oxidative damage, ROS induced double strand breaks cannot be repaired in the oocyte. The DNA repair enzymes Brca1, ATM, Mre11 and Rad51 have decreased expression in oocytes analyzed from both mice and humans of advanced maternal age. All of the enzymes listed are important in repairing ROS-induced DNA damage (41). Whether the decreased expression was due to mutations to DNA by ROS or other changes in the oocyte (such as rates of transcription) were not tested. But, decreased expression of DNA repair enzymes makes the oocytes from older females more susceptible to DNA damage by ROS.

Human oocytes also demonstrate higher levels of oxidative damage. Oocytes from aged women showed increased accumulation of protein markers of oxidative stress as well as markers of protein degradation and apoptosis (42). Additionally, when compared to MII oocytes from younger patients, those from women over 38 years old had upregulation of pro-apoptotic genes and down-regulation of anti-apoptotic genes (43). Likely, oxidative damage is initiating apoptosis in aging oocytes.

A6. Compensation Mechanisms

Oocytes also have mechanisms to reduce oxidative damage. One such mechanism could involve Sirtuin-1 (SIRT1), a master regulator of gene expression within cells. SIRT1 gene expression is elevated in oocytes from aged mice (30). In addition, oocytes from young mice upregulated SIRT1 mRNA if exposed to increased ROS levels, inducing a subsequent increase in the transcription of the ROS scavenger Manganese Superoxide Disumutase (MnSOD). SIRT1 expression in oocytes from aged mice was not as high as in ROS exposed oocytes from young mice. Despite increased SIRT1 transcript, there were significantly lower levels of SIRT1 protein in the oocytes of aged females as compared to young controls. Therefore, aged females were unable to activate the proper SIRT1-induced stress response seen in oocytes from younger females. Unlike young oocytes, oocytes from aged females also demonstrated elevated basal levels of MnSOD expression independent of SIRT1 expression (30). This data suggests that oocytes from older females are unable to properly respond to the age-induced increase in oxidative damage.

Human oocytes are extremely difficult to obtain for research purposes, thus to gain insight into oocyte physiology many studies focus on the cumulus cells which have a close relationship with the oocyte throughout folliculogenesis. Cumulus cells from IVF patients demonstrated abundant expression of two ROS scavenging enzymes, MnSOD and CuZnSOD, which are negatively correlated with increasing age (44). A decrease in these enzymes could make the entire follicle more susceptible to oxidative stress and lead to decreased fertility.

Further studies conducted in IVF patients demonstrated that high levels of H_2O_2 in follicular fluid were positively correlated with poor embryo quality while low levels were

positively correlated with empty follicles. Investigators found that intermediate levels of follicular fluid H_2O_2 correlated with good quality embryos (45). Therefore, ROS are both necessary for successful oocyte retrieval and embryo development, but if the concentration in the follicular fluid is too high, then the oocytes derived from these follicles will give rise to poor quality embryos with decreased developmental competence.

A7. Clinical Effects of Aging

Fertilization

Damage to oocyte mitochondria and low levels of ATP production also lead to decreased fertilization rates. Sperm binding triggers calcium (Ca^{2+}) oscillations within the oocyte, resulting in the completion of meiosis II (Figure 1e). Inhibiting ATP production causes Ca^{2+} levels to drop in the oocyte cytosol. To compensate, the endoplasmic reticulum (ER) releases its Ca^{2+} stores prior to fertilization. Therefore, there is no longer sufficient Ca^{2+} remaining in the ER to trigger the appropriate response in the oocyte when fertilization does occur (46). A similar premature Ca^{2+} release could be occurring in oocytes as females age, since these oocytes are ATP deficient (38).

Recently, Wakai et al showed that the fertilization induced Ca^{2+} oscillations are dependent on both ER Ca^{2+} stores and extracellular Ca^{2+} influx via two ATP-dependent channels, the plasma membrane Ca^{2+}-ATPase (PMCA) and SERCA (sarco/endoplasmic reticulum Ca^{2+}-ATPase), an ER-specific, ATP dependent Ca^{2+} transporter. In order to maintain the appropriate concentrations of Ca^{2+} necessary for Ca^{2+} oscillations and successful fertilization, ATP produced by the mitochondria is utilized. Disruption of mitochondrial function in oocytes rapidly depleted Ca^{2+} concentrations within the cytoplasm and the ER. Mitochondrial disruption

also severely attenuated and rapidly eliminated oscillations prematurely (47). This further supports a critical role of healthy, functional mitochondria for successful fertilization. Because oocytes from aged females have insufficient ATP levels and damaged mitochondria, the ability of the oocytes to trigger the appropriate Ca^{2+} oscillations after sperm binding may be attenuated, preventing fertilization (Figure 1).

After fertilization is achieved, maintaining a proper redox balance is necessary to ensure embryo viability. Inducing oxidative damage to mitochondria during oocyte maturation *in vitro* caused increased apoptosis prior to fertilization and decreased blastocyst formation after fertilization. This was likely caused by the uncoupling of mitochondrial respiration and a subsequent decrease in ATP content (48). Increased levels of ROS were positively correlated with increased frequency of embryo fragmentation and apoptosis in human embryos after IVF (49). If embryos with damaged mitochondria progress past initial cell divisions, development does not occur normally. When two-cell mouse embryos were cultured briefly with agents to damage mitochondria, the embryos developed more slowly and had decreased cell numbers at the blastocyst stage. After being transferred into recipient females, fetuses were smaller at embryonic day 18 (50). Culturing oocytes with the dye rhodamine-123 and irradiating them induces mitochondrial damage. Applying this technique to mouse oocytes adversely affected the resulting embryos which demonstrated significantly fewer cells in the trophectoderm and decreased implantation rates (51). These data support the notion that oxidative damage to oocyte mitochondria prior to ovulation and fertilization has negative effects on embryo development.

Spindle structure and cohesin proteins
Sufficient ATP production is critical for appropriate spindle assembly. When oocytes were exposed to increased levels of H_2O_2 to induce oxidative stress, there was a subsequent

159

decrease in ATP production and a corresponding increase in the proportion of spindle and chromosome segregation abnormalities (52). In a study using oocyte-cumulus complexes taken from a diabetic female mouse model, cumulus cells exhibited decreased glucose uptake. The decrease in glucose availability within cumulus cells correlated with decreased ATP production and an increase in spindle abnormalities in the oocytes of the diabetic females (53). Similarly, there is a decrease in ATP production in oocytes after oxidative damage. Induced oxidative damage in culture also caused abnormal meiotic spindles and misaligned chromosomes (52). While these studies use two very different models, the striking similarity is a decrease in ATP production in the oocytes paired with an increase in abnormal spindles. Therefore, sufficient energy production is critical for normal spindle structure.

Chromosome alignment at the spindle equator requires coordinated localization of the cohesin protein complex (Figure 1b'). If chromosomes are misaligned, spindles cannot attach and meiosis is delayed (54). This suggests that not only spindle formation but also chromosome alignment and therefore cohesin proteins are important in meiotic maturation and allowing the oocyte to be ovulated in a fertilizable state.

Cohesin proteins create a ring-like complex around chromosomes in all dividing cells. The cohesin proteins have roles in DNA repair and holding sister chromatids together during mitosis and meiosis (Figure 1b'). During meiosis, cohesins also facilitate homologous recombination and resolve the DNA breaks that occur as a result of crossovers. Because cohesins have unique functions in germ cells, oocytes and sperm have specific meiotic homologs of all of the cohesin molecules. These cohesin molecules make up a complex known as the synaptonemal complex (SC) that is present in meiosis I and meiosis II. The SC forms a ring like structure around chromosomes and is made of four subunits (Figure 1b'). In meiosis, the two Structural

Maintenance of Chromosome (SMC) subunits, SMC1β and SMC3, form the 'arms' of the ring. The non-SMC proteins REC8 and STAG3 hold the SMC subunits together. SMC3 is the only cohesin protein involved in both meiosis and mitosis (55). During prophase I of meiosis, SC assembly begins along the length of the chromosomes and forms the axial element of the SC. The SC aids in creating the synapses of crossover events during homologous recombination. In addition to the role in crossover events, the SC also holds sister chromatids together during meiosis I to prevent premature pre-division of sister chromatids (55) (Figure 1).

Due to the critical role of cohesin proteins in ensuring faithful chromosome segregation as well as the increased frequency of aneuploidy with age, researchers have investigated the roles of cohesin proteins during aging. One mechanism involved in the etiology of increased aneuploidy with advanced maternal age is decreased levels of the cohesin proteins (31). Therefore, investigators created genetic mouse models to mimic this decrease and answer specific questions about the roles of cohesin proteins during meiosis. Deletion of *Rec8* causes sterility in mice. Additionally, oocytes are not able to mature past the primary stage and form a follicle, indicating REC8 is important even early in oocyte cytoplasmic maturation. Finally, *Rec8* knockouts (KO) did not have crossover events, preventing homologous recombination and genetic diversity (56).

To overcome the sterility of *Rec8* KO mice and study the role of REC8 in oocytes, Tachibana-Knowalski et al. (57) created mice with a TEV-protease site in the meiotic cohesin REC8. This allowed mice to be fertile and have oocytes that underwent meiotic maturation. To investigate the role of REC8 in meiosis, investigators arrested oocytes at either MI or MII and injected the oocytes with mRNA for TEV-protease to induce cleavage of Rec8. Oocyte injection at MI induced premature separation of sister chromatids into bivalents. Similarly, oocyte

161

injection at MII resulted in premature separation of centromeres. Therefore, Rec8 is necessary for appropriate chromosome segregation during MI and MII (57).

Corroborating this finding, when female mice were generated to be heterozygous for *Rec8*, the number of synaptic errors during prophase I in oocytes was significantly increased as compared to controls. *Rec8* heterozygotes also had significantly fewer crossover sites, indicating *Rec8* has a role in holding sister chromatids together and initiating crossovers (58). When sections of human ovaries were analyzed for REC8 and SMC1β expression, accumulation of these cohesin proteins decreased significantly in aged ovaries as compared to young ovaries (59). This suggests that age-associated increases in aneuploidy may be due in part to reduced chromosome cohesion during meiosis.

To assess how frequently MI and MII errors occur with increasing maternal age, the polar body DNA content can be analyzed for hyperploidy (an inappropriate increase in chromosome number). Analysis of polar bodies taken from the oocytes of women undergoing IVF for infertility related to advanced maternal age were analyzed and compared to reproductive outcomes from the same oocytes. Analysis revealed a high percentage of oocytes from older women did not progress through MI or MII faithfully. Additionally, faithful segregation of chromosomes at MI did not guarantee MII segregation would occur without error. One of the most frequently involved chromosomes in aneuploidy was chromosome 21 (60). Corroborating evidence from mouse models for advanced maternal age show aneuploidy rates due to nondisjunction at MI increased significantly at 12 months of age and are even higher in 15 months. These events were due mainly to nondisjunction during MI, not premature sister chromatid division during MII (61). In women, MI errors and trisomy 21 positively correlate with increasing age (62).

Meiosis II errors also increase with maternal age and may be in part due to changes to expression of proteins involved in centromere cohesion. One such protein is SGO2 (Shugosin-2). A decrease in SGO2 levels in murine oocytes was correlated with increased interkinetochore (iKT) distance and premature sister chromatid segregation during MII arrest. Increased iKT caused oscillation of chromatid pairs at the spindle equator, which would increase the likelihood for aneuploidy at fertilization (63). Data from this work led the authors to postulate that a decrease in cohesins changes chromosome dynamics during MII due to prolonged MII arrest. Oscillation of chromosomes can also occur if microtubule reattachment to spindles cannot be maintained, which requires the correct expression of cohesin proteins (63). In a more recent publication, increased iKT distance was positively correlated with attachment of both kinetochores to the same spindle pole (64), which would lead to aneuploidy.

Changes in iKT distance also occur in women of advanced maternal age. In a study of human oocytes received without ovarian hyperstimulation, there was an increase in iKT distance and hyperploidy with increasing age (65). This suggests not only that the increased iKT distance is a maternal aging phenotype, but also that it is occurring independently of exposure to high levels of exogenous gonadotropins used for infertility treatment. Supporting evidence from aged mice shows that increased iKT distance is positively correlated with age (64, 66). Additionally, absolute iKT distance in all oocytes from aged mice was on average similar to iKT distance in aneuploid oocytes at all other ages (66), predisposing oocytes to erroneous segregation events and aneuploidy. Furthermore, the significant increase in aneuploidy of oocytes with increased iKT distance suggests some mechanism of cohesin protein loss is leading to aneuploidy.

A8.   Possible Therapies

ROS impact oocyte quality by damaging the mitochondria, DNA, and spindles. However, understanding these mechanisms can guide potential therapeutic strategies using readily available antioxidants and vitamins. Currently, an active area of research uses antioxidant compounds to lower levels of oxidative damage in oocytes, which is promising for women over 35 attempting to conceive. For example, investigators showed that administration of 0.1 mM N-acetyl-L-cysteine (NAC, an antioxidant) to mice for one year was able to improve fertility and increase trophoblast size in aged mice. There was an also slight improvement to oocyte spindle structure and a decrease in oocyte apoptosis in NAC treated females. But, the number of oocytes retrieved at MII was not increased in aged females by NAC (67). This highlights that age-induced oxidative damage to oocytes, not decreased ovarian reserve, is one cause of decreased fertility.

Vitamins E and C also have antioxidant activity in aging females. Dietary supplementation of female mice with vitamins E and C both long term (from weaning) and short term (from 32 months old to sacrifice; 10-15 weeks) increased the number of cytologically normal, retrievable GV and MII oocytes. These vitamins also decreased the percentage of oocytes that were degraded or undergoing apoptosis at older ages (32). Corroborating evidence from a retrospective clinical study recorded increased intake of vitamin E in women over 35 years old undergoing IVF decreased time to pregnancy as compared to women of the same age who did not conceive (68). Together, these studies suggests that the antioxidant actions of vitamins E and C are able to improve oocyte quality, and thereby fertility, in both mice and humans.

In addition to antioxidants, enhancing mitochondrial metabolism with specific substrates is also beneficial to oocyte quality. Fatty acids are metabolized in the oocyte mitochondria by β-

oxidation, a biochemical process that converts fatty acids to acetyl-CoA in order to be used as a substrate for the TCA cycle and generate ATP. Transport of fatty acids into the mitochondria to be utilized for energy production is dependent on L-carnitine (69). In oocytes from aged female mice, microinjection of oocytes with L-carnitine and the signaling molecule ceramide reversed age-induced mitochondrial damage and decreased the percentage of oocytes that underwent apoptosis (35). L-carnitine supplementation to the culture medium during murine IVF reduced apoptosis and increased the percentage of fertilized embryos that develop to blastocysts. Importantly, L-carnitine was protective against H_2O_2 induced apoptosis (70). Therefore, L-carnitine may play a dual role during oocyte maturation; one in protecting oocytes and oocyte mitochondria against oxidative damage and one in stimulating fatty acid metabolism in the oocytes.

Dietary supplementation with antioxidants is a feasible treatment. However, care must be taken to avoid overcompensation of antioxidant supplementation. Evidence from mice showed the antioxidant alpha lipoic acid (ALA) exposure in high concentrations was detrimental to follicular development, oocyte maturation, and preimplantation development despite benefits at lower concentrations (71). This study demonstrates that antioxidant supplementation can be beneficial, but also that ROS are a necessary component of oocyte maturation and conception, so dosage must be monitored and controlled.

A9.   Conclusions

Maternal age causes an increase in oxidative damage in oocytes. Oxidative damage is linked to spindle abnormalities, decreased ATP content, increased nuclear DNA and mtDNA damage, and inabilities to repair DNA damage efficiently. While an association between oxidative damage and changes to cohesin proteins has not been shown, a feasible hypothesis is

165

that ROS-induced damage to meiotic cohesins causes decreased levels of these proteins. Cohesin decreases cause an inability to maintain chromosome cohesion (58), leading to an increase in aneuploidy as females get older.

Accumulation in mitochondrial damage also occurs as females continue to age. This increased damage is likely the root of many issues in oocytes. The oocytes may have mechanisms to counteract this damage (28), but whether or not the mechanisms are sufficient to overcome the rate of damage has not been addressed. Mechanisms to overcome mitochondrial damage include removal of damaged mtDNA and mitophagy (removal of damaged mitochondria) (72). Whether these processes are highly active in aged oocytes has not been studied.

Finally, treatments to improve oocyte quality may help older women maintain fertility as they age. In particular, targeted treatments to regain the appropriate oxidative balance should be tested. Restoring homeostasis to oocytes would be ideal in preventing age-induced damage. Currently, investigation into antioxidant supplementation is ongoing. However, understanding the underlying mechanism of action of antioxidants within the oocytes is needed. A basic understanding of antioxidants in oocytes will improve two types of therapies: dietary supplementation to women as preventative measure, and as a component of oocyte and embryo culture media during IVF to improve outcomes for all patients. In recent years, advances have been made in understanding the cell biology of mammalian oocytes, but large gaps remain. Until these gaps are filled at the basic science level, oocyte quality and a woman's reproductive potential will continue to decline with age.

A10. References

1. Johnson J, Bagley J, Skaznik-Wikiel M, Lee HJ, Adams GB, Niikura Y, et al. Oocyte generation in adult mammalian ovaries by putative germ cells in bone marrow and peripheral blood. Cell. 2005;122(2):303-15.

2. Johnson J, Canning J, Kaneko T, Pru JK, Tilly JL. Germline stem cells and follicular renewal in the postnatal mammalian ovary. Nature. 2004;428(6979):145-50.

3. te Velde ER, Scheffer GJ, Dorland M, Broekmans FJ, Fauser BC. Developmental and endocrine aspects of normal ovarian aging. Molecular and cellular endocrinology. 1998;145(1-2):67-73.

4. Tarin JJ, Perez-Albala S, Cano A. Cellular and morphological traits of oocytes retrieved from aging mice after exogenous ovarian stimulation. Biology of reproduction. 2001;65(1):141-50.

5. McClellan KA, Gosden R, Taketo T. Continuous loss of oocytes throughout meiotic prophase in the normal mouse ovary. Developmental biology. 2003;258(2):334-48.

6. Sauer MV, Paulson RJ, Lobo RA. Pregnancy after age 50: application of oocyte donation to women after natural menopause. Lancet. 1993;341(8841):321-3.

7. Richards JS, Midgley AR, Jr. Protein hormone action: a key to understanding ovarian follicular and luteal cell development. Biology of reproduction. 1976;14(1):82-94.

8. Dumont J, Desai A. Acentrosomal spindle assembly and chromosome segregation during oocyte meiosis. Trends in cell biology. 2012;22(5):241-9.

9. Gougeon A. Dynamics of follicular growth in the human: a model from preliminary results. Human reproduction (Oxford, England). 1986;1(2):81-7.

10.   Sathananthan AH, Trounson AO. Mitochondrial morphology during preimplantational human embryogenesis. Human reproduction (Oxford, England). 2000;15 Suppl 2:148-59.

11.   Sathananthan AH, Selvaraj K, Girijashankar ML, Ganesh V, Selvaraj P, Trounson AO. From oogonia to mature oocytes: inactivation of the maternal centrosome in humans. Microscopy research and technique. 2006;69(6):396-407.

12.   Li R, Albertini DF. The road to maturation: somatic cell interaction and self-organization of the mammalian oocyte. Nature reviews Molecular cell biology. 2013;14(3):141-52.

13.   De La Fuente R, Eppig JJ. Transcriptional activity of the mouse oocyte genome: companion granulosa cells modulate transcription and chromatin remodeling. Developmental biology. 2001;229(1):224-36.

14.   Philpott CC, Ringuette MJ, Dean J. Oocyte-specific expression and developmental regulation of ZP3, the sperm receptor of the mouse zona pellucida. Developmental biology. 1987;121(2):568-75.

15.   Harris SE, Adriaens I, Leese HJ, Gosden RG, Picton HM. Carbohydrate metabolism by murine ovarian follicles and oocytes grown in vitro. Reproduction (Cambridge, England). 2007;134(3):415-24.

16.   Wang Y, Mohsen AW, Mihalik SJ, Goetzman ES, Vockley J. Evidence for physical association of mitochondrial fatty acid oxidation and oxidative phosphorylation complexes. The Journal of biological chemistry. 2010;285(39):29834-41.

17.   Van Blerkom J, Davis PW, Lee J. ATP content of human oocytes and developmental potential and outcome after in-vitro fertilization and embryo transfer. Human reproduction (Oxford, England). 1995;10(2):415-24.

18.   Yu Y, Dumollard R, Rossbach A, Lai FA, Swann K. Redistribution of mitochondria leads to bursts of ATP production during spontaneous mouse oocyte maturation. Journal of cellular physiology. 2010;224(3):672-80.

19.   Lodish HF, Berk A, Kaiser AK, Krieger M, Scott MP, Bretscher A, et al. Molecular Cell Biology. 6th ed. New York: W. H. Freeman and Company; 2007.

20.   Gaziev AI, Abdullaev S, Podlutsky A. Mitochondrial function and mitochondrial DNA maintenance with advancing age. Biogerontology. 2014.

21.   Heytler PG. Uncouplers of oxidative phosphorylation. Methods in enzymology. 1979;55:462-42.

22.   Ge H, Tollner TL, Hu Z, Dai M, Li X, Guan H, et al. The importance of mitochondrial metabolic activity and mitochondrial DNA replication during oocyte maturation in vitro on oocyte quality and subsequent embryo developmental competence. Molecular reproduction and development. 2012;79(6):392-401.

23.   Takeuchi T, Neri QV, Katagiri Y, Rosenwaks Z, Palermo GD. Effect of treating induced mitochondrial damage on embryonic development and epigenesis. Biology of reproduction. 2005;72(3):584-92.

24.   Shkolnik K, Tadmor A, Ben-Dor S, Nevo N, Galiani D, Dekel N. Reactive oxygen species are indispensable in ovulation. Proceedings of the National Academy of Sciences of the United States of America. 2011;108(4):1462-7.

25.   Biggers JD WD, Dnoahue RP. The pattern of energy metabolism in the mouse oocyte and zygote. Proceedings of the National Academy of Sciences of the United State of America. 1967;58(2):560-7.

26.   Dumollard R, Duchen M, Carroll J. The role of mitochondrial function in the oocyte and embryo. Current topics in developmental biology. 2007;77:21-49.

27.   Zuelke KA, Jeffay SC, Zucker RM, Perreault SD. Glutathione (GSH) concentrations vary with the cell cycle in maturing hamster oocytes, zygotes, and pre-implantation stage embryos. Molecular reproduction and development. 2003;64(1):106-12.

28.   Hill JH, Chen Z, Xu H. Selective propagation of functional mitochondrial DNA during oogenesis restricts the transmission of a deleterious mitochondrial variant. Nature genetics. 2014;46(4):389-92.

29.   Schriner SE, Linford NJ, Martin GM, Treuting P, Ogburn CE, Emond M, et al. Extension of murine life span by overexpression of catalase targeted to mitochondria. Science (New York, NY). 2005;308(5730):1909-11.

30.   Di Emidio G, Falone S, Vitti M, D'Alessandro AM, Vento M, Di Pietro C, et al. SIRT1 signalling protects mouse oocytes against oxidative stress and is deregulated during aging. Human reproduction (Oxford, England). 2014.

31.   Schwarzer C, Siatkowski M, Pfeiffer MJ, Baeumer N, Drexler HC, Wang B, et al. Maternal age effect on mouse oocytes: new biological insight from proteomic analysis. Reproduction (Cambridge, England). 2014;148(1):55-72.

32.   Tarin JJ, Perez-Albala S, Cano A. Oral antioxidants counteract the negative effects of female aging on oocyte quantity and quality in the mouse. Molecular reproduction and development. 2002;61(3):385-97.

170

33. Bogliolo L, Murrone O, Di Emidio G, Piccinini M, Ariu F, Ledda S, et al. Raman spectroscopy-based approach to detect aging-related oxidative damage in the mouse oocyte. Journal of assisted reproduction and genetics. 2013;30(7):877-82.

34. Schie IW, Huser T. Methods and applications of Raman microspectroscopy to single-cell analysis. Applied spectroscopy. 2013;67(8):813-28.

35. Kujjo LL, Acton BM, Perkins GA, Ellisman MH, D'Estaing SG, Casper RF, et al. Ceramide and its transport protein (CERT) contribute to deterioration of mitochondrial structure and function in aging oocytes. Mechanisms of ageing and development. 2013;134(1-2):43-52.

36. Yamada-Fukunaga T, Yamada M, Hamatani T, Chikazawa N, Ogawa S, Akutsu H, et al. Age-associated telomere shortening in mouse oocytes. Reproductive biology and endocrinology : RB&E. 2013;11(1):108.

37. Wilding M, Dale B, Marino M, di Matteo L, Alviggi C, Pisaturo ML, et al. Mitochondrial aggregation patterns and activity in human oocytes and preimplantation embryos. Human reproduction (Oxford, England). 2001;16(5):909-17.

38. Simsek-Duran F, Li F, Ford W, Swanson RJ, Jones HW, Jr., Castora FJ. Age-associated metabolic and morphologic changes in mitochondria of individual mouse and hamster oocytes. PloS one. 2013;8(5):e64955.

39. Piko L, Taylor KD. Amounts of mitochondrial DNA and abundance of some mitochondrial gene transcripts in early mouse embryos. Developmental biology. 1987;123(2):364-74.

40. Murakoshi Y, Sueoka K, Takahashi K, Sato S, Sakurai T, Tajima H, et al. Embryo developmental capability and pregnancy outcome are related to the mitochondrial DNA copy number and ooplasmic volume. Journal of assisted reproduction and genetics. 2013;30(10):1367-75.

41. Titus S, Li F, Stobezki R, Akula K, Unsal E, Jeong K, et al. Impairment of BRCA1-related DNA double-strand break repair leads to ovarian aging in mice and humans. Science translational medicine. 2013;5(172):172ra21.

42. Matsumine M, Shibata N, Ishitani K, Kobayashi M, Ohta H. Pentosidine accumulation in human oocytes and their correlation to age-related apoptosis. Acta histochemica et cytochemica. 2008;41(4):97-104.

43. Santonocito M, Guglielmino MR, Vento M, Ragusa M, Barbagallo D, Borzi P, et al. The apoptotic transcriptome of the human MII oocyte: characterization and age-related changes. Apoptosis : an international journal on programmed cell death. 2013;18(2):201-11.

44. Matos L, Stevenson D, Gomes F, Silva-Carvalho JL, Almeida H. Superoxide dismutase expression in human cumulus oophorus cells. Molecular human reproduction. 2009;15(7):411-9.

45. Elizur SE, Lebovitz O, Orvieto R, Dor J, Zan-Bar T. Reactive oxygen species in follicular fluid may serve as biochemical markers to determine ovarian aging and follicular metabolic age. Gynecological endocrinology : the official journal of the International Society of Gynecological Endocrinology. 2014:1-3.

46. Dumollard R, Marangos P, Fitzharris G, Swann K, Duchen M, Carroll J. Sperm-triggered [Ca2+] oscillations and Ca2+ homeostasis in the mouse egg have an

absolute requirement for mitochondrial ATP production. Development (Cambridge, England). 2004;131(13):3057-67.

47. Wakai T, Zhang N, Vangheluwe P, Fissore RA. Regulation of endoplasmic reticulum Ca(2+) oscillations in mammalian eggs. Journal of cell science. 2013;126(Pt 24):5714-24.

48. Thouas GA, Trounson AO, Wolvetang EJ, Jones GM. Mitochondrial dysfunction in mouse oocytes results in preimplantation embryo arrest in vitro. Biology of reproduction. 2004;71(6):1936-42.

49. Yang HW, Hwang KJ, Kwon HC, Kim HS, Choi KW, Oh KS. Detection of reactive oxygen species (ROS) and apoptosis in human fragmented embryos. Human reproduction (Oxford, England). 1998;13(4):998-1002.

50. Wakefield SL, Lane M, Mitchell M. Impaired mitochondrial function in the preimplantation embryo perturbs fetal and placental development in the mouse. Biology of reproduction. 2011;84(3):572-80.

51. Thouas GA, Trounson AO, Jones GM. Developmental effects of sublethal mitochondrial injury in mouse oocytes. Biology of reproduction. 2006;74(5):969-77.

52. Zhang X, Wu XQ, Lu S, Guo YL, Ma X. Deficit of mitochondria-derived ATP during oxidative stress impairs mouse MII oocyte spindles. Cell research. 2006;16(10):841-50.

53. Wang Q, Chi MM, Schedl T, Moley KH. An intercellular pathway for glucose transport into mouse oocytes. American journal of physiology Endocrinology and metabolism. 2012;302(12):E1511-8.

54.   Nagaoka SI, Hodges CA, Albertini DF, Hunt PA. Oocyte-specific differences in cell-cycle control create an innate susceptibility to meiotic errors. Current biology : CB. 2011;21(8):651-7.

55.   Lee J. Roles of cohesin and condensin in chromosome dynamics during mammalian meiosis. The Journal of reproduction and development. 2013;59(5):431-6.

56.   Xu H, Beasley MD, Warren WD, van der Horst GT, McKay MJ. Absence of mouse REC8 cohesin promotes synapsis of sister chromatids in meiosis. Developmental cell. 2005;8(6):949-61.

57.   Tachibana-Konwalski K, Godwin J, van der Weyden L, Champion L, Kudo NR, Adams DJ, et al. Rec8-containing cohesin maintains bivalents without turnover during the growing phase of mouse oocytes. Genes & development. 2010;24(22):2505-16.

58.   Murdoch B, Owen N, Stevense M, Smith H, Nagaoka S, Hassold T, et al. Altered cohesin gene dosage affects Mammalian meiotic chromosome structure and behavior. PLoS genetics. 2013;9(2):e1003241.

59.   Tsutsumi M, Fujiwara R, Nishizawa H, Ito M, Kogo H, Inagaki H, et al. Age-related decrease of meiotic cohesins in human oocytes. PloS one. 2014;9(5):e96710.

60.   Fragouli E, Wells D, Delhanty JD. Chromosome abnormalities in the human oocyte. Cytogenetic and genome research. 2011;133(2-4):107-18.

61.   Merriman JA, Jennings PC, McLaughlin EA, Jones KT. Effect of aging on superovulation efficiency, aneuploidy rates, and sister chromatid cohesion in mice aged up to 15 months. Biology of reproduction. 2012;86(2):49.

62.   Dailey T, Dale B, Cohen J, Munne S. Association between nondisjunction and maternal age in meiosis-II human oocytes. American journal of human genetics. 1996;59(1):176-84.

63.   Yun Y, Lane SI, Jones KT. Premature dyad separation in meiosis II is the major segregation error with maternal age in mouse oocytes. Development (Cambridge, England). 2014;141(1):199-208.

64.   Shomper M, Lappa C, FitzHarris G. Kinetochore microtubule establishment is defective in oocytes from aged mice. Cell cycle (Georgetown, Tex). 2014;13(7):1171-9.

65.   Duncan FE, Hornick JE, Lampson MA, Schultz RM, Shea LD, Woodruff TK. Chromosome cohesion decreases in human eggs with advanced maternal age. Aging cell. 2012;11(6):1121-4.

66.   Merriman JA, Lane SI, Holt JE, Jennings PC, Garcia-Higuera I, Moreno S, et al. Reduced chromosome cohesion measured by interkinetochore distance is associated with aneuploidy even in oocytes from young mice. Biology of reproduction. 2013;88(2):31.

67.   Liu J, Liu M, Ye X, Liu K, Huang J, Wang L, et al. Delay in oocyte aging in mice by the antioxidant N-acetyl-L-cysteine (NAC). Human reproduction (Oxford, England). 2012;27(5):1411-20.

68.   Ruder EH, Hartman TJ, Reindollar RH, Goldman MB. Female dietary antioxidant intake and time to pregnancy among couples treated for unexplained infertility. Fertil Steril. 2014;101(3):759-66.

69. Houten SM, Wanders RJ. A general introduction to the biochemistry of mitochondrial fatty acid beta-oxidation. Journal of inherited metabolic disease. 2010;33(5):469-77.

70. Abdelrazik H, Sharma R, Mahfouz R, Agarwal A. L-carnitine decreases DNA damage and improves the in vitro blastocyst development rate in mouse embryos. Fertil Steril. 2009;91(2):589-96.

71. Talebi A, Zavareh S, Kashani MH, Lashgarbluki T, Karimi I. The effect of alpha lipoic acid on the developmental competence of mouse isolated preantral follicles. Journal of assisted reproduction and genetics. 2012;29(2):175-83.

72. Palikaras K, Tavernarakis N. Mitochondrial homeostasis: The interplay between mitophagy and mitochondrial biogenesis. Experimental gerontology. 2014.

A11. Figure Legend

Figure A-1: The cytoplasmic and nuclear maturation of an oocyte. All lightning bolts indicate points at which oxidative damage can occur to the oocyte. Along the bottom of the figure, the relative levels of hormones are indicated (FSH: follicle stimulating hormone, LH: luteinizing hormone, E2: estradiol), as well as the fluctuation of ROS that are produced during each estrus or menstrual cycle. (a) The primordial oocyte is characterized by one layer of surrounding follicular cells. Mammalian ovaries have hundreds of thousands of primordial oocytes to recruit from at the beginning of oocyte maturation. At this time, the nucleus and cytoplasm are susceptible to systemic ROS and ovarian ROS. (b) The primary, or germinal vesicle (GV), oocyte has undergone cytoplasmic maturation. The oocyte has increased in size and many more layers of follicular cells surround and support the oocyte. It is ready for nuclear maturation. Chromosomes begin to condense and the synaptonemal complex forms (shown in detail in b'). Crossover events occur at this stage. (b') The synaptonemal complex consists of a cohesin ring with two arms of SMC1β and SMC3 (green) held together by Rec8 (blue) and joined to the axial and lateral elements (orange and red, respectively) by Stag3 (purple). (c) The secondary oocyte has responded to the rise in estrogen levels by resuming meiosis. A spindle forms at this time and a reductional division of homologous chromosomes occurs at this point. Half of the chromosomes will be extruded in a polar body. A fluid-filled antrum begins to develop within the follicular cells. ROS can accumulate in the antrum, which can damage the oocyte and cumulus cells. (d) Just prior to ovulation, a large, fluid filled antrum has formed within the follicle and the oocyte is arrested in metaphase II. ROS accumulation occurs within the follicular fluid and can be damaging to the oocyte and cumulus cells. The spindle and proteins that hold the sister chromatids together (detailed in d') are susceptible to oxidative damage (indicated by lightning bolt). (d') The synaptonemal complex helps hold sister chromatids together similar to (b'), and

Sgo2 (blue) holds kinetochores together during MII arrest. (e) Ovulation is induced by a surge in luteinizing hormone (LH). Cumulus cells have disassociated from the oocyte. If a sperm binds, Ca^{2+} oscillations (black arrow) are triggered from the ER (gray). These oscillations are altered by oxidative damage (lightning bolt). Meiosis completes and a second polar body is extruded (purple). The sperm will release its genetic material into the oocyte as a pronucleus (blue) and a female pronucleus will also be visible (pink).
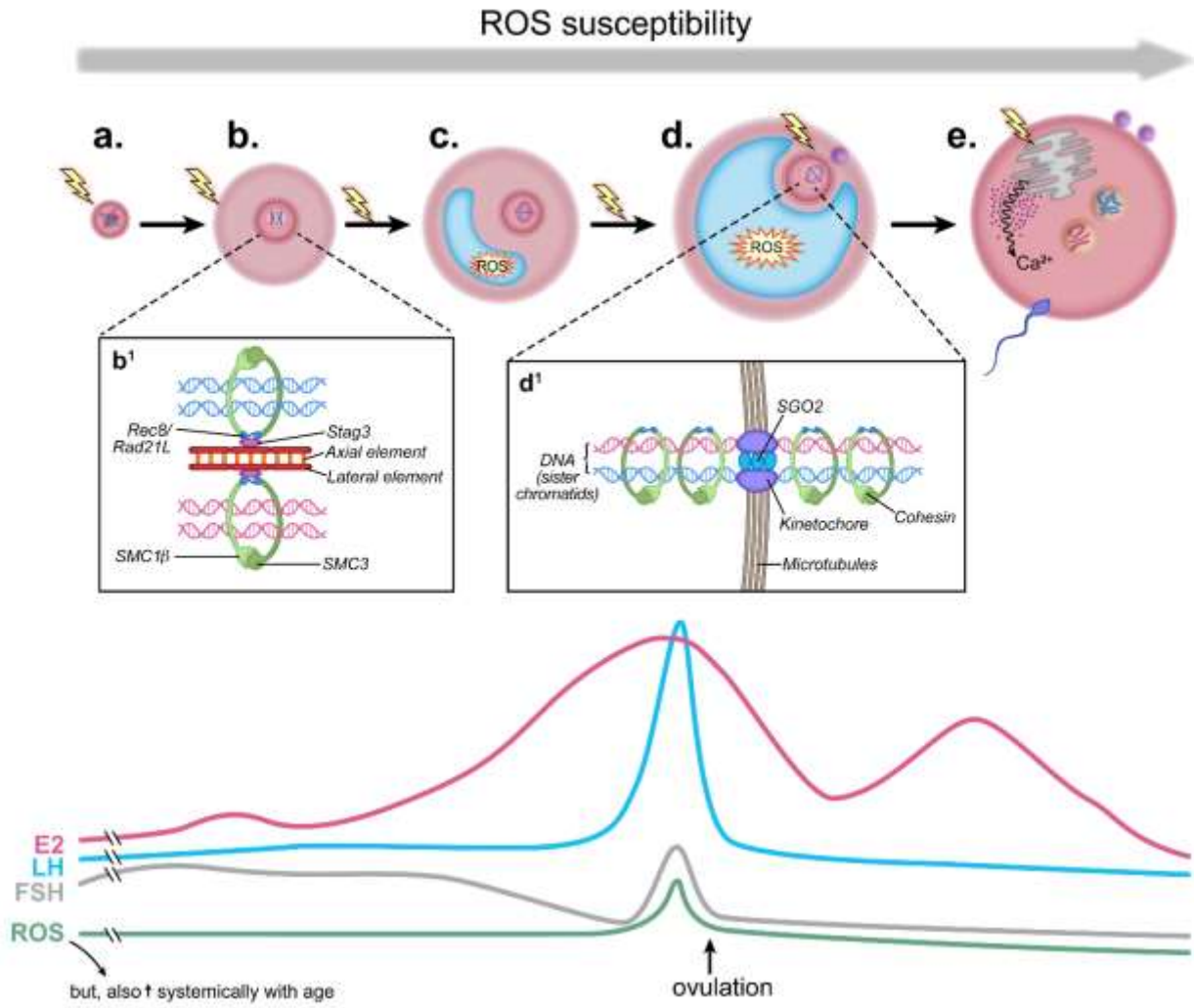
Figure A- 1: Cytoplasmic and nuclear maturation of an oocyte.